



ESCUELA TÉCNICA SUPERIOR DE INGENIERÍA (ICAI)
GRADO EN INGENIERÍA ELECTROMECÁNICA
Especialidad Eléctrica

A DC – to – AC Power Converter for Photovoltaic Stations

Autor: Juan Carlos Martín Valiño

Director: Arijit Banerjee, PhD

Madrid

Julio de 2018

AUTHORIZATION FOR DIGITALIZATION, STORAGE AND DISSEMINATION IN THE NETWORK OF END-OF-DEGREE PROJECTS, MASTER PROJECTS, DISSERTATIONS OR BACHILLERATO REPORTS

1. Declaration of authorship and accreditation thereof.

The author Mr. Juan Carlos Martín Valiño

HEREBY DECLARES that he/she owns the intellectual property rights regarding the piece of work:

A DC-to-AC Converter for Photovoltaic Stations

That this is an original piece of work, and that he/she holds the status of author, in the sense granted by the Intellectual Property Law.

2. Subject matter and purpose of this assignment.

With the aim of disseminating the aforementioned piece of work as widely as possible using the University's Institutional Repository the author hereby **GRANTS** Comillas Pontifical University, on a royalty-free and non-exclusive basis, for the maximum legal term and with universal scope, the digitization, archiving, reproduction, distribution and public communication rights, including the right to make it electronically available, as described in the Intellectual Property Law. Transformation rights are assigned solely for the purposes described in a) of the following section.

3. Transfer and access terms

Without prejudice to the ownership of the work, which remains with its author, the transfer of rights covered by this license enables:

- a) Transform it in order to adapt it to any technology suitable for sharing it online, as well as including metadata to register the piece of work and include "watermarks" or any other security or protection system.
- b) Reproduce it in any digital medium in order to be included on an electronic database, including the right to reproduce and store the work on servers for the purposes of guaranteeing its security, maintaining it and preserving its format.
- c) Communicate it, by default, by means of an institutional open archive, which has open and cost-free online access.
- d) Any other way of access (restricted, embargoed, closed) shall be explicitly requested and requires that good cause be demonstrated.
- e) Assign these pieces of work a Creative Commons license by default.
- f) Assign these pieces of work a HANDLE (*persistent URL*). by default.

4. Copyright.

The author, as the owner of a piece of work, has the right to:

- a) Have his/her name clearly identified by the University as the author
- b) Communicate and publish the work in the version assigned and in other subsequent versions using any medium.
- c) Request that the work be withdrawn from the repository for just cause.
- d) Receive reliable communication of any claims third parties may make in relation to the work and, in particular, any claims relating to its intellectual property rights.

5. Duties of the author.

The author agrees to:

- a) Guarantee that the commitment undertaken by means of this official document does not infringe any third party rights, regardless of whether they relate to industrial or intellectual property or any other type.

- b) Guarantee that the content of the work does not infringe any third party honor, privacy or image rights.
- c) Take responsibility for all claims and liability, including compensation for any damages, which may be brought against the University by third parties who believe that their rights and interests have been infringed by the assignment.
- d) Take responsibility in the event that the institutions are found guilty of a rights infringement regarding the work subject to assignment.

6. Institutional Repository purposes and functioning.

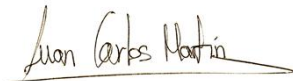
The work shall be made available to the users so that they may use it in a fair and respectful way with regards to the copyright, according to the allowances given in the relevant legislation, and for study or research purposes, or any other legal use. With this aim in mind, the University undertakes the following duties and reserves the following powers:

- a) The University shall inform the archive users of the permitted uses; however, it shall not guarantee or take any responsibility for any other subsequent ways the work may be used by users, which are non-compliant with the legislation in force. Any subsequent use, beyond private copying, shall require the source to be cited and authorship to be recognized, as well as the guarantee not to use it to gain commercial profit or carry out any derivative works.
- b) The University shall not review the content of the works, which shall at all times fall under the exclusive responsibility of the author and it shall not be obligated to take part in lawsuits on behalf of the author in the event of any infringement of intellectual property rights deriving from storing and archiving the works. The author hereby waives any claim against the University due to any way the users may use the works that is not in keeping with the legislation in force.
- c) The University shall adopt the necessary measures to safeguard the work in the future.
- d) The University reserves the right to withdraw the work, after notifying the author, in sufficiently justified cases, or in the event of third party claims.

Madrid, on 9 of May, 2018

HEREBY ACCEPTS

Signature:



Juan Carlos Martín Valiño

Reasons for requesting the restricted, closed or embargoed access to the work in the Institution's Repository

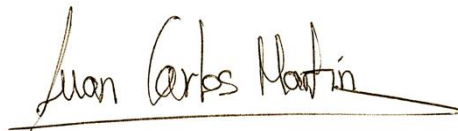
Declaro, bajo mi responsabilidad, que el Proyecto presentado con el título

A DC-to-AC Converter for Photovoltaic Stations

en la ETS de Ingeniería - ICAI de la Universidad Pontificia Comillas en el curso académico 2017/2018 es de mi autoría, original e inédito y no ha sido presentado con anterioridad a otros efectos. El Proyecto no es plagio de otro, ni total ni parcialmente y la información que ha sido tomada de otros documentos está debidamente referenciada.

Fdo.: Juan Carlos Martín Valiño

Fecha: 04/05/2018

A handwritten signature in black ink that reads "Juan Carlos Martín Valiño". The signature is written in a cursive style and is underlined with a single horizontal line.

Autorizada la entrega del proyecto

EL DIRECTOR DEL PROYECTO

Fdo.: Arijit Banerjee, PhD

Fecha: 04/05/2018

A handwritten signature in black ink that reads "Arijit Banerjee". The signature is written in a cursive style and is underlined with a single horizontal line.



ESCUELA TÉCNICA SUPERIOR DE INGENIERÍA (ICAI)
GRADO EN INGENIERÍA ELECTROMECÁNICA
Especialidad Eléctrica

A DC – to – AC Power Converter for Photovoltaic Stations

Autor: Juan Carlos Martín Valiño

Director: Arijit Banerjee, PhD

Madrid

Julio de 2018

To my parents

Acknowledgments

I would like to express the deepest appreciation to the two institutions that have taken me in during these four years of the degree. First, the Universidad Pontificia Comillas at Madrid, in which I have been most of the time and in which I have grown, not only as a professional but as a person and second, the University of Illinois at Urbana–Champaign which has helped me to finish my studies and who has helped me to grow in many aspects of life.

I really would like to express my gratitude to Professor Arijit Banerjee, who has been my professor, adviser and director. For all the time he has been teaching and helping me and my colleagues during this year, especially during this project. Also to Kevin J. Colravy who has helped us with a great effort.

I would like to appreciate the work of those people in the non–teaching staff that, although they have not been professors, they have been taking care of me during these years.

Finally, to my friends, the ones that I keep since I am a child and all the people that I have met at the school. Thank you because otherwise, it would not have been the same.

Of course, it is impossible for me to forget my family, they are the main reason why I am here. My parents and sister have supported me since the beginning, encouraging me to study an engineering, and have set the basis of what I am as a person. I could not be more grateful to belong to this family.

I would like to mention Alberto González Ortega and Daniel Portillo Quesada. We have been helping each other to accomplish this project and make it possible.

Abstract

A DC–TO–AC POWER CONVERTER FOR PHOTOVOLTAIC STATIONS

Author: Martín Valiño, Juan Carlos

Supervisor: Banerjee, Arijit PhD

Collaborating entity: ICAI – Universidad Pontificia Comillas

Abstract

Energy is a lens through we may view many important aspects these days, economy, human development or the environment. Decisions taken today will shape tomorrow's future.

Energy drives economies and has a fundamental role in taking care of nature. We live in a world where we the energy does not equally share. The most developed societies of the present waste energy, using transports or with an improper use of the electricity, not having a deep concern about its impact and the cost. On the other hand, in other societies, the energy is good as limited as safe water.

The main sources from where the energy comes are from fossil fuels, and, especially, from coal and oil. We must not forget natural gas, in which its use has become more frequent due to the increase in residential places.

At this pace that we are generating and consuming energy, the fossil fuel reserves, that are non-renewable resources, will be depleted. It is interesting to know that technically this fact of the reserves deployed would never happen because before we reach that point, their extraction cost will be high enough that no-economies would be able to afford it. Since we have made a society highly dependent on these fuels, not having a secondary source would make the economies collapse. In fact, not having the energy anymore will bring us to times before the Industrial Revolution. Besides economy issues, another different kind of problem comes with the environment. All CO₂ emissions generated by the combustion of these fuels are accelerating the climate change, and what was a natural greenhouse effect is becoming an artificial one.

This way of generating energy is now an advantage, nevertheless, it is now turning into a threat, and this is why we should look for new alternatives. In the same thought of the new renewables, the main and almost unique candidate is nuclear power, in which the energy stored in a simple pellet of Uranium releases as much energy as one ton of coal or three barrels of oil. Despite its controversies related to healthcare, the main reason why it is not fully used is that now no one has developed a plan to manage all the radioactive disposals.

The most prominent solution and the one that pretends to finish with all the energetic dependencies and healthcare problems are renewables energies. Among them, the most promising ones are wind power and solar power energies, being the first one the main candidate. However, in places where are not fully developed or not at all, where it might be impossible to harvest or to do any other activity and the most plentiful resource is solar light, we must believe that the main solution goes through solar energy. Solar energy is easy to transform into different varieties of energy, in which the most know is electricity. Researchers have found two main ways of doing it, (1) one way is through concentrated solar plants, and (2) through photovoltaic plants. This last one is the most common, and consists of transforming solar energy directly into electricity using photosensitive materials.

Facing this great advantage, we have to add a problem, and it is that the solar panels cannot be connected directly to the grid, because they operate in DC while the other operates in AC.

Therefore, during this last year we thought that it would be convenient to make a photovoltaic plant, so we can show the advantages of this technology. This is why two colleges and I decided to immerse in this project.

Three converters will make the power plant so we can fit the station. The first converter is in charge of optimizing the energy extraction of the solar panel; this is made by Daniel Portillo Quesada. This energy is transformed from DC to AC through another converter, and this will be the scope of this project. Finally, we thought about the intermittencies of the solar energy or the excess of power and we added a battery, which is connected to the system through a bidirectional converter; this is made by Alberto González Ortega.

As mentioned, this thesis is aimed to design a DC-to-AC power converter, also known as an inverter. The design of this project is subjected to certain norms and laws, and for that reason, I have made a detailed study of them, especially when dealing with the harmonic currents.

This project is divided into three blocks to understand the operation of the converter.

1. **State of the Art:** In this block, I will make a quick overview of the different technologies that are used in solar panels. Later, I will show all the families of converters, from the rectifier to the inverter. Besides, I will do a summary of the most common filters that are used in signal processing and power electronics.
2. **Principles:** I will state the principles that drive the converter, from its operation and composition of the inverter to the different filters that are used to accomplish the law. In this block, I will analyze the behaviour of the converter, stating its equations and graphs to understand its behaviour. Moreover, I will calculate its components for carrying out this project, according to the criteria established.
3. **Experiments:** Once all the components are designed, it is required to test through simulations that all the requirements are accomplished and that its operation is correct. Once everything is verified, I will proceed to do the real experiment.

This project is oriented to be able to create photovoltaic stations with all its retrofit for its correct operation. This is a small contribution to a greater good, focused on the progress of the society and care of our planet.

Keywords: Energy · Solar Power · Photovoltaic Panel · Solar Plant · DC-to-AC · Filter · Modeling

Resumen

CONVERTIDOR DE CORRIENTE CONTINUA A CORRIENTE ALTERNA PARA PLANTAS FOTOVOLTAICAS

Autor: Martín Valiño, Juan Carlos

Director: Banerjee, Arijit PhD

Entidad colaboradora: ICAI – Universidad Pontificia Comillas

Resumen del proyecto

La Energía es una lente por la que podemos ver varios aspectos muy importantes en estos tiempos, economía, desarrollo humano o el medio ambiente. Las decisiones tomadas en el presente darán forma al futuro que queremos.

La energía es el principal motor de la economía y mantiene un papel fundamental en el cuidado del medio ambiente. Vivimos en un mundo con gran disparidad energética. Las sociedades más desarrolladas del presente derrochan energía, bien sea por transporte o uso indebido de la electricidad, sin preocuparse en el impacto y coste que supone. En contraposición, en otras sociedades la energía se podría considerar un bien tan escaso como el agua potable.

Las principales fuentes de donde proviene la energía que utilizamos proviene de los combustibles fósiles, y, en especial, del carbón y del petróleo. No hay que olvidarse del gas natural, en el que su uso se hace más frecuente en zonas residenciales.

Al ritmo al que se produce y consume energía, las reservas de combustibles fósiles, que son recursos no renovables, se darán por agotadas. Cabe destacar que técnicamente este hecho no ocurriría, ya que antes de que se acabasen, sus costes de extracción serían tan altos que ninguna economía podría sostenerlo. Por ello, y habiendo creado economías altamente dependientes de los combustibles fósiles, el no tener una vía secundaria acabaría por colapsar todas las economías. El hecho de no tener energía nos volcaría a una época anterior a la Revolución Industrial. Además de las posibles consecuencias económicas, otra gran amenaza que suponen los combustibles fósiles tiene que ver con el medio ambiente. El Efecto Invernadero natural, se está convirtiendo en algo ya artificial, en la que las toneladas de CO₂ que se emiten están acelerando el cambio climático.

Esta forma de generar energía nos supone ahora una ventaja, que poco a poco se está volviendo en amenaza, y es por lo que hay que buscar distintas alternativas. Manteniendo la filosofía de los no renovables, el principal y casi único es la energía nuclear, ya que la energía almacenada en una simple pastilla de Uranio es equivalente a la producida por una tonelada de carbón o tres barriles de petróleo.

A pesar de sus controversias, la principal razón por la que no ha conseguido alzarse como la mejor candidata es debido a que no se tiene un plan para almacenar tanto material radioactivo.

La solución que pretende acabar con dependencias energéticas y con problemas de sanidad pasa por priorizar las energías renovables. De entre estas, las más prometedoras son la energía solar y la eólica, siendo esta última la principal. Sin embargo, en lugares poco desarrollados en los que ni el cultivo ni cualquier otra actividad son viables, y en las que el recurso que más abunda es luz solar, invita a pensar que la principal solución es la energía solar. La energía solar es fácilmente transformable en otros tipos, siendo la más conocida la eléctrica. Los estudios que más lejos han llegado están relacionados con la energía solar concentrada y la fotovoltaica. La más utilizada es esta última, y consiste en transformar la energía solar directamente en electricidad mediante materiales fotosensibles.

Ante esta gran ventaja, hay que añadirle un problema, y es que los paneles solares no se pueden conectar directamente a la red, dado que su funcionamiento se limita a la corriente continua y esta funciona en alterna.

Por lo tanto, durante este último año se creyó conveniente realizar una estación fotovoltaica, para así poder mostrar las ventajas que tendría esta tecnología. Es por ello por lo que dos compañeros y yo decidimos sumergirnos en este proyecto.

La estación consistirá en tres convertidores para acondicionar la instalación. El primer convertidor se encargará de optimizar la extracción de energía del panel solar, trabajo realizado por Daniel Portillo Quesada. Esta energía tendrá que ser transformada desde la corriente continua a la alterna, trabajo en el que se centra este proyecto en particular. Por último, nos faltaba tratar con las intermitencias y con los excesos de potencias características del panel solar, y por ello se decidió añadir una fuente de suministro externo conectado mediante una conexión bidireccional, que ha sido realizado por Alberto González Ortega.

Como se ha mencionado, esta memoria está encaminada a diseñar un convertidor de corriente continua a corriente alterna, comúnmente llamado inversor. El diseño del proyecto está sujeto a ciertas normas y leyes, y por ello se ha realizado un estudio cuidadoso de estas, especialmente cuando se trataban con corrientes armónicas.

Este proyecto está dividido en tres bloques fundamentales para comprender el funcionamiento del convertidor.

1. **Estado del Arte:** En este bloque se realizará un breve repaso sobre las distintas tecnologías que se utilizan los paneles solares, además de un repaso a todas las familias de convertidores, desde transformar corriente alterna a continua hasta realizar lo opuesto. Además, se hará un breve resumen de los filtros más comunes que se utilizan en procesamiento de señales y en electrónica de potencia.
2. **Principios del Convertidor:** Se estudiarán los principios que rigen en el convertidor, desde el funcionamiento y composición del inversor hasta los diversos filtros que son utilizados para cumplir el reglamento. En dicho bloque se analiza el comportamiento de cada parte que conforma el convertidor, derivando las ecuaciones y gráficas para conocer el funcionamiento. Además, se calcularán los componentes necesarios para poder llevar a cabo el proyecto, de acuerdo a criterios de diseño establecidos.
3. **Experimento:** Una vez se hayan diseñado todos los componentes necesarios para ejecutar el proyecto, es necesario comprobar en las simulaciones que se cumplen todas las normas

preestablecidas y que su funcionamiento sea el correcto. Una vez se haya verificado, se realizará un experimento físico.

Este proyecto está orientado a poder realizar una estación fotovoltaica con todos los acondicionamientos para su correcto funcionamiento. Esta es una pequeña contribución a lo que será un bien mayor, enfocado al progreso de la sociedad y al cuidado de nuestro planeta.

Palabras clave: Energía · Energía Solar · Panel Fotovoltaico · Planta Solar · CC-CA · Filtro · Modelado

Contents

Abstract	v
Resumen	vii
1. Introduction	1
2. State of Art	5
2.1. Power Converters	7
2.1.1. AC-to-DC Rectifiers	8
2.1.2. DC-to-DC	9
2.1.3. DC-to-AC Inverters	13
2.2. Filter	15
3. Principles	19
3.1. Inverter	19
3.2. PWM	21
3.3. Output Filter	24
3.3.1. Ideal LCL Filter	24
3.3.2. Damping Effect	30
3.4. Input Filter	32
3.4.1. Principles of Operation	32
3.4.2. Damping Effect	37
4. Components	39
4.1. LCL Filter	39
4.2. Input Filter	44
4.3. Inverter	46
5. Simulation	47
5.1. Simulation Environment	47
5.2. Simulated Results	48
6. Real Experiment	53
6.1. Real Circuit	53
6.2. Results	54
7. Future Steps	57
8. Conclusion	59
A. MOSFET	61
B. Electrolytic Capacitor	71
C. Ceramic Capacitor	75
References	77

List of Figures

Figure 2.1.	Representation and equivalent circuit of a solar cell.	6
Figure 2.2.	Comparison of the solar cell technologies with respect the efficiency through the years. From the National Renewable Energy Laboratory.	6
Figure 2.3.	Top solar producers.	8
Figure 2.4.	Single-phase half-wave passive rectifier.	9
Figure 2.5.	Single-phase full-wave active rectifier with an LC filter in an H-Bridge structure.	9
Figure 2.6.	Buck converter. Also known as step-down converter.	10
Figure 2.7.	Boost converter. Also known as step-up converter.	11
Figure 2.8.	Ideal Flyback converter.	12
Figure 2.9.	Model of an H-Bridge inverter using ideal switches.	13
Figure 2.10.	Diode-clamped three-level converter. Invented by Nabae in 1980.	15
Figure 2.11.	Low-pass first-order filter using a capacitor.	16
Figure 2.12.	Low-pass first-order filter using a capacitor.	16
Figure 2.13.	Low-pass first-order filter using an inductor.	17
Figure 2.14.	Band-pass filter using a capacitor and an inductor.	17
Figure 3.1.	Schematic of the system.	19
Figure 3.2.	Model of an H-Bridge inverter.	20
Figure 3.3.	Output of the inverter by changing the δ	20
Figure 3.4.	An operational amplifier can be used as an analogic method of producing a PWM signal.	21
Figure 3.5.	Illustration of how PWM naturally-sampled techniques work.	22
Figure 3.6.	Example of a PWM output waveform.	23
Figure 3.7.	H-Bridge Inverter connected to a DC-bus with voltage value of u_i and to an output.	23
Figure 3.8.	Current and voltage ratings of the MOSFETs.	24
Figure 3.9.	An LCL Filter without damping branch.	25
Figure 3.10.	High-pass third-order LCL filter connected to a resistor.	26
Figure 3.11.	Detail of the PWM, inductor and capacitor voltages.	26
Figure 3.12.	Illustration of an output voltage during T_s	27
Figure 3.13.	Different ripple factors depending on the modulation index and the modulation time.	29
Figure 3.14.	An LCL Filter without damping branch.	30
Figure 3.15.	Region where the damp should work.	32
Figure 3.16.	Filter labeled as a capacitor in parallel.	34
Figure 3.17.	Different ripple factors depending on the modulation index and the modulation time.	36
Figure 3.18.	Behavior of the capacitor filter and the source facing harmonic load.	37
Figure 3.19.	Input filter design with the damping resistor R_d in parallel with the inductance L_f	38

List of Figures

Figure 4.1.	Process of winding a coil for the inductor L_2 .	42
Figure 4.2.	Inductor L_2 finished.	43
Figure 4.3.	Model of a real capacitor.	44
Figure 4.4.	Equivalent model of a real capacitor.	44
Figure 5.1.	Simulation model of the system.	47
Figure 5.2.	Simulation model of the MOSFETs.	48
Figure 5.3.	Current of the inverter-side inductor and the detail of its ripple	48
Figure 5.4.	Current at the point of common coupling and its ripple.	49
Figure 5.5.	Voltage at the point of common coupling and its ripple.	49
Figure 5.6.	Voltage across the output filter capacitors.	50
Figure 5.7.	THD of the inverter-side and grid-side current and the capacitors' voltage.	50
Figure 5.8.	Current across the voltage source, i.e. PV system or battery.	51
Figure 5.9.	Voltage at the inverter's input.	52
Figure 6.1.	Real schematic of the converter.	53
Figure 6.2.	Parts of the real circuit.	54
Figure 6.3.	Real output waveform of the converter.	54
Figure 6.4.	Real voltage of the output capacitor.	55

1

Introduction

Energy is a lens through which we may view many important topics, economy, human development, or the environment. Decisions taken today will shape tomorrow's environment and society.

Since 1781 when a Scottish engineer James Watt built the first steam engine, a machine that produced a continuous rotatory motion using coal as the main fuel that drove it, the use of fossil fuels has been increasing. Throughout the years, the world's energy consumption has been increasing as well, reaching the 500 quads (quadrillion BTUs or British Thermal Units), in 2012. This trend is not going to change in the future; in fact, it will increase more. The United States consumes roughly 1/5 of this total energy; the electricity sector consumes the most, nearly 40%.

From an environmental perspective, electricity production is the main cause of the climate change. The primary fuel source is coal, followed by natural gas and nuclear power. Coal produces the most CO₂ emissions. In fact, electricity production contributes to 31% percent of the greenhouse gases, which are the main cause of the climate change.

From an economic point of view, although fossil fuel reserves are not going to run out, their cost of extraction will be sufficiently high that economies would not be able to afford them. In a non-renewable energy industry, not having access to these resources will cause a collapse in the economies. Of course, before this situation happens, different decisions and plans will be taken.

There are many alternatives available to face these issues. From a non-renewable point of view, the most promising solution is the use of nuclear energy due to its cost effectiveness. Although the nuclear raw materials reserves may run out sometime in the future, this will take a longer time to exhaust them. The amount of energy produced from a single pellet of uranium can be compared to the energy delivered by one ton of coal or three barrels of oil. It does not produce any greenhouse emissions that will accelerate the climate change, although a wrong disposal of radioactive material could lead to more catastrophic consequences. This is the main reason why nuclear power is not widely used.

With the non-renewable alternatives available, the most promising solution is renewable energies. From these, the most important ones, and the more developed ones, are related to wind power and solar photovoltaic generation. The first one is the main alternative to avoid the use of fossil fuels, and it contributes to a 10% of the total energy consumed in the United States. The second one is the main alternative in the future, before wind power, due to its low maintenance costs.

In wind power generation, the power of the wind is used to move the rotor blades, which at the same time move the rotor of an electrical generator that produces electric power. A brief overview of how electric machines work is explained in [1]. The principle of conversion of mechanical power into electrical power using rotatory machines lies in Galileo Ferraris' Theorem, which says that the magnetic field created by three inductors, separated 120° in space and fed with three sinusoidal currents separated 120° in time, generates a magnetic field with a constant magnitude that rotates at the fed frequency of the inductors, i.e. the electric frequency. However, the opposite is true. A rotatory magnetic field with a constant magnitude induces electric currents of the same value on the inductors and are separated 120° in time. Therefore, applying this principle to the rotatory machines of the wind turbines, they are able to generate an alternating current that goes to the grid. Unfortunately, this is not as easy as explained because the speed of the rotor is not always constant, nor the torque generated by the wind. An additional step must be added before giving power to the grid.

On the other hand, the solar energy harvested in photovoltaic panels does not require any kind of motion, so a different procedure must be used. The principle of transforming solar power into electric power is done by solar cells [2] and this involves theories of semiconductors. Considering a steady irradiation, also called solar power flux, a cell will produce a steady current and voltage value; this is, the outcome of a solar cell will be a direct current. Therefore, a photovoltaic solar power station cannot be connected directly to the grid.

Since the power station must be connected somehow to the grid, the use of power electronics is required, especially the use of devices that are able to transform DC into AC. These devices are called inverters. If they are transforming voltages, they are called voltage source inverters (VSI); otherwise, they are current source inverters (CSI). They use non-linear strategies for changing the polarity of a signal in order to obtain an alternating waveform. The way the alternating signal is created determines which strategy is better to use. It can be as simple as generating a square wave and as complex as generating a multi-level waveform. The main purposes of these converters is to generate a sinusoidal signal, which is the one used in the electric grid.

From all imaginable techniques, the most commonly used is called pulse width modulation (PWM), which will be explained in Section 3.2. Its principle lies in generating a series of pulses with a different width so the output resembles a sinusoidal wave after a filtering. Despite being more complex than generating a square wave, the harmonic load of this last one might create a distortion on the grid and a malfunction of devices. Moreover, within this modulation technique, there are other different kinds of strategies that work under the same principle. Among them, the one that produces less harmonic content is known as a unipolar naturally-sampled double-edge carrier [3], and this is why this technique will be used in this project.

However, the use of inverters is not sufficient for the purpose of connecting DC systems to the grid. Existing standards, such as IEEE Std 519-2014 [4], recommend the use of filtering to reduce, even more, the harmonic load. These filters can be active or passive [5]. In high-power transmission, passive filters are recommended over active ones due to their simplicity. In this project, an LCL filter is proposed. It gives good filtering at the same time that has a simple architecture. Moreover, since it has two inductors, it gives two degrees of freedom that can be used (1) to reduce the inverter-side ripple current, and (2) for reducing the harmonics that go into the grid to achieve the recommendations mentioned in IEEE Std 519-2014.

Another filter might be necessary for the same reason as before, to reduce the harmonic load. However, this time it will be placed in the DC side of the inverter. Due to high-frequency switching, harmonics generated by the inverter can affect the behavior of the DC components. If instead of a solar

panel what is connected is a DC source, this harmonics can affect its behavior. In case of a solar panel, these harmonics can disturb the solar cells, causing serious damage to them. For this reason, an input filter is placed between the inverter and the solar panel (or voltage source). In this project, an LC filter is proposed. A DC Link capacitor is required when converting DC into AC, as described in [6] and in Section 3.4 in this project. However, an inductor will be placed to remove the high-frequency harmonics that go downstream to the solar panel. The use of this filter is preferred among more complex and effective filters, such as another LCL, because the capacitor will handle the most important harmonics, so the use of another inductor would be unnecessary.

For a good understanding of these principles, a DC-AC converter will be built, with its respective filters and modulation technique, as stated before, in order to demonstrate the knowledge acquired while doing this project. Simulations of this project will be done as well.

2

State of Art

Solar energy aims to be one of the energy resources of the future. Among different techniques of harvesting this energy resource, the most promising one is the use of photovoltaic solar plants. In this system, the power that comes from the sun is transformed directly into electric energy.

The principles of this conversion lie in the theory of semiconductors. A semiconductor is a material which can change its properties from being a conductor to an insulator, depending on state conditions. The properties can be altered with the addition of impurities, which is called “doping”, into the crystal structure. If a different element is added to it and creates what are called free holes, the material of that part is called p-type, due to the more positive load; on the other hand, if a region contains free electrons, it is called n-type. When these two regions are placed together, the semiconductor junction is created. They are responsible for how the device works, allowing current in one direction but blocking it in the other direction. These means that ideally, a semiconductor behaves as a short-circuit and as an open-circuit, depending on the conditions. These materials are found in many devices, such as diodes or transistors, which are the most important components in power electronics and electronics in general.

The properties of semiconductors can be applied to solar-to-electricity power conversion. They are placed in what is called a solar or photovoltaic solar cells which can change their voltage, current, or resistance when they are exposed to light. The absorption of light excites the electrons of the material until they escape from their atomic orbits, generating a free hole. The gap is replaced with neighboring electrons. This movement of electrons in the semiconductor material produces an electric current, which is collected in the electrodes of the solar cell, which carries them into the electric circuit.

Although this phenomenon produces a DC current, since it uses semiconductors, it also generates a voltage caused by a voltage drop in a diode. Besides, since it is not ideal, a pair of resistors must be added. Thus, a solar cell can be labelled as shown in Fig. 2.1. Where R_S is the series resistor and R_{SH} the shunt resistor, given by the junction voltage, of the solar cell.

Solar cell technologies have been changing throughout the years. In Fig. 2.2 we can see different of them and their evolution along the years. The current maximum efficiency is reached with multijunction cells, which improves the absorption of different wavelengths of light. With a single junction cell, the theoretical maximum efficiency is up to 33.16%, while with this new technology it can get up to 86.8% [7], both under highly concentrated sunlight. Solar cells are not 100% efficient in part because

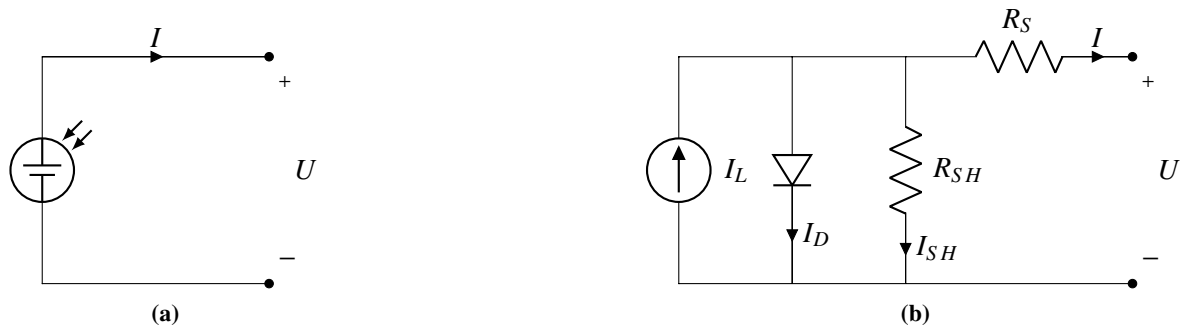


Figure 2.1. Representation and equivalent circuit of a solar cell.

some of the light that goes into the solar panel is reflected; another part is not powerful enough to generate electricity (infrared) or it creates heat instead of electricity, as in the case of ultraviolet light.

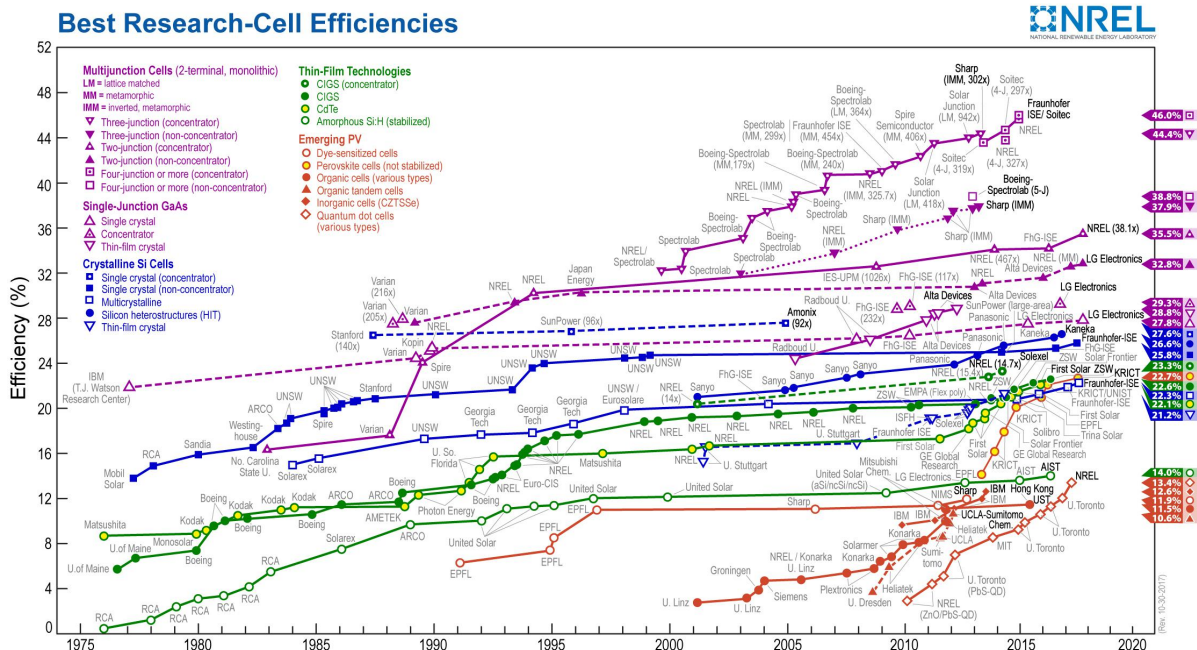


Figure 2.2. Comparison of the solar cell technologies with respect the efficiency through the years. From the National Renewable Energy Laboratory.

The voltage produced by a solar cell is not sufficiently high to be connected to a circuit; besides, the maximum power delivered is not too high. For that reason, solar cells are grouped together forming solar arrays, which at the same time are grouped, creating solar panels. These groups can be made in two different ways. If the solar cells are connected in series, the total voltage of the system will be the sum of each of them. On the other hand, if they are connected in parallel, the total current will be the sum of each current. This idea can be used when grouping solar arrays, and so with solar panels.

The behavior of a solar cell is explained using an $i-u$ curve, which describes the voltage that a solar cell supplies with respect the current provided. The shape of the curves is subjected to the income irradiation and the temperature of the solar cell. The lower the temperature, the greater the admissible voltage, and the higher the irradiation, the higher the current.

If the current is maximum, there is not any voltage and viceversa. This means that at those points the solar cell is not giving any power to the system. Once voltage or current shifts from those positions, the system starts to generate power. There is a point where voltage and current give the maximum

power, the maximum power point (MPP). A solar cell has one of these points in all conditions. There are power converters, which are connected to a group of solar panels, that seek that point, they are DC–DC converters using a modulation technique known as maximum power point tracker (MPPT). The technique that these converters use permits to obtain the maximum power under all conditions.

With this technique, there are many different methods [8], [9] whose their objective is to find the maximum point. The most well known are:

- Perturbation and observation (P&O) [10], [11]: the converter changes the voltage of the array in small quantities. If the power increases it keeps going until the power begins to decrease. At that point, the maximum power is reached.
- Hill climbing [12], [13]: it follows a similar procedure as with P&O; however, instead of perturbing the operation voltage, the duty ratio is modified.
- Incremental conductance [14]: the controller measures the incremental variation of the current and voltage when this last one varies, for predicting the effect of a voltage change.

Although these are the main methods, there are others such as short–circuit current, open–circuit voltage and ripple correlation.

The photovoltaic effect first was discovered in 1839 by the French physicist Alexandre-Edmond Becquerel, however, the first solar cell was built in 1883 when Charles Fritts created the first semiconductor that could work under the experiments. The studies done by Nikola Tesla, Michael Faraday, James Clerk Maxwell about the electromagnetic induction and waves, and electric forces helped to the development of this new technology. The most important contribution came by the hand of Albert Einstein in which stated the bases of the photoelectric effect, the fundament of solar–to–electricity conversion.

After different attempts, in 1946 an American engineer Russel Ohl patented the first modern solar cell, which had an efficiency of 0.5%. The first solar cell that was created with commercial purposes was released in 1954 when the American scientists Gerald Pearson, Calvin S. Fuller and Daryl Chapin, from Nokia Bell Laboratory, accidentally discovered a junction that was highly sensitive to light. This new technology reached an efficiency of a 6%. Between the years 1954 and 1960 Hoffman Electronics achieved an efficiency of 14%.

One of the first applications in real life was during the space race. The new satellites incorporated solar panels in order to produce self–sufficient energy instead of short–life batteries. Due to their extreme success, governments invested in development and research of these devices.

The overall solar capacity today has reached 175 GW and it follows the distribution given in Fig. 2.3.

We can see the need of recent emergent countries for obtaining new and sustainable forms of energy.

However, since solar panels only work in DC, it is impossible to connect them directly to the grid. Here again, the use of power electronics is required to solve this problem.

2.1. Power Converters

As mentioned at the beginning of this chapter, the discovery of semiconductors materials has marked an era in the history of electronics. These materials have been utilized to create devices such as diodes,

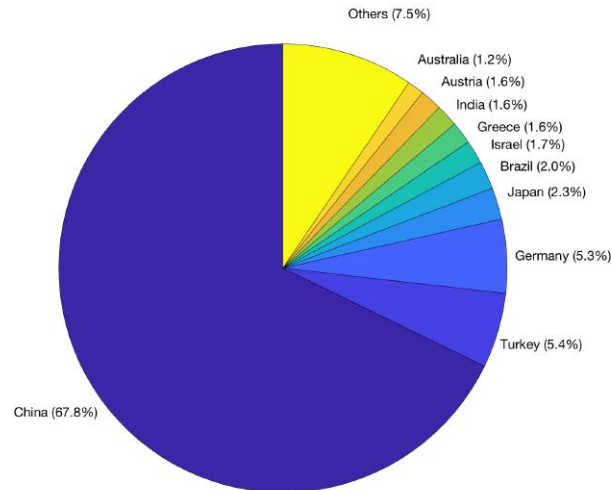


Figure 2.3. Top solar producers.

thyristors and transistors, besides integrated circuits, which among different applications in electronics, they can provide a switching effect.

Linear components are elements that when a signal goes through them, the output is another signal at the same frequency but that could have different magnitude and different phase shift. A clear example of these kind of components in electronics are capacitors, inductances and resistors. Due to their linear nature, they cannot be used alone in power conversion that relates DC with AC. This is why non-linear devices, such as the ones mentioned before, are very important in power electronics. They allow relating DC to AC and vice-versa and DC to DC. And this is the main reason why the study of power electronics is very important when studying about solar power plants because they permit the conversion between the DC power provided by the solar panels into AC power that is used in the grid.

2.1.1. AC-to-DC. Rectifiers

The first mechanism that used power electronics was developed in 1902 by Peter Cooper Hewitt, who invented the first rectifier which permitted the conversion from AC to DC. Although the components he used are not in use anymore, nowadays the rectifier can be labelled with diodes, if it is a passive rectifier, or with thyristors, if it is an active rectifier. In this last case, different components such as transistors can be used as well. An example of a simple rectifier is shown in Fig. 2.4. Besides of the composition, the difference between active and passive rectifiers lies under voltage regulation. While diodes, ideally, always conducts when V_D is greater than 0 or a current is flowing across them, thyristors and transistors may not conduct under those conditions. They need an external signal to be activated. These suppose an advantage with respect to common diodes because they permit voltage regulation.

Rectifiers are AC-to-DC converters and consider the first devices that allowed the transmission of power between two different electric natures. There are more complex topologies about rectifiers involving single-phase AC. The next level brings a full-wave rectification, where all the input-wave during a period is rectified. These principles can be applied to three-phase AC, in which the output will be more steady.

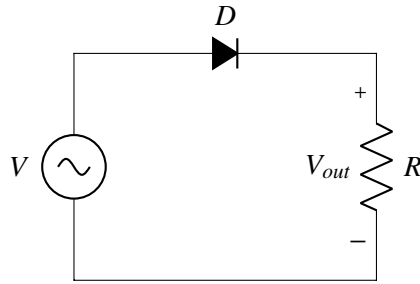


Figure 2.4. Single-phase half-wave passive rectifier.

Moreover, rectifiers come with a filter that makes the output smoother. Fig. 2.5 shows an active rectifier with an LC output filter. The capacitor is used to keep the voltage constant and the inductor to provide a more steady current. In this case, there is no-need of using a free-wheeling diode for preventing a drop in the inductor's current.

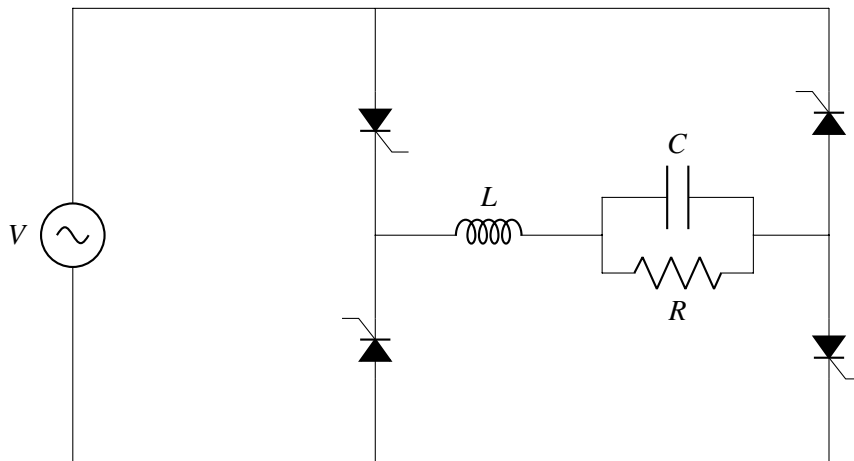


Figure 2.5. Single-phase full-wave active rectifier with an LC filter in an H-Bridge structure.

In the case of Fig. 2.5, if we obtain the average output voltage of the rectifier, the mathematical expression will be

$$V_{out} = \frac{2V}{\pi} \cos \alpha \quad (2.1)$$

where α can go from 0 to π radians. This variable α is the gate signal of the SCR. We can see that if it is equal to $\pi/2$ there rectifier is not working at all. The normal behavior of this kind of converters happens when $\alpha \in [0, \pi/2)$, and this is what is known as rectification. Nevertheless, if $\alpha \in (\pi/2, \pi]$, the average voltage of the output becomes negative. This phenomenon is called inversion, and it is very important for transforming DC-AC.

2.1.2. DC-to-DC

The main purpose of a rectifier is to transform electric power from AC to DC. With the use of active elements it can regulate the output voltage, nevertheless, this can only decrease the output with respect the input, but never increase it. Besides, it involves a low power factor. A possible solution might be to place a transformer before the rectifier for achieving the desired output. Because this is not cost-effective, the main purpose of DC-DC converters is to increase or decrease the voltage in DC very efficiently. This transformation requires the use of switching devices, again, semiconductors.

In contradiction to DC, the use of AC permits to change the voltage of a circuit while conserving the power using linear elements. This is done by the already mentioned transformer. Its operation is based on an induction phenomenon where a coil induces an electric current into another coil which shares the same magnetic core. The cores are usually made of iron or ferrite, otherwise, the power transfer might be more difficult. Being N_1 the number of turns of the first winding and N_2 the number turns of the second winding, the relation between both voltages using a transformer is,

$$\frac{V_2}{V_1} = \frac{N_2}{N_1} \quad (2.2)$$

Since the power transferred must be conserved,

$$\frac{I_2}{I_1} = \frac{N_1}{N_2} \quad (2.3)$$

As mentioned before, this is only possible because of the electromagnetic induction. Using Faraday-Lenz's Law, where Φ is the magnetic flux,

$$\varepsilon = -\frac{d\Phi}{dt} \quad (2.4)$$

We can see from Eq. 2.4 that an electromotive force can be only created if the flux is varying with respect the time. Therefore, since in DC systems de magnetic flux remains steady, any voltage can be induced. This means that a transformer does not work in DC systems, at least not for the moment.

In DC, the use of non-linear active elements are required to achieve the same purpose that transformer [15]. However, the use of linear-elements that are able to store energy are required as well. These are capacitors and inductors. In fact, without them, the converter would not work properly. And schematic of how a converter looks like is shown in Fig. 2.6.

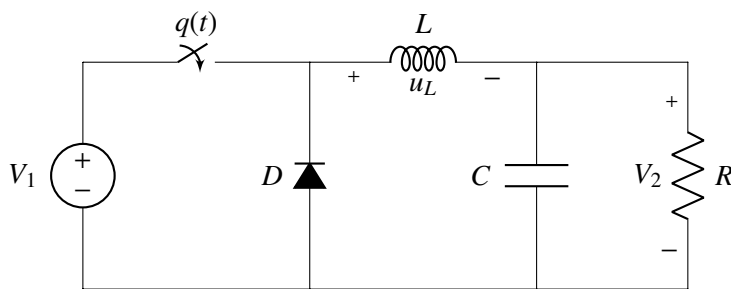


Figure 2.6. Buck converter. Also known as step-down converter.

The switches will work at a switching frequency. In periodic-steady-state, the time when $q(t) = 1$ will be DT_s , where D is named as duty ratio. Since we are in periodic-steady-state, the average voltage across the inductor has to be equal to 0. Looking to the states of the circuit depending on the switch state.

- If $0 < t < DT_s$:

$$u_L = V_1 - V_2 \quad (2.5)$$

- If $DT_s < t < T_s$:

$$u_L = -V_2 \quad (2.6)$$

Doing $\langle u_L \rangle = 0$, the relation between voltages is given by,

$$\frac{V_2}{V_1} = D \quad (2.7)$$

And since the energy must be conserved,

$$\frac{I_2}{I_1} = \frac{1}{D} \quad (2.8)$$

This converter is called Step-down because it decreases the output voltage. However, it does not give any solution if we want to increase it. A different topology must be used to accomplish it, in this case, the new circuit will be as shown in Fig. 2.7,

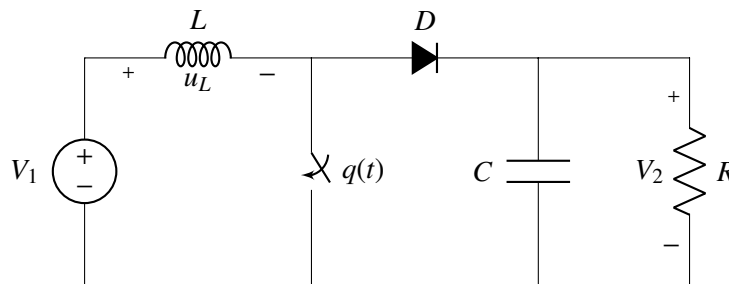


Figure 2.7. Boost converter. Also known as step-up converter.

Doing a similar analysis as before, we get,

$$\frac{V_2}{V_1} = \frac{1}{1 - D} \quad (2.9)$$

$$\frac{I_2}{I_1} = 1 - D \quad (2.10)$$

With this kind of converter, we can increase the voltage, as so with transformers. However, these are two different topologies for two different things, while in a transformer by changing the relation between the number of turns the output voltage can increase or decrease. This can be fixed with the use of more complex converters, such as, the Buck-Boost Converter [15].

All the converters mentioned until this moment does not provide any kind of insulation between the input and the output. It is very important, especially using solar panels, to isolate them, otherwise, they could suffer serious damages when facing a fault or when a malfunctioning of the systems generates an income stream of power. There are existing DC-to-DC converters that provide insulation by using a transformer. Beside providing isolation, this transformer can also help to change the magnitude of the voltage. However, it may require complex circuits due to the leakage inductor, in which its energy will be delivered to the input or released into a resistor with the use of an active or passive clamped-circuit respectively. An example of an isolated DC-to-DC converter is shown in Fig. 2.8,

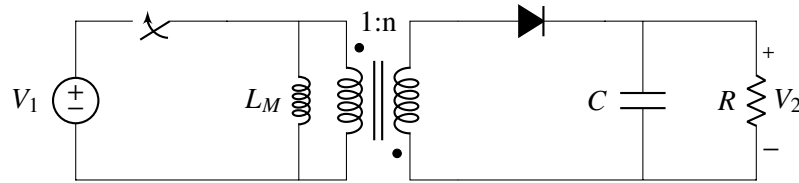


Figure 2.8. Ideal Flyback converter.

In this converter, the magnetic inductor is in charge of storing the energy that the output will need, consequently, the converter does not need any other inductor. Using the same method as before, but in this case with the magnetic inductor of the transformer,

$$\frac{V_2}{V_1} = \frac{nD}{1-D} \quad (2.11)$$

$$\frac{I_2}{I_1} = \frac{1-D}{nD} \quad (2.12)$$

Flyback converters are commonly used in photovoltaic solar plants due to the characteristics mentioned before, insulation of the parts of the converter, upstream and downstream, and the increment of voltage.

DC-to-DC converters can be divided in two groups. The first group are direct converters, in which the input is directly connected to the output, or by an inductor, sometime during the switching period. In this case all the power is given by the source directly. Examples of this are the ones shown in Fig. 2.6 and Fig. 2.7. The second group are indirect converters, in which the input is never connected to the output. In this converters the energy is stored in the inductors as magnetic energy. For this reason the core must have an air-gap. Examples of this kind of converter are the Buck-Boost mentioned before and the one in Fig. 2.8.

Moreover, DC-DC converters have two modes of operation. The first mode is continuous conduction mode (CCM) where the current across the inductor never stops flowing. In this mode the relation between variables are the ones shown before in every converter. The other mode is named as discontinuous conduction mode (DCM). Here, the current across the inductor stops flowing. Although it might be more difficult to get the equations, it is true that this mode presents many advantages. In the case of a Boost converter, the output voltage will increase more for the same duty ratio. The new relation between voltages will be,

$$\frac{V_2}{V_1} = \frac{1}{2} + \frac{\sqrt{1 + \frac{2DRT}{L}}}{2} \quad (2.13)$$

These are only some examples of DC-DC converters, but we can see how powerful non-linear elements can be. Moreover, they show how complex DC-DC conversion can be with respect to the use of a transformer in AC lines. Nevertheless, this kind of converters has several advantages that a transformer does not have. For example, a transformer that works at 50–60 Hz of main frequencies would be large heavy when transferring few watts. It means that they need a big magnetic core which will turn into bigger losses due to eddy currents and winding resistors. On the other hand, since these converters work at high-frequency, the size of inductors and capacitors is reduce considerably, which makes them being more economic and space-efficient.

2.1.3. DC-to-AC. Inverters

This is the last step into AC-to-AC transmission involving a DC transition. The main purpose of an inverter is to transform DC power into AC. If for AC-to-DC we needed the use of non-linear elements, in this conversion we will need to use them as well. In fact, they must be active elements since we will have to control their duty ratios. As shown in (2.1), depending on the gate signal, these active elements, used in an H-Bridge in this case and shown in Fig. 2.9, can work in rectification or inversion modes. For this purpose, they will work in inversion.

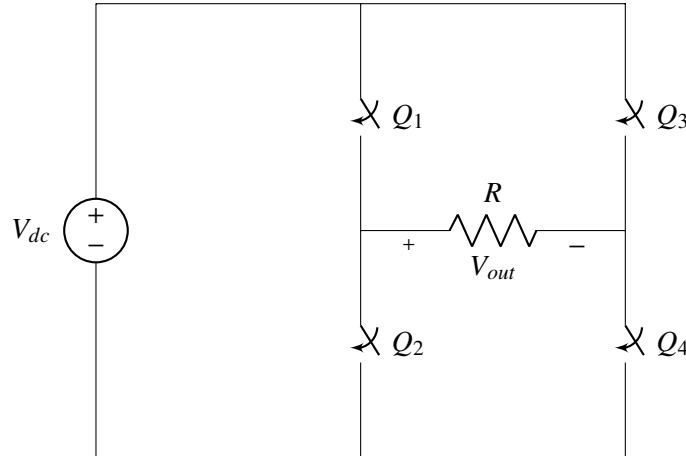


Figure 2.9. Model of an H-Bridge inverter using ideal switches.

The use of power electronics is not necessarily required for a DC-AC power transmission. From the late 19th century to the middle of the 20th century DC-AC conversion was accomplished with the use of rotatory machines and motor generators. Nowadays this method is used as well by coupling a DC machine to an AC by a shaft being this last machine connected to the grid. The output is a three-phase sinusoidal waveform. Although it has many advantages, theoretically the output must be a pure sine-wave, it takes a lot of space and it is not necessarily efficient. For places where the space is a limited resource, such as an aircraft, the use of inverters is required.

Inverters can generate many different waveforms. The simplest one is the square waveform, which is used when using low-sensitive devices. However, if the purpose of the inverter is to transform the power into the grid, the use of this kind of wave is unsuitable. Existing regulations and standards, the most known is [4], does not allow the conversion to AC using a square wave by saying that for total harmonic distortion (THD) of the output must be less or equal to an 8%. Applying Fourier Series and the definition of THD,

$$V_n = \frac{2}{n\pi} (1 - (-1)^n) \text{ for } n \in \mathbb{N} \quad (2.14)$$

$$\text{THD} = \frac{\sqrt{\sum_{n=2}^{\infty} V_n^2}}{V_1} \quad (2.15)$$

In the case of an square wave, the THD is approximately 45%, which is far away from the permitted.

For avoiding this issue, a possible solution could be the addition of a filter which will reduce the harmonic content with the use, in this case, of linear elements. Other filters might use non-linear ones. Although this topic will be mentioned later in the future, the main problem of using a filter resides on the size of the filtering elements. Thus, a problem of size and, consequently, greater losses comes again.

There are two possible solutions:

1. To reduce the magnitude of the harmonics, this will affect the type of inverter used.
2. To push the frequency of the harmonics to the right as much as possible, so the size of the filter is reduced. This will bring different modulation techniques.

The most known modulation technique is named as Pulse Width Modulation (PWM) and presented later when talking about how the inverter works. The basis of this technique is to compare a reference signal with respect a carrier signal. This last one usually is a triangular or sawtooth wave-form. The resulting output waveform will be a train of pulses with value V_{dc} but with different width each of them.

In a PWM technique, there are two main objectives in order to have an adequate output waveform [3]. First, we have to determine the converter switch ON times in order to generate the desired output waveform. Second, it determines the most effective way of switching to minimize unwanted harmonic distortion.

There are many alternatives to obtain the switch ON times; however, only three of them have been successfully proved. These are:

1. Calculating the times looking at the intersection of a reference and a carrier waveform (naturally sampled PWM).
2. Switching at the intersection between a regularly sampled reference and a carrier waveform (regular sampled PWM).
3. Switching so that the integrated area of the target reference waveform over the carrier interval is the same as the integrated area of the converter switched output (direct PWM).

Sinusoidal PWM modulation is the most typical used [16] and it was first introduced 1964 by Schoung and Stemmler [17]. Depending on the modulation, we can have two-level (bipolar) or three-level (unipolar) PWM. The results of a PWM will be presented in the future. When using PWM techniques, the magnitude of the harmonics does not depend on the switching frequency, but their frequency does.

Another kind of modulation is the Space Vector PWM which was introduced in the mid-1980's [18]. In SVPWM the three-phase variables are expressed in space vectors, that were first introduced by the female engineer Edith Clarke [19] and which was improved by Park [20] and Kron [21]. This is based on the fact that every three-phase system can be expressed in 3 different orthogonal axes $\alpha\beta\gamma$, or dqo in some literature. In an equilibrated system, the last component is 0, due to is referred to the homopolar components. By analyzing which are the reactions that the other two components make to each other, this PWM generates the switch ON times that are required. This kind in modulation is widely used in the vectorial control of electric drives because allows knowing the dynamic response of the machine.

The other alternative to reduce harmonic load and, therefore, the size of the filter is by using multi-level converters. While using a PWM the output does not look like a sine wave, in this type of converters the shape of the output looks more similar to it. The higher the number of levels, the more similar will be, so the magnitude will be reduced and some harmonics will be cancelled. An example of how a multi-level converter looks like is shown in Fig. 2.10

The use of multi-level inverters reduce the switch voltage stress. However, the use of this converters is not exclusive for using PWM. There are existing converters that use both techniques combined.

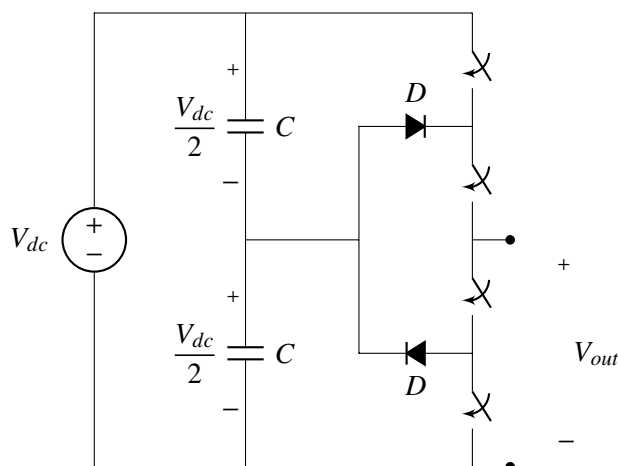


Figure 2.10. Diode-clamped three-level converter. Invented by Nabae in 1980.

As said before, the use of inverters is required when space is limited. The Little Box Challenge was an open competition powered by Google and IEEE and awarded with \$1,000,000 where research groups developed power inverters as small as possible. The prototypes had to be at most 820 cm^3 and a rated power of 2 kVA. Besides many other specifications that must achieve, researchers from the University of Illinois at Urbana-Champaign achieved a 2 kVA inverter in 152 cm^3 [22]. This shows how powerful and useful Power Electronics is, especially in renewable energy.

Inverters are widely used today, not only for renewable energy. One of the main uses of inverters has to be with electric drives in which the speed of the electric machine varies. In this case, the speed control is bounded to a voltage control, otherwise, the magnetic core saturates or the torque decreases. Related to drives, inverters are also used when transferring power from an AC generator to the AC grid. Although it may sound redundant, they are used to connect both systems to the same frequency, due to the frequency of the generator may not be the same as the grid. A perfect example of this phenomenon happens in wind turbines, where the wind does not blow the same and makes a variation in the rotor speed.

They are also used when connecting two grids that have different frequencies, typically 50 Hz and 60 Hz grids. In this case, the power transfer requires a complex topology and an operation of a rectifier and a DC-DC converter in some cases. Nevertheless, some devices convert AC to AC directly without the use of a DC-to-DC step.

This kind of topologies where the use of different converters is required are also present in HVDC systems, which stands for High Voltage DC. As mentioned before, power lines usually operate in AC, however, in long distances they may be inefficient, and this has to be with the frequency the line pulsates. In a 60 Hz system that distance is around 5000 km. Beyond that distance, the use of a DC power line is recommended. For this reason, an AC-to-DC converts the power, a DC-DC elevates the voltage to a high level. At the end of the line another DC-DC decreases the voltage and then a DC-AC inverter transforms the power into AC.

2.2. Filter

Despite PWM techniques or multilevel converters, the use of filters is required as well. They can be active or passive filters, although in high-power transmission the passive ones are more used. Passive filters are made up of linear elements, such as inductors, capacitors and resistors. The simplest filters using capacitors are shown in Fig. 2.11 and Fig. 2.12,

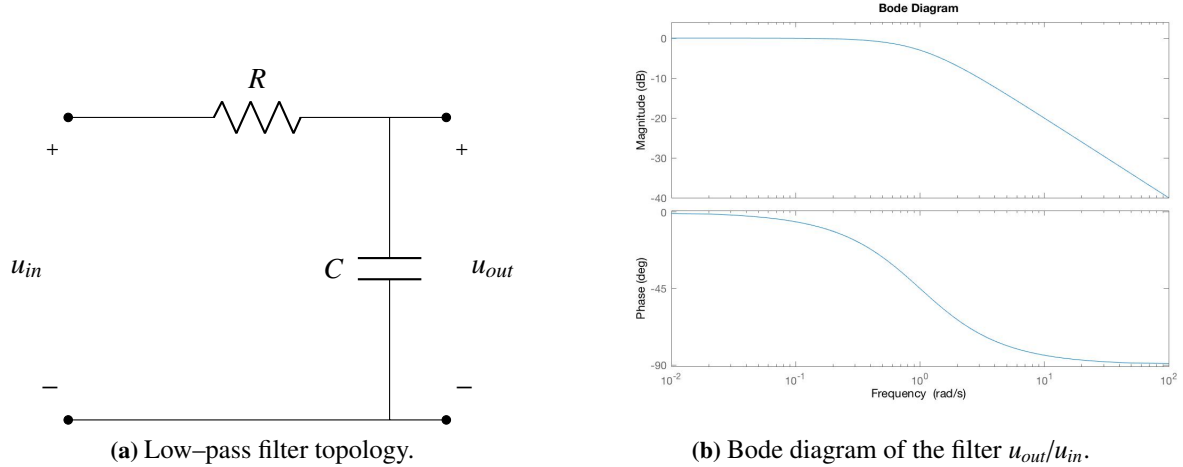


Figure 2.11. Low-pass first-order filter using a capacitor.

In the case of a low-pass filter we can see that high-frequency harmonics are reduced by 20 dB per decade from the cut-off frequency, which depends on the time constant $\tau = RC$. There other topologies depending on the effective use of linear elements where this reduction can be done faster. Using, for example, an inductor and a capacitor, what is known as LC filter [23], the reduction becomes 40 dB per decade. Nevertheless, high-order circuits have a resonant frequency where the gain becomes infinite. Therefore, a damping resistor must be added. The higher the order, the more reduced the harmonics are.

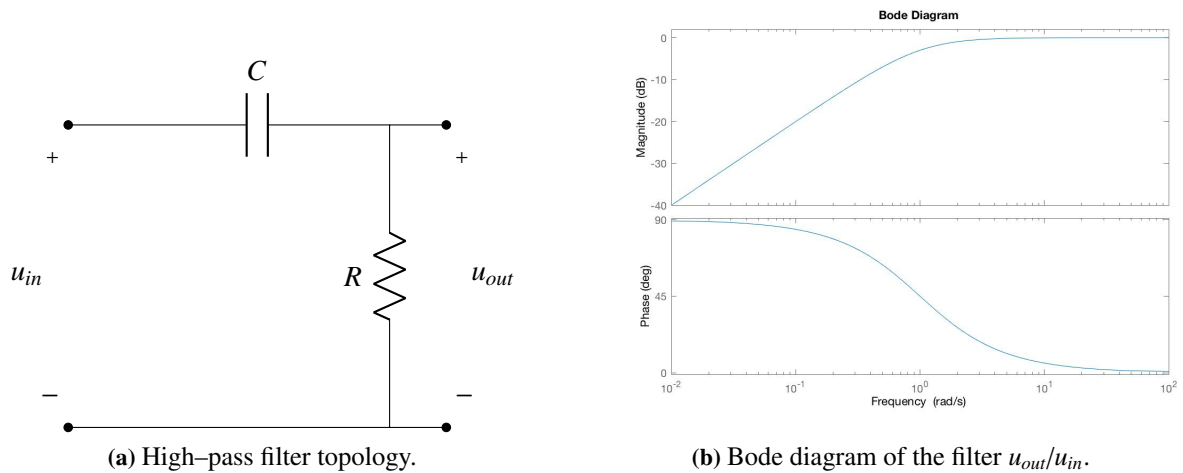


Figure 2.12. Low-pass first-order filter using a capacitor.

In the case of a low-pass filter we can see that high-frequency harmonics are reduced by 20 dB per decade from the cut-off frequency, which depends on the time constant $\tau = RC$. There other topologies depending on the effective use of linear elements where this reduction can be done faster. Using, for example, an inductor and a capacitor, what is known as LC filter [23], the reduction becomes 40 dB per decade. Nevertheless, high-order circuits have a resonant frequency where the gain becomes infinite. Therefore, a damping resistor must be added. The higher the order, the more reduced the harmonics are.

Filters are widely used in different fields related to electronics, from signal processing to power transfer. The first power filters used were placing an inductor between the inverter and the grid as shown

in Fig. 2.13. This is because, commonly, a transformer was used, and its leakage inductance was used as filter. In this case, the grid has been substituted by a resistor, applying the Substitution Theorem and assuming a unity power factor.

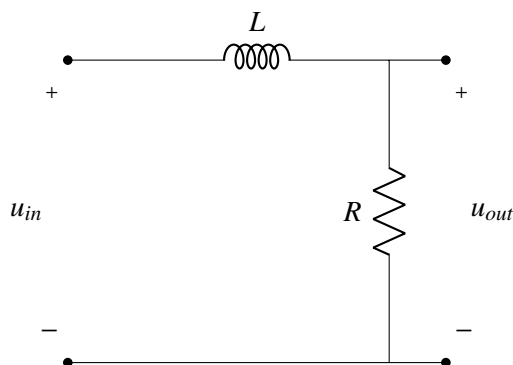


Figure 2.13. Low-pass first-order filter using an inductor.

In DC-to-AC high-power conversion the use of high-order filters is needed. The most common filter is an LCL [24], [25], [26], [27], which are two inductors and a capacitor connected in parallel. It is like an LC filter but with another inductor. This provides a reduction of 60 dB per decade. This filter is chosen among different options because it provides an effective filtering at the same time that the size of the components is reduced. With the use of the two inductors, we can manage the input-ripple while with the other is designed to achieve the regulations.

The behavior of the filter is the same as the one shown in Fig. 2.11. The main problem with this filter is that in order to achieve all the constraints and recommendations [4] the inductor size will be huge and this is translated as high voltage drop and high losses.

There many other filters that are used in power transmission. These filters are designed to reduce all the harmonics that are not at the desired frequency, it could be high-frequency or low-frequency harmonics. This is accomplished with an inductor and a capacitor placed in parallel. The opposite also works, this means that it can also reduce the desire harmonic without reducing the rest of them. An example of this can be seen in Fig 2.14.

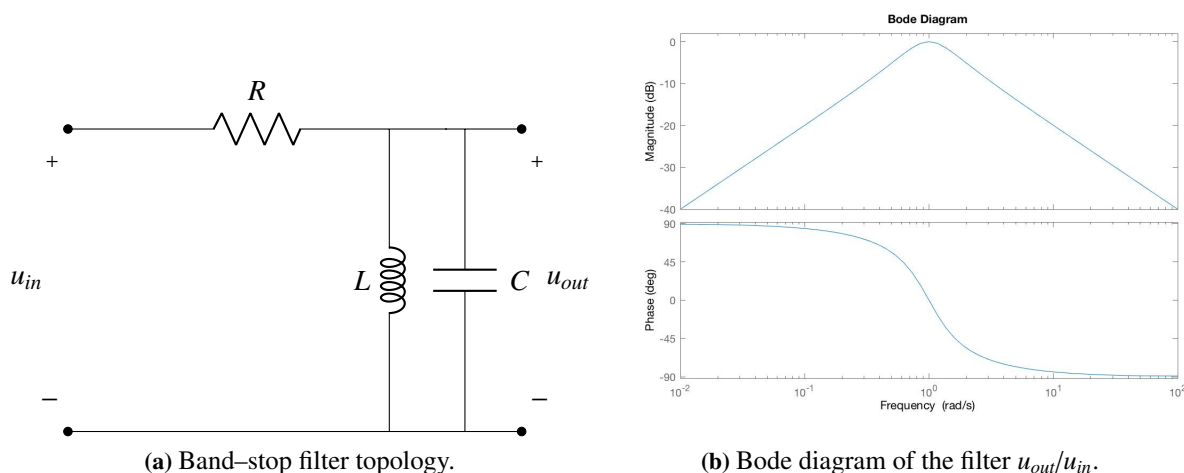


Figure 2.14. Band-pass filter using a capacitor and an inductor.

3

Principles

The main purpose of this chapter is to fully understand how this converter will work, from the input-filter to the output-filter going through the inverter. A schematic of the system is shown in Fig. 3.1. The parts that are going to be studied in this project are related to the DC-Link capacitor and the DC-to-AC transmission.

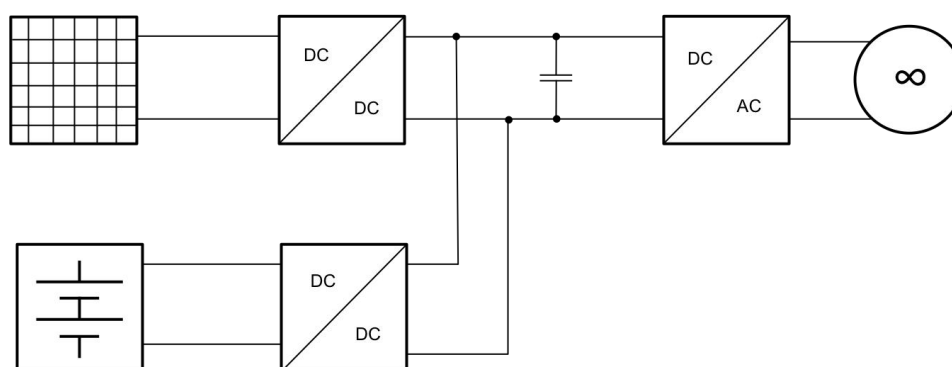


Figure 3.1. Schematic of the system.

3.1. Inverter

The purpose of an inverter, and the purpose of the whole project, is to generate an alternating wave that comes from a DC signal. For this reason, the use of an H-Bridge converter, as it can be seen in Fig. 3.2, is preferred among different architectures.

The main objectives of an inverter technique are:

1. Calculate the converter switch ON times which create the desired (low-frequency) target output voltage or current.
2. Determine the most effective way of minimizing the harmonic distortion.

Starting from the basics of this converter, the first thing to know is that the switches on a same leg cannot be conducting at the same time, otherwise the DC voltage source would be shorted. Being $q(t)$ the driving signal, this can be written as follow,

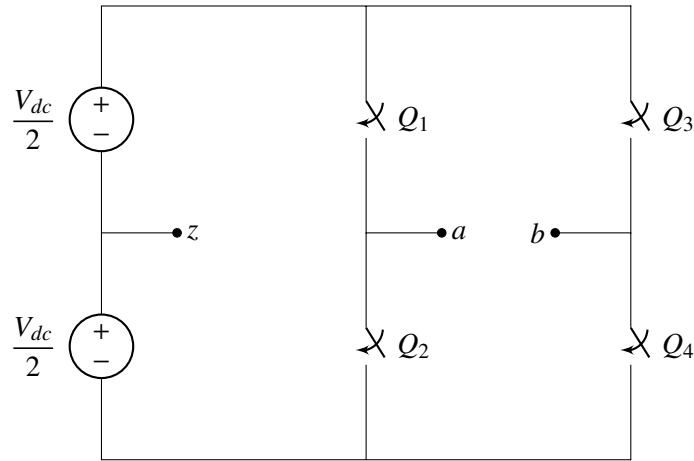


Figure 3.2. Model of an H-Bridge inverter.

$$q_1(t) + q_2(t) = 1$$

$$q_3(t) + q_4(t) = 1$$

Where $q(t) \in \{0, 1\}$. Moreover, if $q_i(t) + q_j(t) \leq 1$ it could happen that both switches are open, this will mean that the node is a floating point, which is undesirable.

Making the following choices,

n	Q_1	Q_2	Q_3	Q_4	U_{ab}
1	1	0	1	0	0
2	1	0	0	1	V_{dc}
3	0	1	0	1	0
4	0	1	1	0	$-V_{dc}$

The choices selected generates an output that looks like Fig. 3.3.

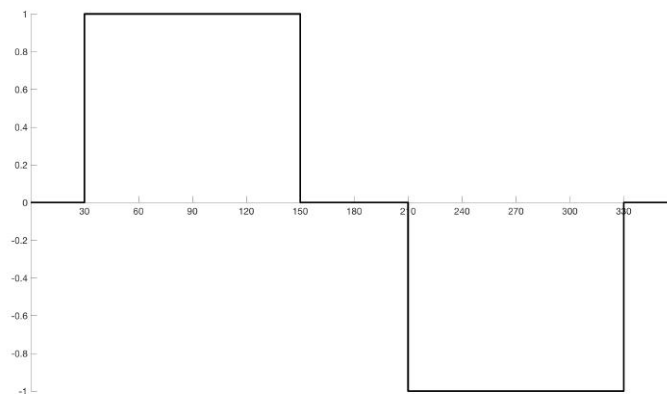


Figure 3.3. Output of the inverter by changing the δ .

Using the Fourier Series, the output voltage can be expressed as,

$$U_{ab} = \sum_{n=1}^{\infty} a_n \cos n\omega_o t + b_n \sin n\omega_o t \quad (3.1)$$

Since in this case the output is an odd wave with half-wave symmetry, their coefficients will be,

$$a_n = 0$$

$$b_n = \frac{2V_{dc}}{n\pi} \cos n\delta (1 - (-1)^n)$$

We can see that by changing the angle δ , i.e. the time where U_{ab} is equal to 0, some harmonics are cancelled. For example, if $\delta = \pi/6$, the third harmonic will be removed. A disadvantage of this method is that the power that can be transferred is less than if $\delta = 0$. Moreover, other harmonics may increase. Since the purpose of this project is to generate a sinusoidal wave, this idea will be taken in Section 3.2, but with some variations.

3.2. PWM

There are more powerful techniques for generating a wave with less harmonic content. These techniques are based on how the switches are modulated. For this explanation, the use of a comparator is required,

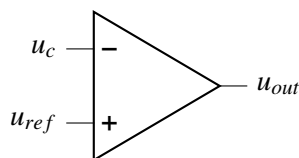


Figure 3.4. An operational amplifier can be used as an analogic method of producing a PWM signal.

Where u_c is the carrier wave, in which in this project is a triangular wave with frequency f_s that goes from 0 to 1, and a reference waveform. The purpose of this comparator is that the output of the comparator will be the gate input $u_{out} = q(t)$. Moreover, the duty ratio of the switches can be written as $d = u_{ref}$. If the reference wave is a sinusoidal wave with an amplitude of M , a frequency of f_o and an offset of $1/2$,

$$d = \frac{1}{2} + M \sin \omega_o t \quad (3.2)$$

Where M varies from 0 to $1/2$. This method is called pulse width modulation (PWM).

This theory can be applied to the four switches. There are different techniques of modulation and they are explained in [3].

In this project the technique used will be a unipolar sine-triangle asymmetrical double-edge carrier. A visual illustration of how it works is shown in Fig. 3.5. This means that the the reference and the carrier waveforms are as said before, besides, both legs will be modulated and the output waveform will have three levels. Mathematically it can be expressed as,

$$Q_1 : d_1(t) = \frac{1}{2} + M \sin \omega_o t$$

$$Q_2 : q_2(t) = \bar{q}_1(t)$$

$$Q_3 : d_3(t) = \frac{1}{2} - M \sin \omega_o t$$

$$Q_4 : q_4(t) = \bar{q}_3(t)$$

Coming back to Fig. 3.2, and looking to a leg,

- During $t = [0, d_1 T]$,

$$U_{az} = V_{dc}$$

- During $t = [d_1 T, T]$,

$$U_{az} = -V_{dc}$$

And the average voltage will be,

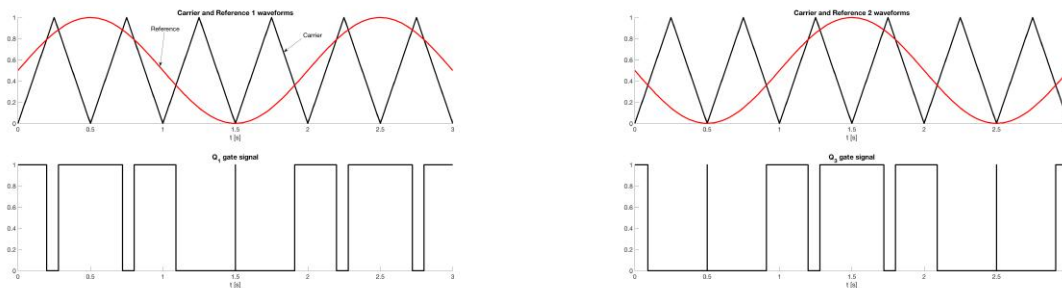
$$\bar{V}_{az} = \frac{V_{dc}}{2}(d_1) - \frac{V_{dc}}{2}(1 - d_1) = V_{dc}(d_1 - \frac{1}{2})$$

Doing the proper thing in case of b leg,

$$\bar{V}_{bz} = \frac{V_{dc}}{2}(d_3) - \frac{V_{dc}}{2}(1 - d_3) = V_{dc}(d_3 - \frac{1}{2})$$

The average voltage at the output will be $\bar{V}_{ab} = \bar{V}_{az} - \bar{V}_{bz}$,

$$\bar{V}_{ab} = V_{dc}(d_1 - d_3) = 2V_{dc}M \sin \omega_o t \quad (3.3)$$



(a) Regarding to Q_1 and Q_2 . The gate signal shown is q_1 and \bar{q}_2 .

(b) Regarding to Q_3 and Q_4 . The gate signal shown is q_3 and \bar{q}_4 .

Figure 3.5. Illustration of how PWM naturally-sampled techniques work.

Although this gives the average voltage of the output in a certain period of time, this does not give how the output will be. Using the Double Fourier Series described in [3],

$$u_{PWM}(t) = 2V_{dc}M \sin(\omega_o t) + \sum_{k=1}^{\infty} \sum_{n=-\infty}^{\infty} \frac{2V_{dc}J_{2n-1}(2k\pi M)}{k\pi} \cos([m+n-1]\pi) \sin(2k\omega_s t + [2n-1]\omega_o t) \quad (3.4)$$

Where J is the Bessel Function and can be expressed as $J_n(x) = \frac{1}{\pi} \int_0^{\pi} \cos(n\pi - x \sin \tau) d\tau$. This corresponds to the technique selected before.

As can be seen in (3.4), this technique gives the desired fundamental component but also generates sideband harmonics of the carrier frequency. From now, the carrier frequency will be named as switching frequency f_s . An output example of a PWM signal is shown in Fig. 3.6. From this figure we can see the different width of the pulses, and the maximum width remains in the middle of them, because there is where the value of the sinusoidal is maximum.

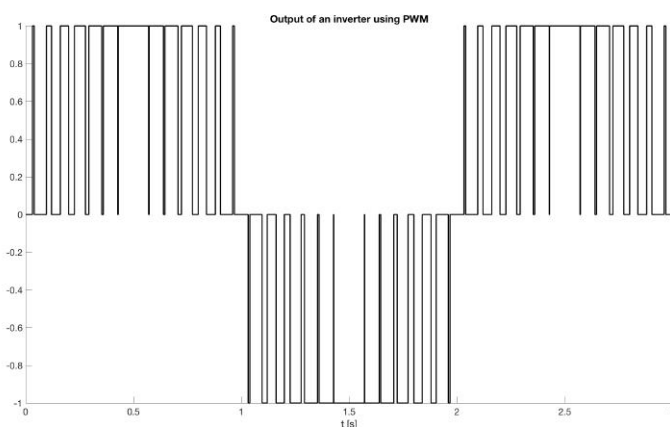


Figure 3.6. Example of a PWM output waveform.

Ideally, Q_1 , Q_2 , Q_3 and Q_4 are non-loss switches. However, in real life, they are not. In this project, they will be replaced by MOSFETs. The behavior of this converter will remain the same. The architecture of the inverter is shown in Fig. 3.7.

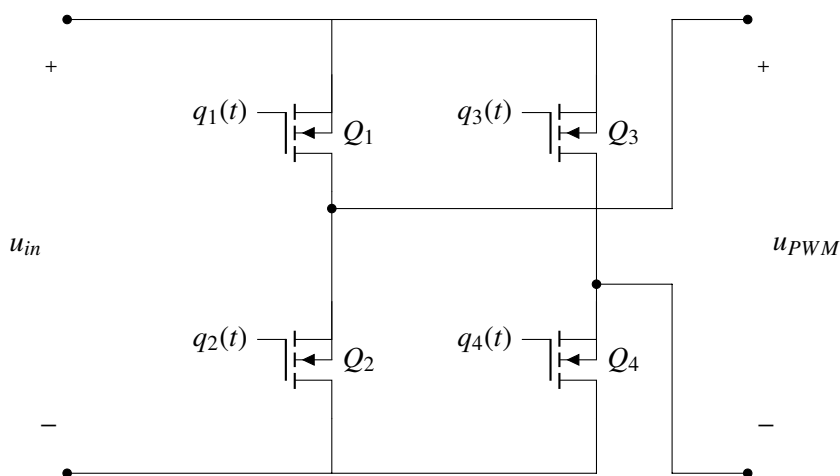


Figure 3.7. H-Bridge Inverter connected to a DC-bus with voltage value of u_i and to an output.

As non-ideal elements, it is required to know their current and voltage ratings.

If $q_1(t) = 1$ and $q_3(t) = 0$,

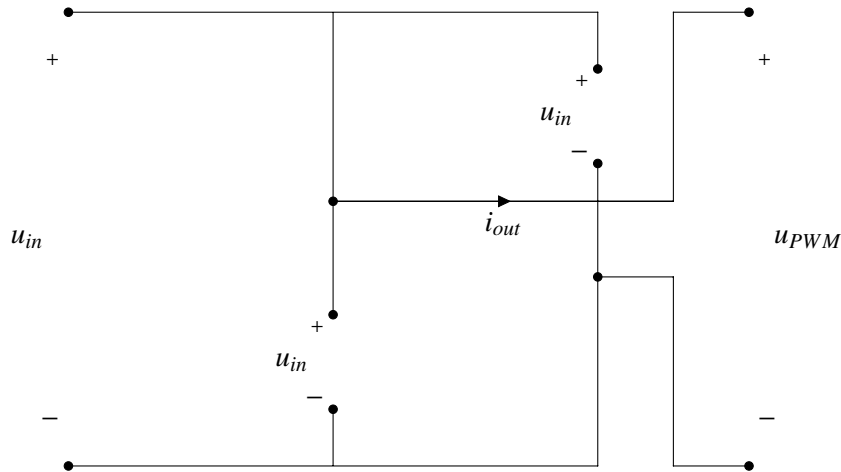


Figure 3.8. Current and voltage ratings of the MOSFETs.

From Fig. 3.8, the voltage and current ratings of the MOSFETs are,

$$I_{MOSFET} = i_{out} \quad (3.5)$$

$$U_{MOSFET} = u_{out} \quad (3.6)$$

Where i_{out} and u_{out} will be discussed in the future.

3.3. Output Filter

The goal of the design is to ensure high quality of grid current as well as to minimize the size of the filter magnetics. In general, the size of inductors is greater than capacitors.

Most of the criteria selected come from [24] and [26], that refer specifically to LCL filters with some variations and for different purposes as discussed here. However, in those, the iteration process does not follow any minimization or optimal criteria. To consider those, other articles such as [25] or [27] have been used.

According to IEEE 1547.2–2008 [28], it is reasonable to suppose that the grid can be considered as a source with infinite power, so the equivalent impedance can be neglected. This also means that the current that goes across it only has one harmonic, the fundamental component.

3.3.1. Ideal LCL Filter

First, a pure LCL filter, as shown in Fig. 3.9 without a damping branch is considered. This step is crucial in the making of the filter because it will follow criteria that are aimed only at filtering. Once the passive components are calculated, the damping resistor will be included.

The Bode diagram of this filter is shown in Fig. 3.10. Unlike a simple first-order filter that can be seen in Fig. 2.13, the reduction of the magnitude of harmonics is higher than in an L-filter, moreover, the phase-shift is also affected by it. In this case, it goes from 0 to 270°. Also, we can see a resonance peak that varies depending on the values of the components of the filter.

The criteria used is the following,

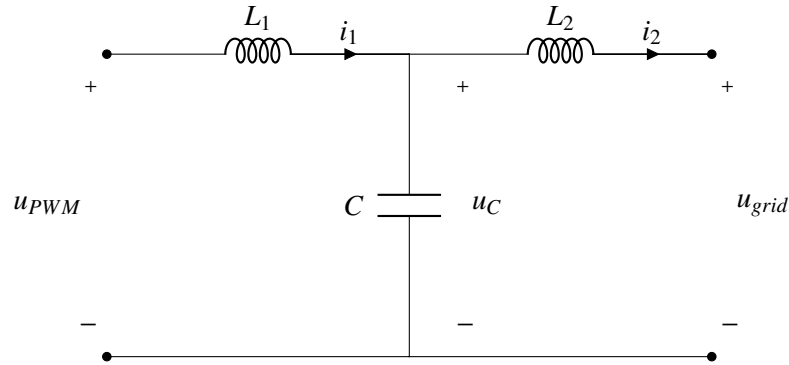


Figure 3.9. An LCL Filter without damping branch.

1. Due to the inductances that the filter has, the capacitor value is limited to decrease the amount of reactive power generated. In this project, the maximum will be set to 3% of the rated power of the converter, although this value can reach the 5% in some cases. Another way of calculating the capacitor is proposed in [29]. In this article, the capacitance is established by the current that goes across the capacitor instead of the reactive power that it is generating. Nevertheless, with normalized units these two processes are equivalent.
2. The maximum voltage drop in the filter must be 5% of the rated voltage. Since the current across the capacitor can be neglected (as stated before), this voltage drop depends on the total inductor L . This is $L = L_1 + L_2$. The lower limit depends on the inverter high-frequency harmonics specifications defined by IEEE 519–2014 standard and that is presented below in 5. It has been discussed in many articles, as [30] and [31], that regarding to stability reasons, L_1 must be greater than L_2 .
3. The value of the ripple of the inverter-side inductor is typically lower than 40%. However, it may not be a good option to reduce it as much as possible because it can involve an enormous value of inductance.
4. The resonance frequency must be greater or equal than ten times the fundamental frequency and at most a half of the switching frequency. This is made to ensure that the resonance frequency is not located at any harmonic frequency generated by the inverter. Although the filter must be damped, this is a common action taken for security reasons.
5. According to the standard mentioned before, if the short-circuit current on the grid-side of the filter is 20 times the rated current, harmonics higher than the 35th must be limited to a 0.3%. Moreover, the THD at the common coupling point must be lower than 5%.

Based on these conditions, the filter can be designed according to the following procedure

1. For the inverter side inductor,

$$0.15 \leq \Delta i_1 \leq 0.4$$

If the current ripple increases, the inductance required is lower, and therefore, the size of L_1 will be lower $L \propto A_c / I_c$. To derive the expression that allows calculate this ripple, knowing how the inverter works is required.

From the equations derived in (3.2), the period of time when the switches are operating is known.

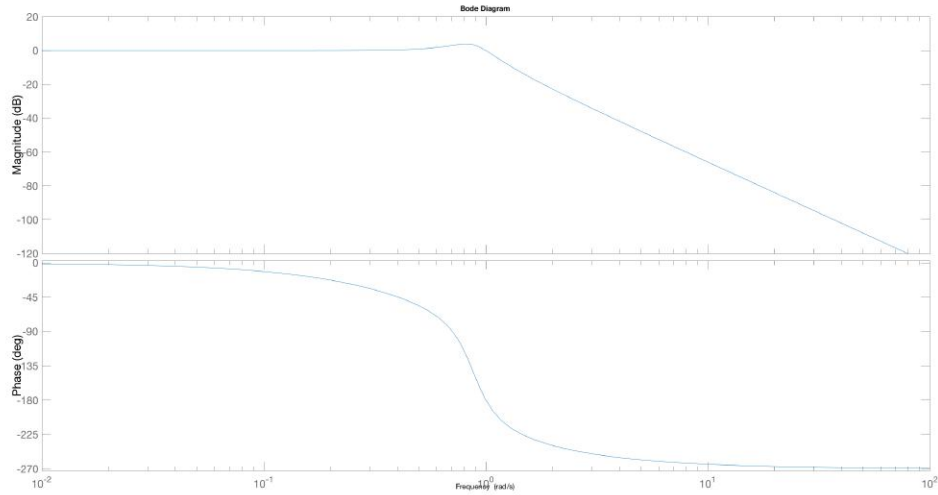


Figure 3.10. High-pass third-order LCL filter connected to a resistor.

$$d_1 = \frac{1}{2} + M \sin \omega_o t$$

$$d_3 = \frac{1}{2} - M \sin \omega_o t$$

The inductor fundamental equation is also required since the objective is to calculate the voltage ripple. So, it can be written as,

$$u_L = L \frac{di_L}{dt} \tag{3.7}$$

$$\frac{u_L}{L} = \frac{di_L}{dt} \tag{3.8}$$

Being u_L as shown in Fig. 3.11,

$$u_L = u_{PWM} - u_C \tag{3.9}$$

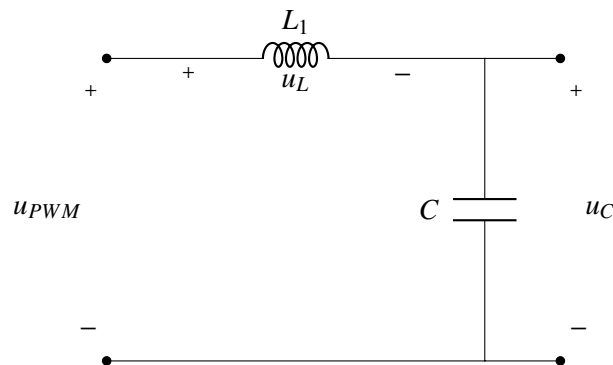


Figure 3.11. Detail of the PWM, inductor and capacitor voltages.

It is not trivial to calculate the voltage of the inductor in a certain period of time because the values of the variables will be changing with the fundamental frequency f_0 . However, since this calculation is focused on the ripple caused by the switching frequency, at $T_s = 1/f_s$, it can be assumed that the width of the pulses caused by the modulation remain the same during certain periods T_s , as shown in Fig. 3.12, because $f_s \gg f_0$. This assumption is only valid at the switching domain where the sinusoidal reference almost does not change.

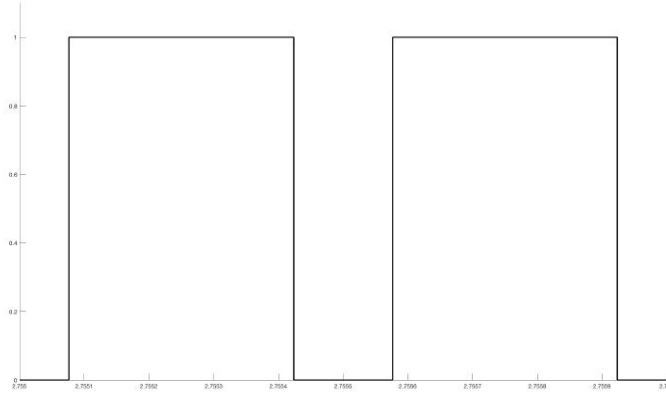


Figure 3.12. Illustration of an output voltage during T_s .

If the pulses have the same width and knowing that the average voltage across an inductor has to be equal to zero, $\langle u_L \rangle = 0$,

$$\langle u_{PWM} \rangle = \langle u_L \rangle + \langle u_C \rangle \rightarrow \langle u_{PWM} \rangle = \langle u_C \rangle \quad (3.10)$$

Therefore, and as derived in (3.3), the average voltage of the capacitor at the switching frequency follows this expression,

$$U_C = \langle u_C \rangle = 2V_{dc}M \sin \omega_o t \quad (3.11)$$

Once this value is achieved, and knowing that the value of the pulse given by the inverter is constant, and so is U_C during T_s since the voltage across the capacitor cannot change sharply, the current ripple can be calculated. Again, under the assumption that f_s is much higher than f_0 .

$$\Delta i_L = \frac{V_{dc}(1 - 2M \sin \omega_o t)T_{on}}{L} \quad (3.12)$$

It can be seen from Fig. 3.12 that during a switching period, there are two pulses instead of one. This is all because of the double-edge modulation and this means that the harmonics generated are multiples of two times the switching frequency. Therefore, half of the period can be taken for this analysis.

$$T_{on} = (d_1 - d_3) \frac{T_s}{2} = \frac{d_1 - d_3}{2f_s}$$

$$d_1 = \frac{1}{2} + M \sin \omega_o t$$

$$d_3 = \frac{1}{2} - M \sin \omega_o t$$

And therefore, it can be said that,

$$T_{on} = \frac{M \sin \omega_o t}{f_s} \quad (3.13)$$

Using Equations (3.12) and (3.13),

$$\Delta i_L = \frac{V_{dc}}{Lf_s} M(1 - 2M \sin \omega_o t) \sin \omega_o t \quad (3.14)$$

That can be written as,

$$\Delta i_L = \frac{V_{dc}}{Lf_s} R_p(M, t) \quad (3.15)$$

Where $R_p(M, t) = M(1 - 2M \sin \omega_o t) \sin \omega_o t$.

Taking derivatives with respect the time t and M to analyze where is the maximum ripple, we get that,

$$\frac{\partial \Delta i_L}{\partial M} = 0 \rightarrow M = \frac{1}{4 \sin \omega_o t} \quad (3.16)$$

$$\frac{\partial \Delta i_L}{\partial t} = 0 \rightarrow \sin \omega_o t = \frac{1}{4M} \quad (3.17)$$

These provide the same solution, so substituting this value in (3.15),

$$\Delta i_L = \frac{1}{8} \frac{V_{dc}}{Lf_s} \quad (3.18)$$

From Fig. 3.13 we can see how the maximum ripple changes with respect the modulation index M and the modulation time. In each case the maximum ripple coefficient is 1/8.

2. For the capacitor, r is defined as the amount of reactive power generated. In real units, it can be established as,

$$C = \frac{r \cdot P_n}{U_n^2 \omega_o} \quad (3.19)$$

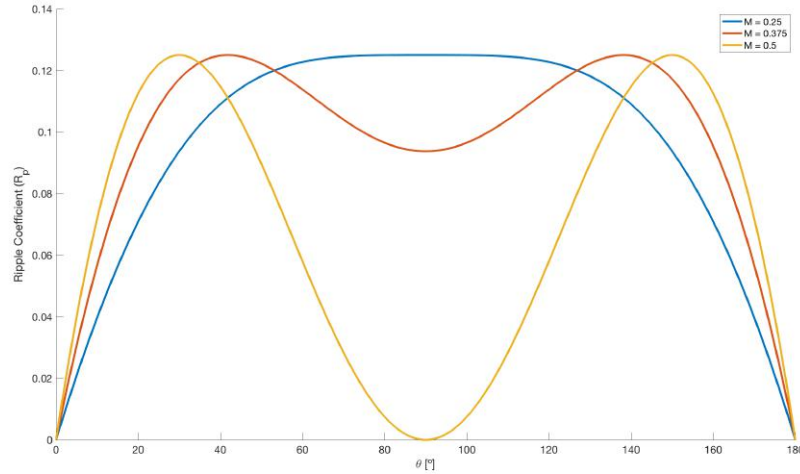


Figure 3.13. Different ripple factors depending on the modulation index and the modulation time.

3. L_2 depends on the attenuation of the switching harmonics. The value of this harmonics can be calculated using (3.4) and considering that the converter is operating under the condition of unipolar, sine–triangle and asymmetrical naturally–sampled PWM. Then,

$$U_h(n, k) = \left| \frac{2V_{dc} J_{2n-1}(k\pi M)}{k\pi} \cos([m + n - 1]\pi) \right| \quad (3.20)$$

Using normalized units and according to the standard mentioned before and [26], which says that the harmonic load that goes into grid should be less or equal than 0.3% of the rated fundamental current.

$$\frac{2u_{dc} \cdot \max(|J_n(k\pi M)|) \cdot F'_{21}(s)_{s \rightarrow j\omega^*}}{k\pi} \leq 0.3\% \quad (3.21)$$

In which,

$$\omega^* = 2k\omega_s + [2n - 1]\omega_o \quad (3.22)$$

$$F_{21}(s) = \frac{I_2(s)}{U_1(s)} = \frac{1}{s(CL_1L_2s^2 + L_1 + L_2)} \quad (3.23)$$

And F'_{21} is the same transfer function but with normalized units.

4. Once all the parameters are calculated, all the constraints must be satisfied. Otherwise the iteration method must start again, by changing the absorbed reactive power or the inverter–side inductor ripple. These constraints are ¹,

$$10\omega_o \leq \omega_r = \sqrt{\frac{L_1 + L_2}{CL_1L_2}} \leq \frac{\omega_s}{2} \quad (3.24)$$

$$l_t = l_1 + l_2 \leq 0.05 \quad (3.25)$$

¹Notice the difference between real and normalized units.

3.3.2. Damping Effect

For attenuating as much as possible a resonance caused by the LCL power filter, a damping branch must be added. There are different ways for an effective damp, such as passive or active damping. The simplest and cheapest way is using a passive damping method, however, sometimes it might be difficult to get low power losses and an effective damp. Nevertheless, this method is the one used the most, generally when high-power transfer is required. The new circuit will result as shown in Fig. 3.14.

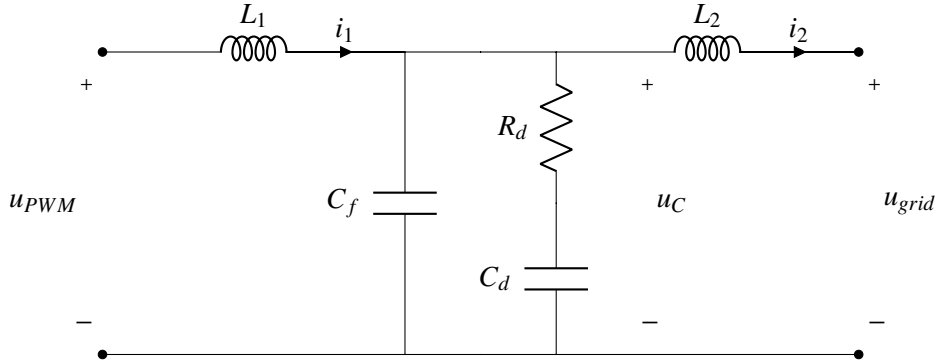


Figure 3.14. An LCL Filter without damping branch.

In this project, the value of the capacitor C will be split into two capacitors according to [25] and [32], otherwise, the requirements given above would not be satisfied. From now on, regarding the output filter, there are going to be two capacitors named as C_f and C_d , that are related as follow,

$$\begin{aligned} C_f + C_d &= C \\ C_d &= nC_f \end{aligned}$$

C_f will be the capacitor in charge of filtering, still C_d will be used for filtering the output, but it will have in series a resistor aimed to reduce the damp. This damping branch is called the R_d-C_d branch.

The addition of the R_d-C_d branch changes the system, so the transfer function described in Eq. (3.23) does not represent the system when the frequency is around the resonance frequency ω_r . The new transfer function that involves $I_2(s)$ and $U_1(s)$ can be expressed now as,

$$G_{21}(s) = \frac{I_2(s)}{U_1(s)} = \frac{R_d C_d s + 1}{s(L_1 L_2 R_d C_f C_d s^3 + L_1 L_2 (C_d + C_f) s^2 + R_d C_d (L_1 + L_2) s + L_1 + L_2)} \quad (3.26)$$

Now, calculating the resonance frequency is not easy, since there are more terms than the ones before, however, ω_r can be enclosed into an interval that is calculated by changing the value of the damping resistor from 0 to ∞ .

If $R_d \rightarrow 0$

$$\omega_{r_{min}} = \sqrt{\frac{L_1 + L_2}{L_1 L_2 (C_f + C_d)}} \quad (3.27)$$

And, if $R_d \rightarrow \infty$

$$\omega_{r_{max}} = \sqrt{\frac{L_1 + L_2}{L_1 L_2 C_f}} \quad (3.28)$$

In both cases the system is undamped.

If L_c is defined as $L_c = \frac{L_1 L_2}{L_1 + L_2}$, the characteristic impedance can be defined as,

$$Z_c = \sqrt{\frac{L_c}{C_f + C_d}}$$

And the quality factor (Q) as,

$$Q = \frac{R_d}{Z_c}$$

Somewhere in between the $\omega_{r_{min}}$ and $\omega_{r_{max}}$ the resonance frequency may be optimal and this is achieved by making $Q = Q_{opt}$. After many considerations described in [27], it is finally given that,

$$Q_{opt} = \sqrt{\frac{(5n + 4)(n + 2)(n + 1)}{2n^2(4 - n)}} \text{ for } n \in (0, 1.3] \quad (3.29)$$

Another consideration regarding to the damping branch is that it should work in an interval around the resonance frequency, while it should not work in any other situation. The effect of the capacitors must be eliminated during this interval. Looking at the impedance made of the R_d - C_d and C_f branches,

$$Z_p = \frac{R_d C_d s + 1}{(R_d C_d C_f s + C_d + C_f) s}$$

The two frequencies where the effects of the capacitor are cancelled are during the frequencies below,

$$\omega_z = \frac{1}{R_d C_d} = \frac{n + 1}{n R_d C}$$

$$\omega_p = \frac{C_d + C_f}{R_d C_d C_f} = \frac{(n + 1)^2}{n R_d C}$$

And it is derived that,

$$\omega_z \leq \omega_r \leq \omega_p \quad (3.30)$$

From the (3.27), (3.28) and (3.30), the rule of selecting the resistance R_d is taken as,

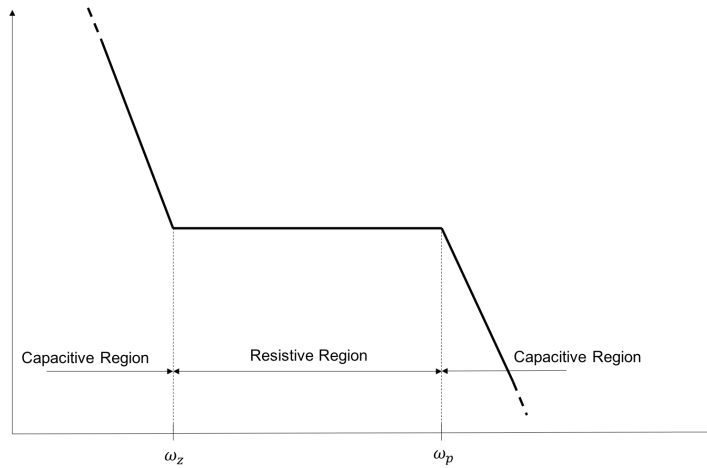


Figure 3.15. Region where the damp should work.

$$\frac{1}{R_d C_d} \leq \omega_{r_{min}} \quad (3.31)$$

$$\frac{C_d + C_f}{R_d C_d C_f} \geq \omega_{r_{max}} \quad (3.32)$$

Both, combined, establish the interval of a possible value of R_d .

$$\frac{\sqrt{n+1}}{n} \sqrt{\frac{L_c}{C_f}} \leq R_d \leq \frac{n+1}{n} \sqrt{\frac{L_c}{C_f}} \quad (3.33)$$

In case of variation in the parameters, if R_d does not meet (3.33), an increase in the value of n or L_2 might be needed.

Another consideration regarding this kind of damping is that by increasing $\frac{C_d}{C_f}$, and therefore n , the damping effect improves. On the other side, this improvement brings greater losses in the damping resistor. Thus, probably a good alternative that is discussed in [32] is to set C_f equal to C_d . By doing this, the damping effect and damping losses are balanced.

3.4. Input Filter

The DC part of the converter requires the use of an input filter in order to filter all the possible non-DC noise that can affect the operation of the batteries or solar panel. In the theory, what is commonly used is a DC link capacitor. This is because we have to satisfy the conservation of energy between two ports [6], in this case the DC source and the AC port, that can be labeled as an AC source.

3.4.1. Principles of Operation

The size of the capacitor cannot be chosen arbitrarily, it must be chosen regarding design parameters in order to maintain, mainly, a steady DC voltage. The process is described below.

The power provided by the DC source is equal to

$$P_{dc} = U_{dc} I_{dc} \quad (3.34)$$

The AC port has a time-varying power flow that can be written as

$$\begin{aligned} p_{ac}(t) &= u_{ac}(t)i_{ac}(t) \\ u_{ac}(t) &= U_{out} \sin(\omega_o t + \psi_u) \\ i_{ac}(t) &= I_{out} \sin(\omega_o t + \psi_i) \end{aligned}$$

Where U_{out} and I_{out} are the amplitudes of the first harmonic at the fundamental frequency and $U_{out} = 2 \cdot M \cdot U_{dc}$. M is the modulation index. Doing some trigonometrics,

$$p_{ac}(t) = \frac{U_{out}I_{out}}{2} \cos(\psi_u - \psi_i) - \frac{U_{out}I_{out}}{2} \cos(2\omega_o t - (\psi_u - \psi_i)) \quad (3.35)$$

In this analysis, a unity power factor is assumed. This makes $\psi_i = \psi_u$,

$$p_{ac}(t) = \frac{U_{out}I_{out}}{2} - \frac{U_{out}I_{out}}{2} \cos 2\omega_o t$$

$$\text{If } P_1 = \frac{U_{out}I_{out}}{2}$$

$$p_{ac}(t) = P_1 - P_1 \cos 2\omega_o t \quad (3.36)$$

P_1 can be seen as the mean value of the power generated by the fundamental component.

Regarding to the input side, and as mentioned in [33],

$$i_{in} = I_{dc} + \tilde{i} + \Delta i \quad (3.37)$$

$$u_{in} = u_c = U_{dc} + \tilde{u} + \Delta u \quad (3.38)$$

Where I_{dc} and U_{dc} are the DC components, \tilde{i} and \tilde{u}_c are the double-frequency fundamental component that are caused by the AC system at the output, and Δi and Δu are the components caused by the switching frequency caused by the inverter. The main problem about a ripple in the voltage is that it produces a ripple in the power.

Using the conservation of energy and neglecting the input/output harmonics,

$$p_{in}(t) = p_{ac}(t)$$

$$U_{dc}(I_{dc} + \tilde{i}) = P_1 - P_1 \cos 2\omega_o t$$

$$U_{dc}I_{dc} + U_{dc}\tilde{i} = P_1 - P_1 \cos 2\omega_o t \quad (3.39)$$

Since I_{dc} is the direct current and \tilde{i} the alternating one, the equation can be divided looking at the different components of the power. In the case of the DC component and looking to the voltage amplitude of the fundamental component at (3.4),

$$P_{dc} = P_1$$

$$I_{dc} = \frac{2M \cdot I_1}{2} = MI_1 \quad (3.40)$$

And in the case of the alternating component,

$$\tilde{i}_c = -MI_1 \cos 2\omega_o t \quad (3.41)$$

Despite the output current of the converter has an angular frequency of ω_o as the fundamental component, the current on the other side has two times this angular frequency.

At this point where both components of the input current i_{in} are calculated, it is time to get a look at them. The DC source can only provide a steady power flow since its voltage is ideally fixed to a DC value. However, someone must give the alternating power that the output-side requires.

There are different kind of solutions to this problem, it can be solved using passive and active filters. In this project, a passive filter will be used. So, the problem described above can be accomplished by placing a capacitor in parallel with the inverter and the DC source, as shown in Fig. 3.16.

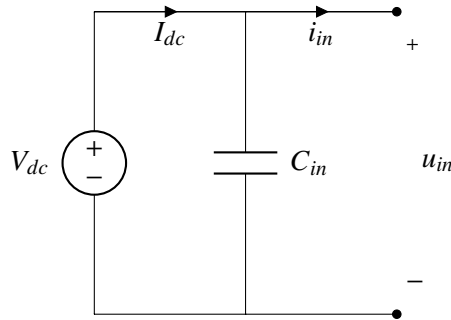


Figure 3.16. Filter labeled as a capacitor in parallel.

Once the DC and alternating current are derived, the next component that must be calculated is the current ripple caused by high frequency harmonics.

$$\begin{aligned} \bar{i} &= I_{dc} + \tilde{i}_c = MI_1(1 - \cos 2\omega_o t) = 2M \cdot I_1 \sin^2 \omega_o t \\ \Delta i &= i_{in} - \bar{i} = I_1 \sin \omega_o t(1 - 2M \sin \omega_o t) \end{aligned} \quad (3.42)$$

Once all the current components have been calculated, it is the turn for the voltage ones. However, a consideration has to be made. With a relatively large capacitance, the voltage at the DC side can be considered as constant. The main problem is that a double-frequency alternating power must be caused by an alternating current, and consequently an alternating voltage that contradicts what it is said before.

Nevertheless, there is a solution to this complication, this can be fixed by using a coupled inductor filter, which is described in [34].

Considering the capacitor's voltage and being $p_c(t)$ the power provided by the capacitor,

$$p_c(t) = u_c(t)i_c(t) \quad (3.43)$$

And neglecting the effects of the ripple,

$$u_c(t) = U_{dc} + \tilde{u}_c$$

Using the capacitor's fundamental equation $i(t) = C \frac{du_c}{dt}$ and since U_{dc} is a constant,

$$i_c(t) = C_{in} \frac{d}{dt} (U_{dc} + \tilde{u}_c) = C_{in} \frac{d\tilde{u}_c}{dt} \quad (3.44)$$

$$d\tilde{u}_c = \frac{\tilde{i}_c(t)}{C_{in}} dt \quad (3.45)$$

$$\tilde{u}_c = \int_0^t \frac{M \cdot I_1}{C_{in}} \cos 2\omega_o t dt = \frac{1}{2\omega_o C_{in}} MI_1 \sin(2\omega_o t) \quad (3.46)$$

The maximum amplitude of the double-frequency voltage happens when $\sin(2\omega_o t) = 1$. Thus, to complete the requirements,

$$C_{in} \geq \frac{MI_1}{2\omega_o \tilde{u}_c} = \frac{MI_1}{2\pi f_o \Delta U} \quad (3.47)$$

With $\Delta U = 2\tilde{u}$.

All the parameters of (3.47) are fixed with the exception of M and I_1 . The bigger those parameters are, the greater capacitance will be required. I_1 depends on the power, so the assumption will be that the converter is operating at its maximum point. The modulation index will be fixed to 0.5. This result can be obtained with a similar method as explained in [6], where all the calculations are done with respect the output power instead of the current. The main problem of the description of this article is that it does not consider the effect of the ripple caused by the PWM.

The solution to this problem is given by [33], where the ripple caused by the PWM can be calculated as

$$\Delta u = \frac{1}{C_{in}} \int_0^{T_{on}} \Delta i dt \quad (3.48)$$

Where T_{on} is the on-time interval shown in Fig. 3.12, and it has been derived in Eq. (3.13)

$$T_{on} = \frac{M \sin \omega_o t}{f_s} \quad (3.49)$$

Integrating the expression above,

$$\Delta u = \frac{I_1}{f_s C_{in}} r_{pp}(M, t) \quad (3.50)$$

Being r_{pp} the normalized peak-to-peak voltage switching ripple.

$$r_{pp}(M, t) = |M \sin(\omega_o t)^2 (1 - M \sin(\omega_o t))| \quad (3.51)$$

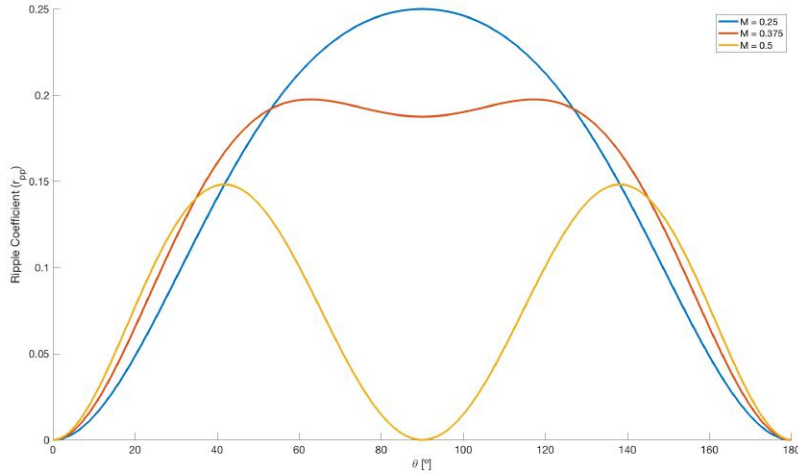


Figure 3.17. Different ripple factors depending on the modulation index and the modulation time.

As shown in Fig. 3.17, the maximum r_{pp} occurs when $M = 0.25$ and takes a maximum value of 0.25. Therefore, the voltage ripple caused by the switching can be expressed as,

$$\Delta u_{max} = \frac{1}{4} \frac{I_1}{f_s C_{in}} \quad (3.52)$$

And,

$$C_{in} \geq \frac{1}{4} \frac{I_1}{f_s \Delta u_{max}} \quad (3.53)$$

Comparing the capacitor's maximum voltage ripple caused by the double-frequency voltage and the effects of the switching,

$$\frac{\Delta u}{\tilde{u}_c} = \frac{\frac{1}{4} \frac{I_1}{f_s C_{in}}}{\frac{I_1}{8\pi f_o C_{in}}} = 2\pi \frac{f_o}{f_s} \simeq 0 \quad (3.54)$$

From here, it is shown that the voltage ripple is mainly caused by the doubled-frequency component of the input current. So, apparently there is no need of another capacitor due to switching harmonics.

The statement before would be true if C_{in} is small, so it would not be necessary a ceramic or film capacitor. Since C_{in} use to be big, the use of an electrolytic capacitor is required. A concern about this kind of capacitor is explained in [35]. An electrolytic capacitor can be labelled as a capacitor in series with a resistor and an inductor. Regarding the doubled-frequency harmonic it will work properly since the impedance of the inductance would not be high enough. However, from the point of view of the high-frequency harmonics, the inductive component will be greater than the rest. Consequently, it will be considered as a big impedance facing high-frequency harmonics. This causes that the high-frequency harmonic current will go across another path which is the voltage source. Actually, since the voltage source would be a photovoltaic solar panel or a battery, this harmonics can disturb their behavior, causing serious damages.

For avoiding this effect, these high-frequency harmonics must flow through a different path. The solution proposed is using a non-electrolytic capacitor that will be placed in parallel to the other one. This capacitor will absorb all the high-frequency harmonics at the same time that it controls the voltage ripple caused by them.

As in the case of the output filter, the new names of the capacitor will be changed to C_f and C_h . C_f is referred to the capacitor in charge of providing the doubled-frequency current, and C_h is in charge of reducing the high-frequency load.

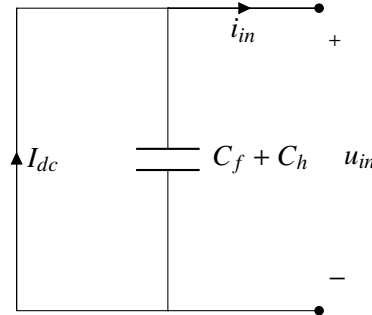


Figure 3.18. Behavior of the capacitor filter and the source facing harmonic load.

Another consideration that must be taken is, again, regarding the frequency harmonics. As said before, the capacitor placed in parallel to the voltage source is designed to provide the extra amount of power that the inverter needs or to store it. And in this project, the capacitor has been designed with respect these criteria. However, and considering an ideal circuit, for a non-DC component, the voltage source behaves as a short-circuit, as it is supposed to. This involves that all the harmonic current will flow through the voltage source, although it would not generate power, not only the switching but also the doubled-frequency harmonics. This can cause a failure in the solar panel or battery. This can be seen in Fig. 3.18.

3.4.2. Damping Effect

The solution proposed in this project is the use of an LC filter, where the capacitors will be the same as calculated before. This filter has been selected before another LCL filter due to its simplicity and because the use of another inductance may affect the power transfer of the capacitor. The filter inductor L_f has been chosen to reduce the harmonic content that goes through the voltage source, especially the switching harmonics.

Being $F_{I_{dc}}$ the transfer function that involves the current of the source and the current that goes into the inverter,

$$F_{I_{dc}} = \frac{I_{dc}(s)}{I_{in}(s)} = \frac{1}{L_f(C_f + C_h)s^2 + 1} \quad (3.55)$$

The resonance frequency of this filter will be equal to,

$$\omega_r = \sqrt{\frac{1}{L_f(C_f + C_h)}} \quad (3.56)$$

Since the filter inductor is selected to reduce the harmonic content that goes through the source, it is required that ω_r is lower than the sideband harmonics of the switching frequency, but it is not required to be smaller than the doubled-frequency fundamental harmonic for two reasons:

1. A very small ω_r requires of high inductance, which will increase the size of the magnetic core and, consequently, the power losses will be increased.
2. Since the ripple voltage caused by the capacitor C_f is very small, the voltage that sees the inductor will be very small and, therefore, not many currents will flow through it.

Nevertheless, the system will be undamped. As mentioned with the output filter, it is required the use of a damping resistor R_d . In this project, the input filter is designed as shown in Fig. 3.19. Despite the other filter the damping resistor has been placed in series with a capacitor, in this case, it makes more sense if it is in parallel with the inductor.

The main reason because it is not placed in series with a capacitor is because harmonic current will flow through them. This becomes in high power losses: however, if the resistor is placed in parallel with the inductor, not many currents will flow across it. As said before, the current of the source will be mainly DC with a small harmonic content. From a DC perspective, the resistor will be shorted because of the inductor. After many considerations, this is the simplest and least lossy way for damping this filter.

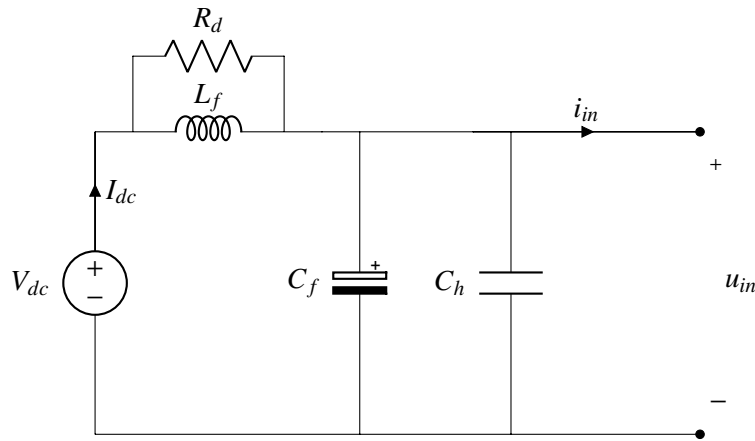


Figure 3.19. Input filter design with the damping resistor R_d in parallel with the inductance L_f .

In the same way as in the other filter, a transfer function of the new system can be derived,

$$F_{I_{dc}} = \frac{I_{dc}(s)}{I_{in}(s)} = \frac{\frac{L_f}{R_d}s + 1}{L_f(C_f + C_h)s^2 + \frac{L_f}{R_d}s + 1} \quad (3.57)$$

Where $\omega_z = \frac{R_d}{L_f}$. As talked about during the output filter, we would like the damping branch to act when ω_r . However, if it is not high enough the harmonics would not be filtered and they will go into the source.

At this point, the overall input filter has been designed. Moreover, we know from Eq. 3.40 the relation between currents. The maximum current will be when $M = 1/2$, and so,

$$I_1 = 2I_{dc} = 2 \cdot \frac{P_{dc}}{U_{dc}} \quad (3.58)$$

4

Components

The main purpose of this chapter is to calculate the components that are needed in order to build the DC-to-AC converter. Using the last part equations we are able to calculate these components.

The majority of the parameters has been calculated using normalized units, therefore, it is worthy to present the base units

Side	U_{base} [V]	S_{base} [VA]	I_{base} [A]	Z_{base} [Ω]	f_{base} [Hz]	ω_{base} [rad/s]	L_{base} [mH]	C_{base} [μ F]
AC	120	120	1	120	60	$2\pi 60$	320	22
DC	$120\sqrt{2}$	120	$\sqrt{2}/2$	240	60	$2\pi 60$	640	11

4.1. LCL Filter

The first thing to do is to calculate the current and voltage ratings of the filter. From Eq. (3.15) we can see that at nominal conditions, i.e. nominal load and nominal voltage, the current ripple through the inverter-side inductor when it reaches its maximum point is 0. This is when $M = 1/2$ and $\sin \omega_o t = 1$. Although with different modulation the ripple current will be located at its maximum point, still it would not reach the maximum value of the current when $M = 1/2$,

$$\Delta i_L = \frac{V_{dc}}{L f_s} M(1 - 2M \sin \omega_o t) \sin \omega_o t$$

A similar procedure can be done to the grid-side inductor.

This means that the maximum current that flows through the inductors is

$$I_\rho = \sqrt{2} I_n = \sqrt{2} = 1.44 \text{ A}$$

Moreover, the maximum voltage will be when $M = 0.25$, a designed parameter that establish the minimum modulation factor.

$$U_\rho = \frac{2U_{dc}}{2M} = \frac{240}{0.5} \sqrt{2} = 680 \text{ V}$$

The design parameter has been chosen according to what it has been stated. These are,

$$\Delta i_1 = 30\%$$

$$r = 2\%$$

Using the Equations(3.18) and (3.19), assuming nominal conditions and a unity power factor $\cos \varphi = 1$,

$$l_1 = \frac{1}{8} \frac{V_{dc}}{\Delta i_1 f_s} = \frac{1}{8 \cdot 0.3 \cdot \frac{40 \cdot 10^3}{60}} = 6.3 \cdot 10^{-3} \text{ p.u.}$$

$$c = \frac{r \cdot P_n}{U_n^2 \omega_o} = r = 0.02 \text{ p.u.}$$

Using these parameters, L_2 is calculated as follow using Equations (3.21) and (3.23). Both give an inductance value of,

$$l_2 = 1.1 \cdot 10^{-3} \text{ p.u.}$$

The resonance frequency of this filter, without considering the damping branch yet, is equal to,

$$\omega_r = \sqrt{\frac{l_1 + l_2}{l_1 l_2 c}} = \sqrt{\frac{(6.3 + 1.1) \cdot 10^{-3}}{6.3 \cdot 1.1 \cdot 10^{-6} \cdot 0.02}} = 227 \text{ p.u.}$$

All the constraints stated (3.24) are satisfied,

$$l_1 + l_2 = (6.3 + 1.1) \cdot 10^{-3} = 0.0074 \leq 0.05$$

$$10 \leq 227 \leq 667$$

Once the damping branch C_d-R_d is added, and as established in when talking about the damping branch, the relation between C_d and C_f , for getting the most efficient damping with respect the power losses, must be equal to 1. Consequently,

$$c_f = \frac{c}{2} = 0.01 \text{ p.u.}$$

$$c_d = \frac{c}{2} = 0.01 \text{ p.u.}$$

Looking to the optimal quality factor, with this parameters the damping resistor would be out of the interval (3.33). This is why the resistor has been chosen as the mean value of both $R_{d_{min}}$ and $R_{d_{max}}$. Otherwise, by changing the parameters, the filter would be out of specifications.

$$l_c = \frac{l_1 l_2}{l_1 + l_2} = 0.22 \text{ p.u.}$$

$$r_{d_{min}} = \frac{\sqrt{n+1}}{n} \sqrt{\frac{l_c}{l_f}} = 0.44 \text{ p.u.}$$

$$r_{d_{max}} = \frac{n+1}{n} \sqrt{\frac{l_c}{c_f}} = 0.62 \text{ p.u.}$$

$$r_d = 0.53 \text{ p.u.}$$

Therefore, changing normalized units to real values,

$$L_1 = 2 \text{ mH}$$

$$L_2 = 365 \text{ } \mu\text{H}$$

$$C_f = C_d = 221 \text{ nF}$$

$$R_d = 64 \text{ } \Omega$$

These are the theoretical values of the components to achieve the specifications. However, in most of the components, these are not going to be their final values.

In case of the inductors, since it is very difficult to find inductances with the required specifications, the propose alternative has been to build them. This involves using the materials available at the ECE building in the University of Illinois at Urbana–Champaign.

On the specifications, besides the physical characteristics of the core, the magnetic characteristic, or unitary inductance is expressed as A_L : [nH/turn²]. Using the inductor's fundamental equation and Faraday's Law (2.4),

$$u_L = L \frac{di_L}{dt} = \frac{dN^2 A_L i_L}{dt}$$

$$\varepsilon = \frac{d\lambda}{dt} = \frac{dN\Phi}{dt}$$

So,

$$\Phi = N A_L i_L$$

Being Φ the magnetic flux,

$$\Phi = \oiint \vec{B} \circ d\vec{A} = B A_e$$

Therefore, the main equations for designing an inductance are,

$$N = \sqrt{\frac{L}{A_L}} \quad (4.1)$$

$$i_{max} = \frac{B_{sat}A_e}{NA_L} \quad (4.2)$$



Figure 4.1. Process of winding a coil for the inductor L_2 .

Where A_e is the equivalent area and B_{sat} is the maximum magnetic field value before the magnetic material starts to be saturated.

Starting from the inverter-side inductor L_1 , the core proposed is P36/22–3F3–E400. The characteristics of this core are:

$$A_L = 400 \text{ nH}$$

$$B_{sat} = 450 \text{ mT}$$

$$A_e = 202 \text{ mm}^2$$

With this specifications, the design parameters to build this inductor are,

$$N_{L_1} = \sqrt{\frac{2 \cdot 10^6}{400}} \approx 80 \text{ turns}$$

$$i_{max} = \frac{0.45 \cdot 202 \cdot 10^{-6}}{80 \cdot 400 \cdot 10^{-9}} \approx 3.6 \text{ A} > I_p$$

In the case of the grid-side inductor L_2 , the core proposed is P26/11–3C81–A315. The characteristics of this core are:

$$\begin{aligned}
 A_L &= 315 \text{ nH} \\
 B_{sat} &= 450 \text{ mT} \\
 A_e &= 93.9 \text{ mm}^2
 \end{aligned}$$

The design parameters for building this inductor are,

$$\begin{aligned}
 N_{L_2} &= \sqrt{\frac{365 \cdot 10^3}{315}} \approx 34 \text{ turns} \\
 i_{max} &= \frac{0.45 \cdot 93.9 \cdot 10^{-6}}{34 \cdot 315 \cdot 10^{-9}} \approx 4 \text{ A} > I_\rho
 \end{aligned}$$

The process of creating a inductor is shown in Fig. 4.1 and Fig. 4.2.

After creating these inductors, they have been tested. Their real values of inductance and resistance are:

$$\begin{aligned}
 L_1 &= 2.33 \text{ mH} \\
 R_{s_1} &= 0.3 \Omega
 \end{aligned}$$

And,

$$\begin{aligned}
 L_2 &= 418.5 \text{ mH} \\
 R_{s_2} &= 0.12 \Omega
 \end{aligned}$$

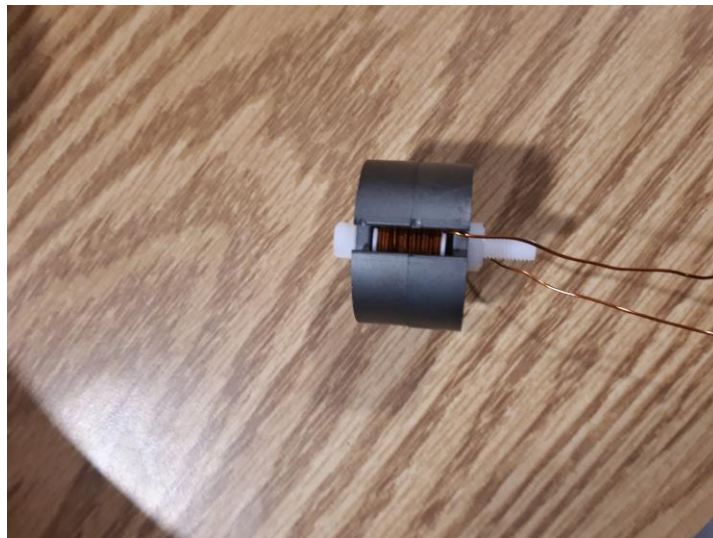


Figure 4.2. Inductor L_2 finished.

In the case of the capacitors, we will choose ceramic capacitors due to their low equivalent resistance. The ones chosen are C3216X7T2W104M160AA, which datasheet is shown in the Appendix. It has a capacitance of 100 nF, which means that we are going to use two of them for each leg. It is true that this

will not reach what it has been specified before, but, the difference is small and otherwise the reactive power generated will increase. Moreover, its dissipation factor is at most 2.5%.

A real capacitor can be labelled as an ideal capacitor in parallel with a resistor, named R_{leak} which represents the dielectric resistance, and both in series with another resistor R_{lead} ,

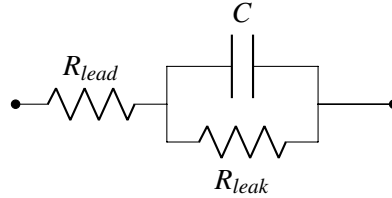


Figure 4.3. Model of a real capacitor.

Nevertheless, calculating impedance between the two point of the capacitor we get that,

$$Z_{AB} = (R_{lead} + \frac{1}{\omega^2 C^2 R_{leak}}) - j \frac{1}{\omega C} \quad (4.3)$$

Considering that R_{lead} is close to 0, we can neglect that term. Therefore, the equivalent model of a capacitor can be written as,

$$Z_{AB} = \frac{1}{\omega^2 C^2 R_{leak}} - j \frac{1}{\omega C} \quad (4.4)$$

And the new element can be labeled as $ESR = \omega C \tan \delta$, where the dissipation factor $\tan \delta = \frac{1}{\omega C R_{leak}}$.

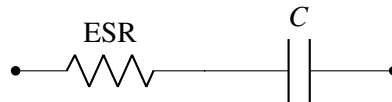


Figure 4.4. Equivalent model of a real capacitor.

At f_o the filter behaves as a pure inductive one, this means that the capacitors' legs will be open circuits. So, through the capacitors only will flow high-frequency current. In this case, for calculating this capacitor's resistance the frequency that must be used is $2f_s$, as stated in Chapter 3.

$$ESR = 2\pi \cdot 2 \cdot 40 \cdot 10^3 \cdot 68 \cdot 10^{-6} \cdot 0.025 = 0.8544 \Omega$$

4.2. Input Filter

A similar process can be done in the case of the input filter. In this part, the capacitors have been chosen so they can absorb the switching-frequency harmonics and the doubled-frequency fundamental component.

The input-current will have as well switching harmonics, however, the same thing happens to it. At nominal operation and with a nominal voltage the current ripple is zero. Since the voltage ripple allowed is a 5%, the voltage ratio will be $\mathcal{R}_u = 2.5\%$. Moreover, the maximum voltage that the DC bus can reach has been set to when $M = 0.25$. Therefore,

$$I_\rho = 2I_{dc} = \sqrt{2} = 1.44 \text{ A}$$

$$U_\rho = \frac{U_n}{2M}(1 + \mathcal{R}_u) = \frac{U_n}{0.5} \sqrt{2}(1 + 0.025) = 350 \text{ V}$$

Using the Equations (3.47), (3.53), (3.58) and allowing a voltage ripple of 5% caused by the doubled-frequency current and a 1% caused by the switching-frequency current,

$$c_f = \frac{4MP_{dc}}{\omega_o V_{dc}^2 \tilde{u}} = \frac{2 \cdot 0.5}{1 \cdot 0.05} = 20 \text{ p.u.}$$

$$c_h = \frac{1}{4} \frac{I_1}{f_s \Delta u} = \frac{1}{4 \cdot \frac{40 \cdot 10^3}{60} \cdot 0.01} = 0.0375 \text{ p.u.}$$

As mentioned in the previous parts, if the resonance frequency of the converter ω_r is set to be ten times lower than the switching frequency,

$$l_f = \frac{1}{\omega_r^2(c_f + c_h)} = \frac{1}{67^2 \cdot (20 + 0.0375)} = 1.12 \cdot 10^{-5} \text{ p.u.}$$

The cut-off frequency of the zero $\omega_z = r_d/l_f$ has been set to be 10 times the resonance frequency ω_r , therefore,

$$r_d = l_f \omega_z = 1.12 \cdot 10^{-5} \cdot 6667 = 0.7486 \text{ p.u.}$$

These parameters in real units are calculated multiplying the normalized units by the DC bases,

$$L_f = 7.15 \mu\text{H}$$

$$C_f = 221 \mu\text{F}$$

$$C_h = 414 \text{ nF}$$

$$R_d = 180 \Omega$$

As done with the output filter inductors, the best way of having the desire inductance is to build it. In this case, the core selected is P14/8-3C81-A100. The characteristics of this core are,

$$A_L = 100 \text{ nH}$$

$$B_{sat} = 450 \text{ mT}$$

$$A_e = 25.1 \text{ mm}^2$$

With these specifications, the design parameters to build this inductor are,

$$N_{L_f} = \sqrt{\frac{7.15 \cdot 10^3}{100}} \approx 9 \text{ turns}$$

$$i_{max} = \frac{0.45 \cdot 25.1 \cdot 10^{-6}}{9 \cdot 100 \cdot 10^{-9}} \approx 11.2 \text{ A} > I_p$$

As done before, the real values of the inductor are,

$$L_f = 10.46 \mu\text{H}$$

$$R_{s_f} = 0.09 \Omega$$

In the case of C_f , since its value is very big, the capacitors used are electrolytic. This will mean a high ESR, which stands for Equivalent Series Resistance. The capacitor used is a UCY2V680MHD, which has a capacitance of $68 \mu\text{F}$. To achieve the requirements four of them will be placed in parallel. This capacitor has a dissipation factor of $\tan \delta = 0.24$ at a measured frequency of 120 Hz. We will use this frequency because as explained in Chapter 3, the electrolytic capacitors will handle the doubled-frequency harmonic, and so, the frequency that they see is $2\omega_o$.

$$\text{ESR} = 0.24 \cdot 2\pi \cdot 120 \cdot 68 \cdot 10^{-6} = 0.0123\Omega \quad (4.5)$$

In the case of the ceramic capacitors that are placed in parallel to the electrolytic ones, their ESR can be neglected, in fact, any information about their $\tan \delta$ is given. The one chosen are C3216X7T2W104M160AA. The same procedure can be used in case of this one. In this case four of them will be placed in parallel. Moreover, they will handle the same harmonic load, and therefore, their ESR will be the same as in the case of the capacitors of the output filter.

4.3. Inverter

In the case of the inverter, its voltage and current rating depends on the components it is made of. In this case, the most important ones are the MOSFETs, which are behaving as switches. From Chapter 3 and (3.5), the voltage and current ratings must be calculated and in(3.5),

$$U_p = U_{in} \approx 350 \text{ V}$$

$$I_p = I_{out} \approx 1.44 \text{ A}$$

For achieving the specifications, the MOSFET chosen is IRF740 which fits in the project. The datasheet of this components is presented in the Appendix.

5

Simulation

In Chapter 4, we have calculated the real values of the components that are going to be used in the converter. The main purpose of this chapter is to simulate the behavior of the converter under specific conditions.

5.1. Simulation Environment

The simulation comes from Matlab–Simulink. The simulation model can be shown in Fig. 5.1,

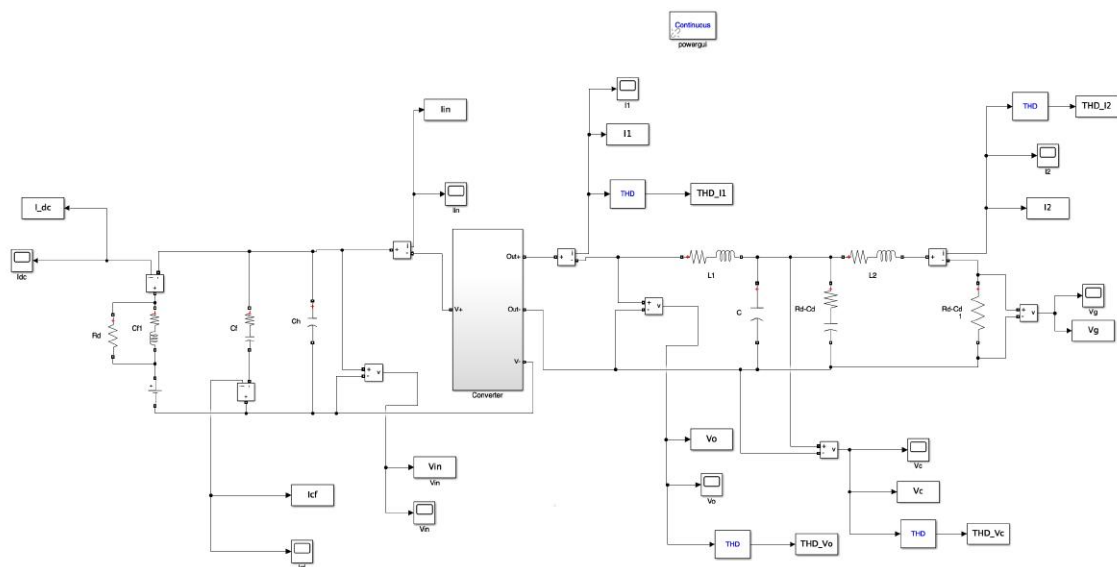


Figure 5.1. Simulation model of the system.

And the block of the MOSFETs can be seen in Fig. 5.2

The simulation has been chosen as follow,

- Solver Method: variable–step ode45.
- Minimum Step–Size: $0.1/f_s$.
- Relative Tolerance: 10^{-12} .
- Absolute Tolerance: 10^{-15} .

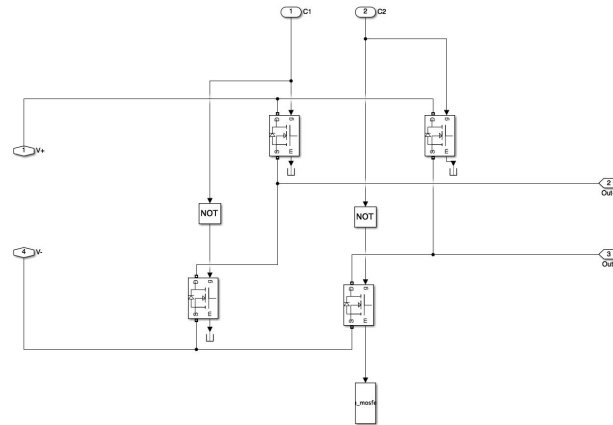


Figure 5.2. Simulation model of the MOSFETs.

This values of tolerance and step-size has been chosen in order to be able to see the pulses generated by the PWM, otherwise, we would miss some of them.

5.2. Simulated Results

In this part of the chapter the simulated results will be presented.

Inverter-side Output Current

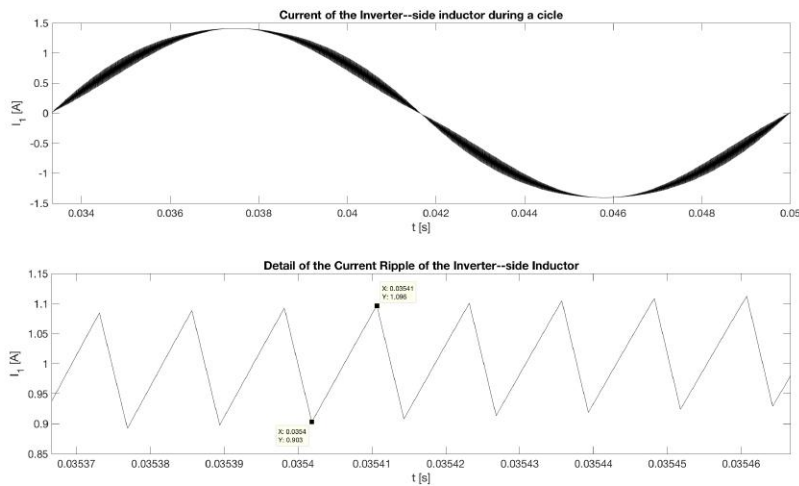


Figure 5.3. Current of the inverter-side inductor and the detail of its ripple

As we can see in Fig. 5.3, the ripple current has a sawtooth shape due to what it has been commented in Chapter 3. The voltage across the inductor can be seen as a train of pulses. Since the pulses have a constant value, the current across the inductor follows a linear expression, assuming that the voltage of the capacitor remains constant during certain periods of T_s .

From the graph, we can see that the current ripple has a value of 0.193 A, which is roughly a 20% of the current of the fundamental component. Therefore, Eq. 3.15 represents the behavior of the current across the inverter-side inductor. It is useful to observe that in the case of a simple L filter, this fact

would not be happening. Therefore, the use of a capacitor as a low-pass filter also allows controlling the current ripple across the inverter-side inductor. From Fig. 5.7 we can see that in fact, this waveform achieves the specifications and recommendations stated before.

Point of Common Coupling

Here are two variables of interest, current and voltage, and both are fixed to the standard and regulations mentioned before [4]. In both, the THD of the waveforms must be less than 5% and 8% respectively for systems under 1 kV. In the case of the current, it must satisfy another constraint, the value of the harmonics over 35th must be less or equal than 0.3%. The figures obtained by the simulation are shown below in Fig. 5.4 and Fig. 5.5.

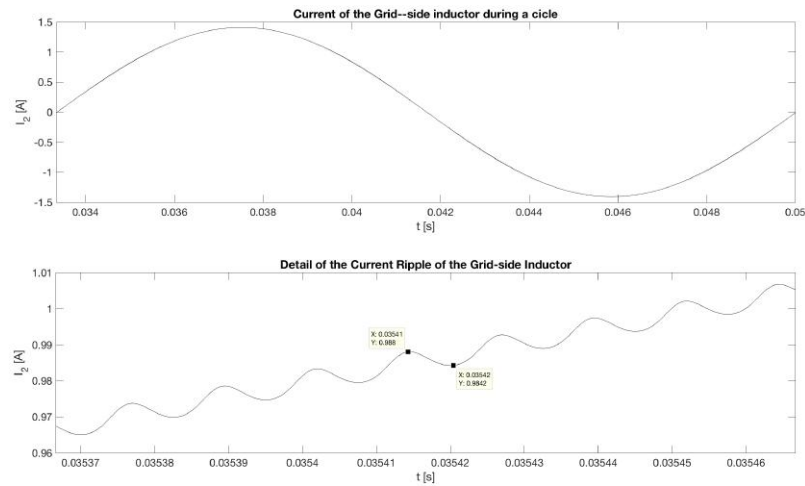


Figure 5.4. Current at the point of common coupling and its ripple.

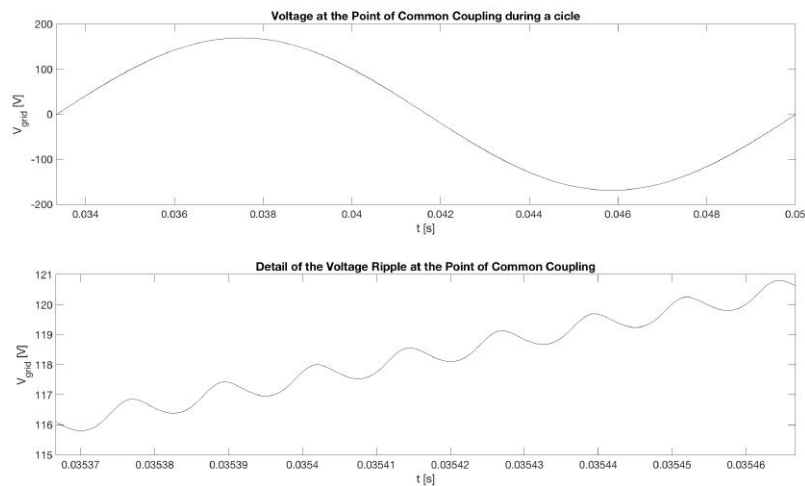


Figure 5.5. Voltage at the point of common coupling and its ripple.

In this case, the shape of the voltage and current is the same because the grid has been substituted by an equivalent resistor, according to the Substitution Theorem. In both pictures, from the graph above we can see the effectiveness of the filter and the effectiveness of the PWM. The output variables are smooth sine-waveforms but with a little bit of ripple. This is not a problem since the impedances of the grid will filter the signal as well.

Output Filter Capacitors

The main purpose of showing the simulated results of this component is because, according to [28], for reducing the complexity of the problem, the grid can be labelled as a source of infinite power, i.e. it does not have any equivalent impedance. Therefore, at the point of common coupling, the voltage at the output of the filter will be the same as the grid's voltage.

The solution proposed is to satisfy all the restrictions [4] at the capacitor's node. At least regarding the voltage. The current must be filtered through the grid-side inductor.

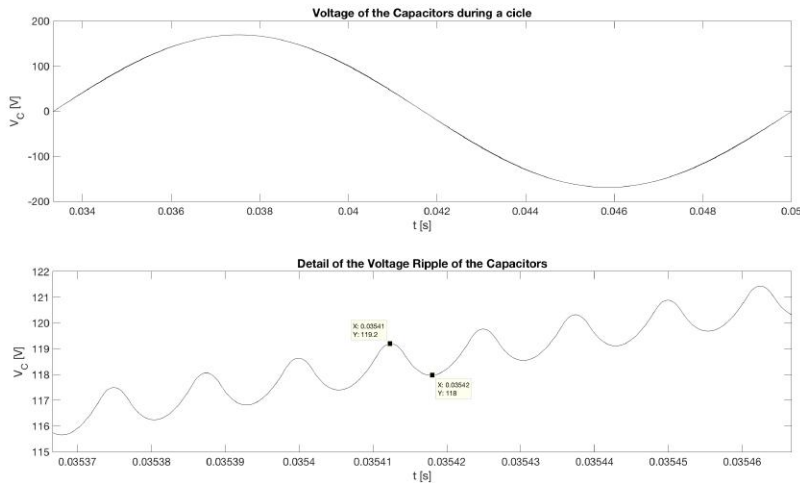


Figure 5.6. Voltage across the output filter capacitors.

From Fig. 5.6 we can see that the shape of the waveform is almost the same as in Fig. 5.5. Nevertheless, here we have more ripple, which is logical since the inductor is not filtering the signal.

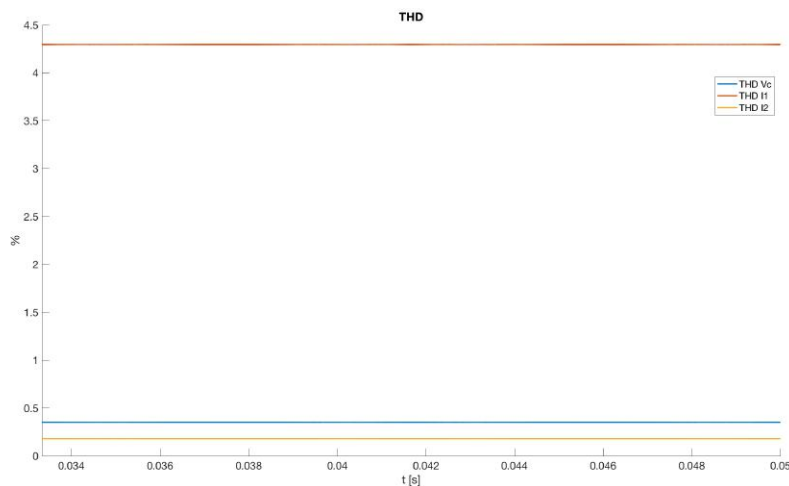


Figure 5.7. THD of the inverter-side and grid-side current and the capacitors' voltage.

However, as can be seen in Fig. 5.7, the THD of the voltage across the capacitor has a very small THD, roughly a 0.5%, which is acceptable.

From Fig. 5.7 we can see that none of the variables is over 5% which proves the effectiveness of the filter.

DC Source Current

The current across the DC Source is very important because it is the equivalent model of a PV system or a battery. The ideal case must be a DC current that might have some noise.

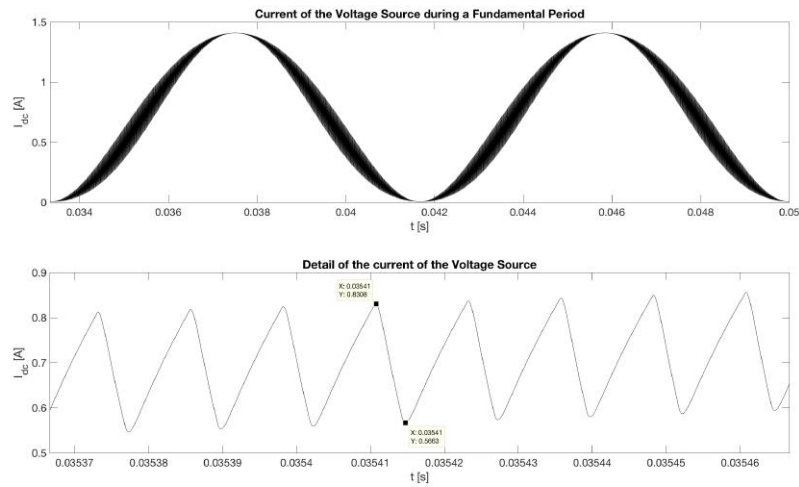


Figure 5.8. Current across the voltage source, i.e. PV system or battery.

As we can see from Fig. 5.8 the source is not giving a steady value of current but also is giving an alternating current.

If we look back to Chapter 3, we placed an input capacitor in order to provide the extra amount of power that the inverter needs or to store it. Therefore the capacitor was designed to provide an alternating current that creates a ripple in the voltage. However, looking again to Fig. 5.8, this alternating current is the one provided by the source.

Therefore, the first consequence of this fact is to assume that the filter is not working properly, which is the case, and it has to be regarding the inductor. Nevertheless, in an attempt to change its value, the current across the source became steady, but the input voltage of the inverter behaved strangely.

Therefore, the solution adopted was to keep the inductor the same as in the first moment, although it will provide a variable DC current. This is not the best case but since is not purely alternating is not the worst case.

Notice that the ripple of this current is very similar to the one of the inverter–side inductor. However, it is smoother.

Input Voltage

As we have mentioned in the last part, the fact that the variable current goes across the source involves that the current across the capacitor in charge of the doubled–frequency harmonic is almost neglected. This brings a steady voltage at the input, as shown in Fig. 5.9,

As we can see in at the bottom of the Fig. 5.9, although the waveform is almost steady, there are some ripple. This is because the high–frequency harmonics caused by the inverter.

In the simulation they have been considered the ESR of the capacitors and sthe inductors' serie resistors. Moreover, the MOSFETs have been chosen as real. Considering all these resistors, besides the damping ones, the DC–to–AC converter has an efficiency of,

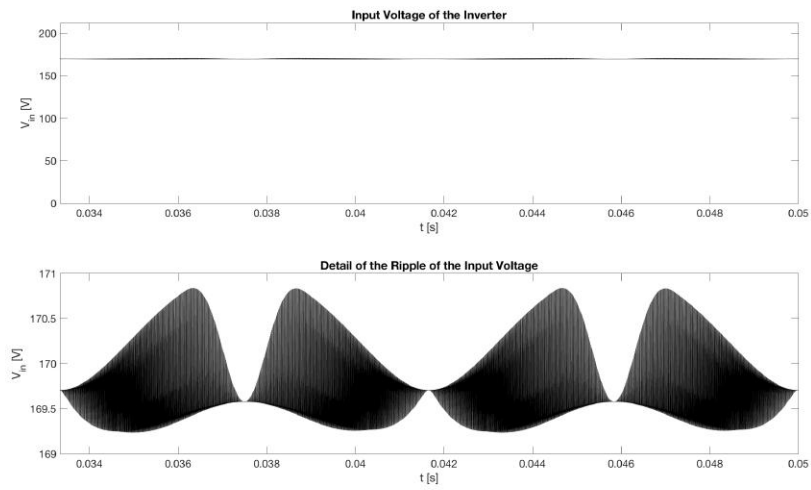


Figure 5.9. Voltage at the inverter's input.

$$\eta = 88 \%$$

6

Real Experiment

As said at the beginning of this project, the aimed purpose of this project, besides fully understanding of how a DC-to-AC converter works and how to build some parts of it, the other objective was to build it. In Chapter 4 we have calculated the values we must use in order to create the desired waveforms.

6.1. Real Circuit

In this section, the parts of the circuit will be presented. to represent the grid, it has been substituted by a resistor. The input is not connected to the following pictures.

In Fig. 6.1 we can see the whole system placed on a breadboard.

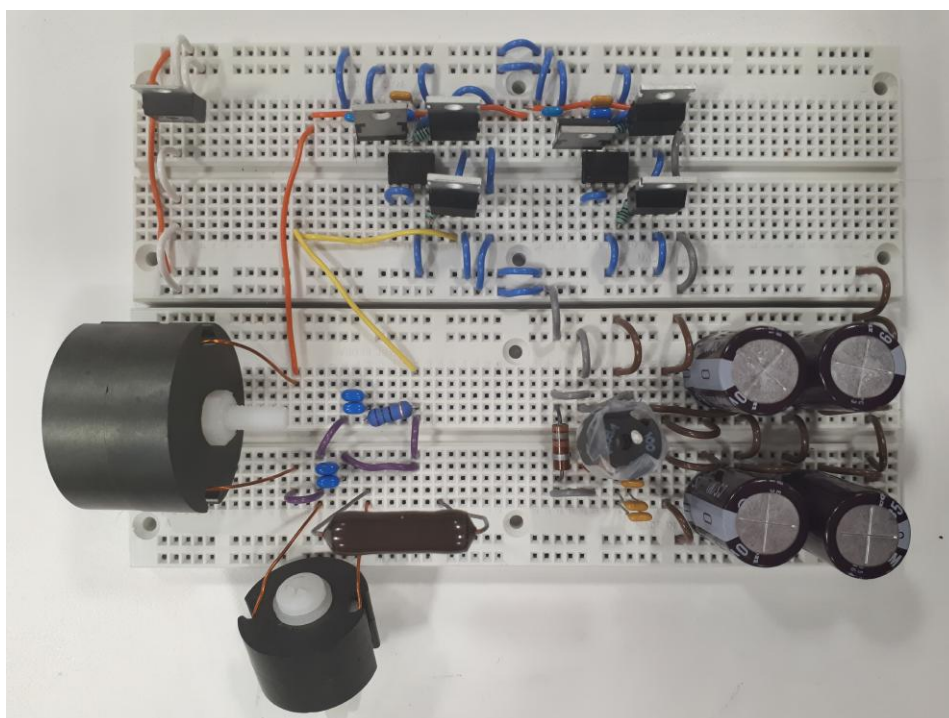
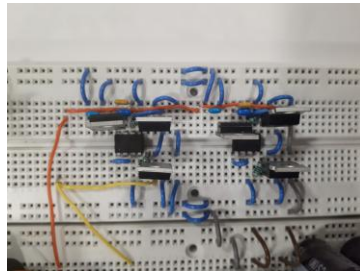


Figure 6.1. Real schematic of the converter.

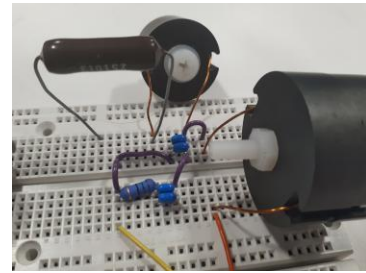
A detail representation of each part is presented in Fig. 6.2,



(a) [Real schematic of the input filter.



(b) Real schematic of the inverter.



(c) Real schematic of the output filter with a load.

Figure 6.2. Parts of the real circuit.

6.2. Results

First, due to the lack of knowledge in programming, the desire PWM waveform has not been achieved. Nevertheless, a PWM has been generated. It does not have the required quality, but for the purpose of showing how the inverter and the filters work, it is useful.

In the graphs, the yellow waveform represents the voltage provided by the DC Source, which is a real case must be the PV system or a battery.

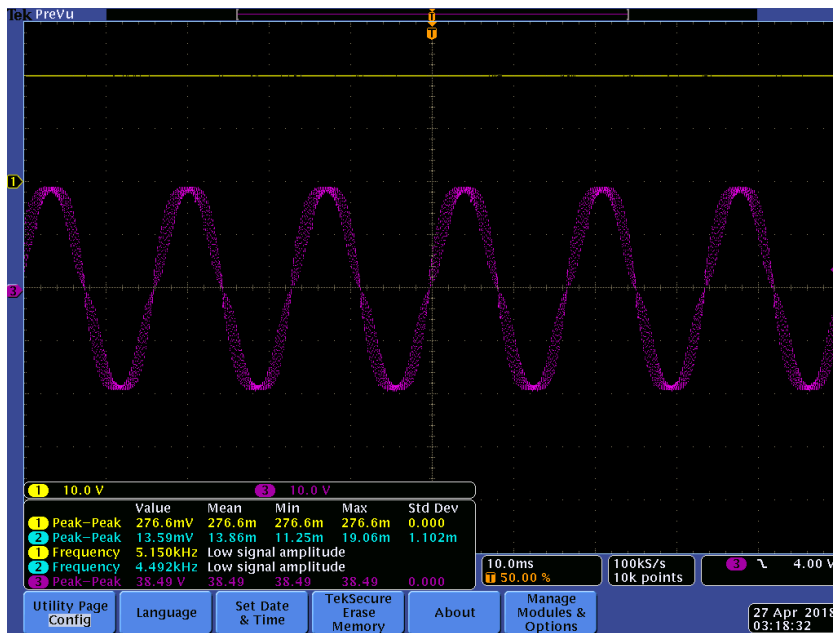


Figure 6.3. Real output waveform of the converter.

In Fig. 6.3 we can see that despite how good the PWM is, the inverter works. First, a Sine PWM waveform has been generated and also we can see that the filter is working as well.

The ripple of this waveform is huge and, of course, it cannot be connected to the grid. However, we can see the ripple caused by the PWM pulses is similar to the one in Fig. 5.5.

As said before in Chapter 5, since we can consider grid as an infinite power source, the point of common coupling will have the voltage of the grid. Therefore, it is useful to have the voltage across the output capacitor. This output can be seen in Fig. 6.4,

It has a lot of harmonics, but we can see that it almost has a sinusoidal shape.

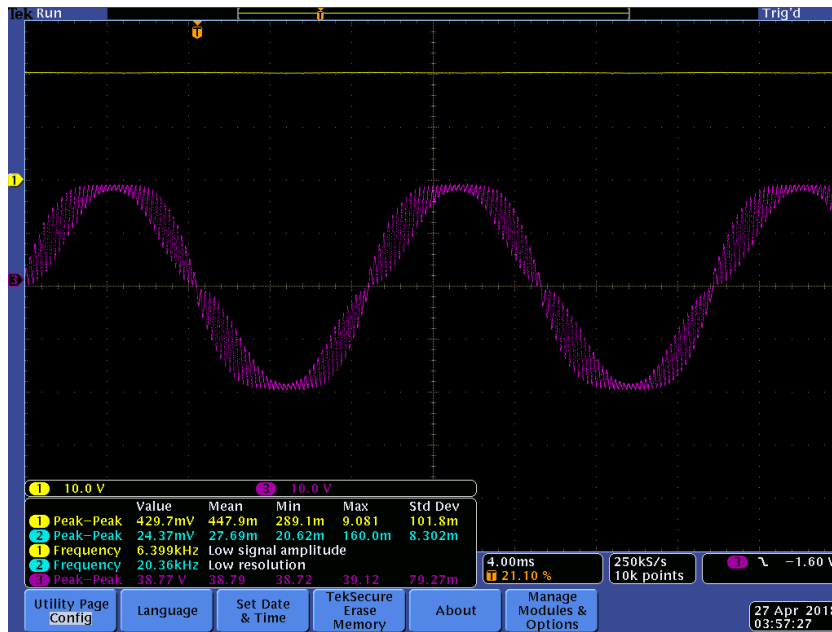


Figure 6.4. Real voltage of the output capacitor.

Again, despite the PWM was not accomplished, the overall converter has worked properly. The inverter gave a PWM, although it was not the desire, and the filters worked properly.

With the desire PWM, the waveforms should look like the simulations.

7

Future Steps

During this project, the behavior of a DC-to-AC power converter and two kinds of filters have been studied. The converter operated under nominal conditions most of the time and with a resistive load, which gave a unitary power factor. Although it have been built and tested, the final objective of the project has not been accomplished due to the lack of knowledge about programming.

The most important step on this project will be to generate the desire PWM waveform using the technique explained in previous chapters.

Moreover, since during these analyses the converter has been tested under a resistive load, it has not be tested under different conditions, such as an inductive or capacitive load. This is because for controlling the converter, first, it will need a control that regulates the amount of power that goes into the load, in this case, the grid. Due to the lack of knowledge about control systems, this has not be done too.

Therefore, the future steps must be to generate a PWM waveform and the control of the converter. These two are key points in the attempt of connecting it to the grid.

8

Conclusion

In this project, the analysis and construction of a DC-to-AC converter has been done.

From the two kinds of power converters, in this project Voltage Source Inverter topology has been chosen since the input of the inverter came from a PV Solar Power Plant or from a battery. To generate the AC waveform a PWM unipolar naturally-sampled double-edge carrier has been chosen because it is the one that produces less harmonic load.

For the Output Filter, it has been designed an LCL filter that is capable of reducing the ripple current of the inverter-side inductor at the same time that it satisfies the constraints imposed by regulations. This has been a complex filter but it has achieved a reduction in passive elements. A simple L filter or an LC would need greater values which involves a bigger size and more losses.

From the input-side, an LC filter has been used in order to reduce any possible harmonic that goes to the battery or PV solar system. A more complex filter has not been considered necessary.

All the inductors have been created since it is hard to find one with the required specifications. Their value has been very close to what it was calculated and in all the cases they are oversized. Which can be due to many reasons, such as more turns than expected.

From the simulation, the converter and all the designed components worked properly except the input filter. Nevertheless, the output filter and the inverter worked successfully, allowing a better performance than expected. In this case, where the rated power has been small, the use of high-frequency switch has helped on the duty of filtering. When turning to high-power converters, the switching frequency would be lower, and therefore the performance of the filter would be worse. Nevertheless, more powerful filters can be used.

From the real experiment, it cannot be considered a failure because the output filter and the inverter worked as expected. However, the lack of knowledge in programming has made the objective to not be accomplished, and so the project.

For a future perspective, a real PWM must be done and since it has to be connected to the grid a control must be set as well.

In this project, the knowledge about power inverters and filters has been acquired and the construction of a real DC-to-AC converter has been created. Here are exposed the principles of power conversion and a practical case in Photovoltaic Solar Power Plants.

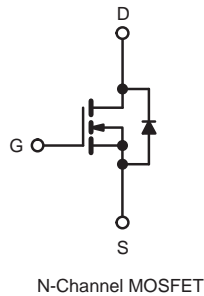
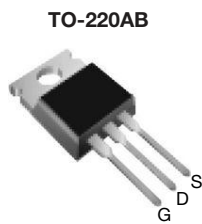
A

MOSFET

In this annex we can find the datasheet of the MOSFET used in this project. It consists on a transistor made by VISHAY and named as IRF740.

Power MOSFET

PRODUCT SUMMARY	
V_{DS} (V)	400
$R_{DS(on)}$ (Ω)	$V_{GS} = 10\text{ V}$ 0.55
Q_g (Max.) (nC)	63
Q_{gs} (nC)	9.0
Q_{gd} (nC)	32
Configuration	Single



FEATURES

- Dynamic dV/dt Rating
- Repetitive Avalanche Rated
- Fast Switching
- Ease of Paralleling
- Simple Drive Requirements
- Compliant to RoHS Directive 2002/95/EC


RoHS*
COMPLIANT

DESCRIPTION

Third generation Power MOSFETs from Vishay provide the designer with the best combination of fast switching, ruggedized device design, low on-resistance and cost-effectiveness.

The TO-220AB package is universally preferred for all commercial-industrial applications at power dissipation levels to approximately 50 W. The low thermal resistance and low package cost of the TO-220AB contribute to its wide acceptance throughout the industry.

ORDERING INFORMATION	
Package	TO-220AB
Lead (Pb)-free	IRF740PbF SiHF740-E3
SnPb	IRF740 SiHF740

ABSOLUTE MAXIMUM RATINGS ($T_C = 25\text{ }^\circ\text{C}$, unless otherwise noted)				
PARAMETER	SYMBOL	LIMIT	UNIT	
Drain-Source Voltage	V_{DS}	400	V	
Gate-Source Voltage	V_{GS}	± 20		
Continuous Drain Current	V_{GS} at 10 V	$T_C = 25\text{ }^\circ\text{C}$	10	A
		$T_C = 100\text{ }^\circ\text{C}$	6.3	
Pulsed Drain Current ^a		I_{DM}	40	
Linear Derating Factor			1.0	W/ $^\circ\text{C}$
Single Pulse Avalanche Energy ^b		E_{AS}	520	mJ
Repetitive Avalanche Current ^a		I_{AR}	10	A
Repetitive Avalanche Energy ^a		E_{AR}	13	mJ
Maximum Power Dissipation	$T_C = 25\text{ }^\circ\text{C}$	P_D	125	W
Peak Diode Recovery dV/dt^c		dV/dt	4.0	V/ns
Operating Junction and Storage Temperature Range		T_J, T_{stg}	- 55 to + 150	$^\circ\text{C}$
Soldering Recommendations (Peak Temperature)	for 10 s		300 ^d	
Mounting Torque	6-32 or M3 screw		10	lbf · in
			1.1	N · m

Notes

- Repetitive rating; pulse width limited by maximum junction temperature (see fig. 11).
- $V_{DD} = 50\text{ V}$, starting $T_J = 25\text{ }^\circ\text{C}$, $L = 9.1\text{ mH}$, $R_g = 25\text{ }\Omega$, $I_{AS} = 10\text{ A}$ (see fig. 12).
- $I_{SD} \leq 10\text{ A}$, $dI/dt \leq 120\text{ A}/\mu\text{s}$, $V_{DD} \leq V_{DS}$, $T_J \leq 150\text{ }^\circ\text{C}$.
- 1.6 mm from case.

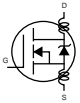
* Pb containing terminations are not RoHS compliant, exemptions may apply

IRF740, SiHF740

Vishay Siliconix

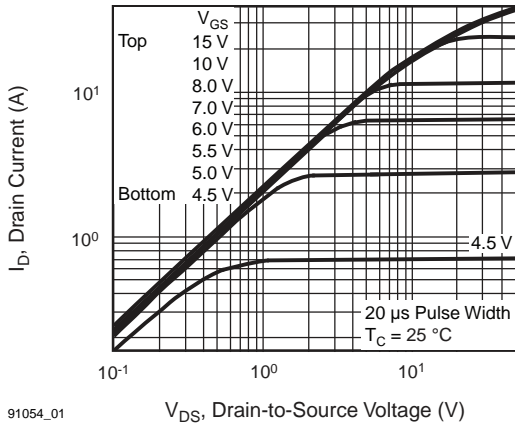


THERMAL RESISTANCE RATINGS				
PARAMETER	SYMBOL	TYP.	MAX.	UNIT
Maximum Junction-to-Ambient	R_{thJA}	-	62	°C/W
Case-to-Sink, Flat, Greased Surface	R_{thCS}	0.50	-	
Maximum Junction-to-Case (Drain)	R_{thJC}	-	1.0	

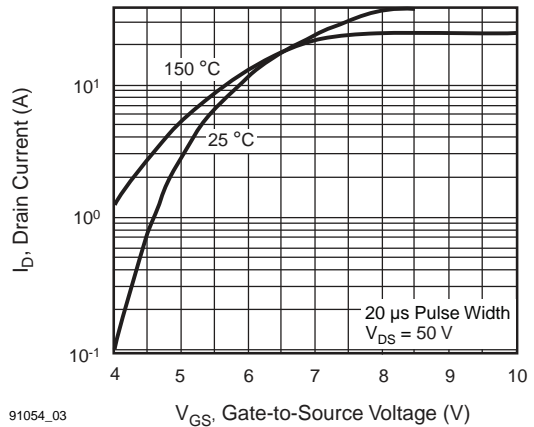
SPECIFICATIONS ($T_J = 25\text{ }^\circ\text{C}$, unless otherwise noted)						
PARAMETER	SYMBOL	TEST CONDITIONS	MIN.	TYP.	MAX.	UNIT
Static						
Drain-Source Breakdown Voltage	V_{DS}	$V_{GS} = 0\text{ V}, I_D = 250\text{ }\mu\text{A}$	400	-	-	V
V_{DS} Temperature Coefficient	$\Delta V_{DS}/T_J$	Reference to $25\text{ }^\circ\text{C}, I_D = 1\text{ mA}$	-	0.49	-	V/°C
Gate-Source Threshold Voltage	$V_{GS(th)}$	$V_{DS} = V_{GS}, I_D = 250\text{ }\mu\text{A}$	2.0	-	4.0	V
Gate-Source Leakage	I_{GSS}	$V_{GS} = \pm 20\text{ V}$	-	-	± 100	nA
Zero Gate Voltage Drain Current	I_{DSS}	$V_{DS} = 400\text{ V}, V_{GS} = 0\text{ V}$	-	-	25	μA
		$V_{DS} = 320\text{ V}, V_{GS} = 0\text{ V}, T_J = 125\text{ }^\circ\text{C}$	-	-	250	
Drain-Source On-State Resistance	$R_{DS(on)}$	$V_{GS} = 10\text{ V}, I_D = 6.0\text{ A}^b$	-	-	0.55	Ω
Forward Transconductance	g_{fs}	$V_{DS} = 50\text{ V}, I_D = 6.0\text{ A}^b$	5.8	-	-	S
Dynamic						
Input Capacitance	C_{iss}	$V_{GS} = 0\text{ V},$ $V_{DS} = 25\text{ V},$ $f = 1.0\text{ MHz, see fig. 5}$	-	1400	-	pF
Output Capacitance	C_{oss}		-	330	-	
Reverse Transfer Capacitance	C_{rss}		-	120	-	
Total Gate Charge	Q_g	$V_{GS} = 10\text{ V}, I_D = 10\text{ A}, V_{DS} = 320\text{ V},$ see fig. 6 and 13 ^b	-	-	63	nC
Gate-Source Charge	Q_{gs}		-	-	9.0	
Gate-Drain Charge	Q_{gd}		-	-	32	
Turn-On Delay Time	$t_{d(on)}$	$V_{DD} = 200\text{ V}, I_D = 10\text{ A}$ $R_g = 9.1\text{ }\Omega, R_D = 20\text{ }\Omega, \text{ see fig. 10}^b$	-	14	-	ns
Rise Time	t_r		-	27	-	
Turn-Off Delay Time	$t_{d(off)}$		-	50	-	
Fall Time	t_f		-	24	-	
Internal Drain Inductance	L_D	Between lead, 6 mm (0.25") from package and center of die contact 	-	4.5	-	nH
Internal Source Inductance	L_S		-	7.5	-	
Drain-Source Body Diode Characteristics						
Continuous Source-Drain Diode Current	I_S	MOSFET symbol showing the integral reverse p - n junction diode 	-	-	10	A
Pulsed Diode Forward Current ^a	I_{SM}		-	-	40	
Body Diode Voltage	V_{SD}	$T_J = 25\text{ }^\circ\text{C}, I_S = 10\text{ A}, V_{GS} = 0\text{ V}^b$	-	-	2.0	V
Body Diode Reverse Recovery Time	t_{rr}	$T_J = 25\text{ }^\circ\text{C}, I_F = 10\text{ A}, dI/dt = 100\text{ A}/\mu\text{s}^b$	-	370	790	ns
Body Diode Reverse Recovery Charge	Q_{rr}		-	3.8	8.2	μC
Forward Turn-On Time	t_{on}	Intrinsic turn-on time is negligible (turn-on is dominated by L_S and L_D)				

Notes

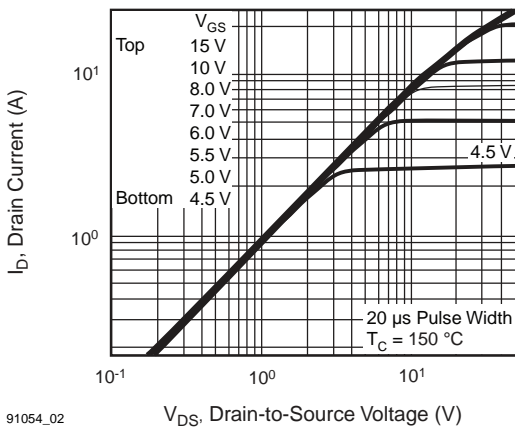
- Repetitive rating; pulse width limited by maximum junction temperature (see fig. 11).
- Pulse width $\leq 300\text{ }\mu\text{s}$; duty cycle $\leq 2\%$.

TYPICAL CHARACTERISTICS (25 °C, unless otherwise noted)


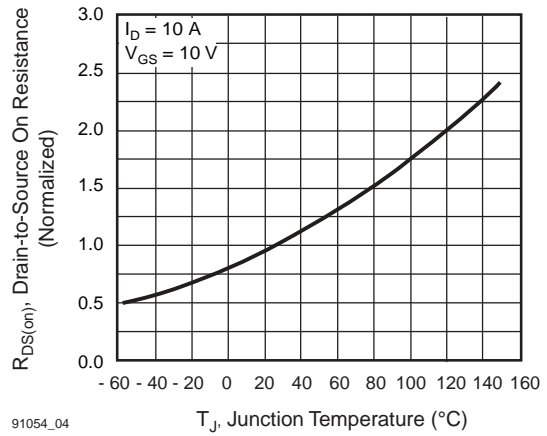
91054_01

Fig. 1 - Typical Output Characteristics, $T_C = 25\text{ }^\circ\text{C}$


91054_03

Fig. 3 - Typical Transfer Characteristics


91054_02

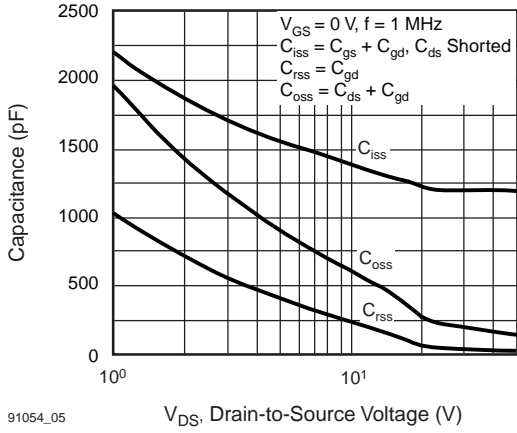
Fig. 2 - Typical Output Characteristics, $T_C = 150\text{ }^\circ\text{C}$


91054_04

Fig. 4 - Normalized On-Resistance vs. Temperature

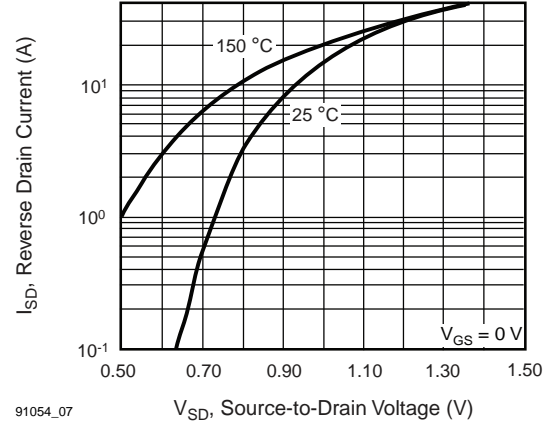
IRF740, SiHF740

Vishay Siliconix



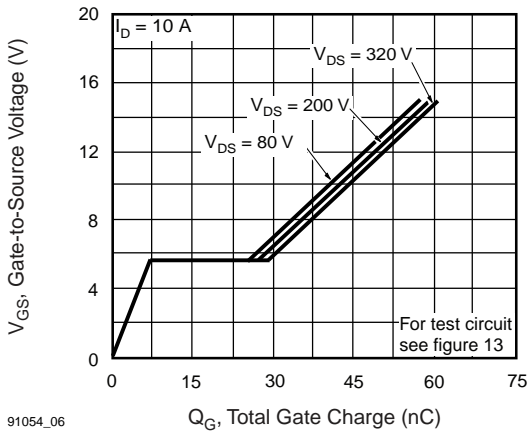
91054_05

Fig. 5 - Typical Capacitance vs. Drain-to-Source Voltage



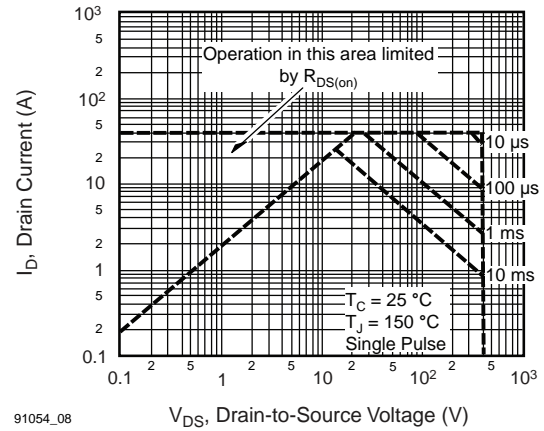
91054_07

Fig. 7 - Typical Source-Drain Diode Forward Voltage



91054_06

Fig. 6 - Typical Gate Charge vs. Drain-to-Source Voltage



91054_08

Fig. 8 - Maximum Safe Operating Area

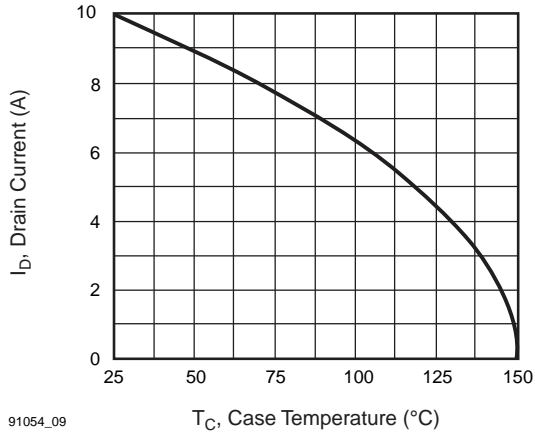


Fig. 9 - Maximum Drain Current vs. Case Temperature

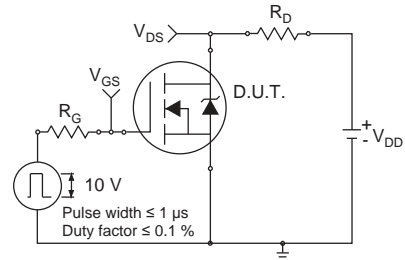


Fig. 10a - Switching Time Test Circuit

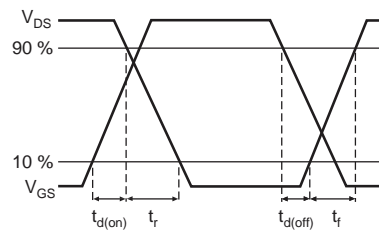


Fig. 10b - Switching Time Waveforms

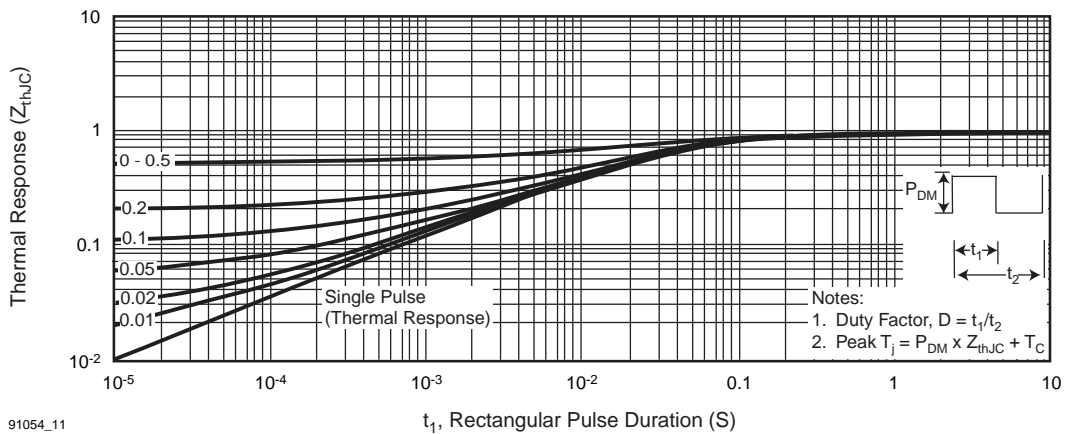


Fig. 11 - Maximum Effective Transient Thermal Impedance, Junction-to-Case

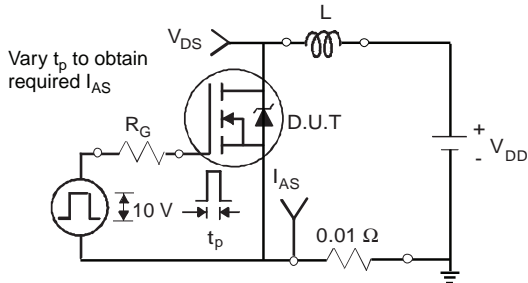


Fig. 12a - Unclamped Inductive Test Circuit

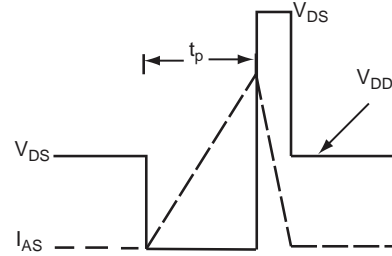
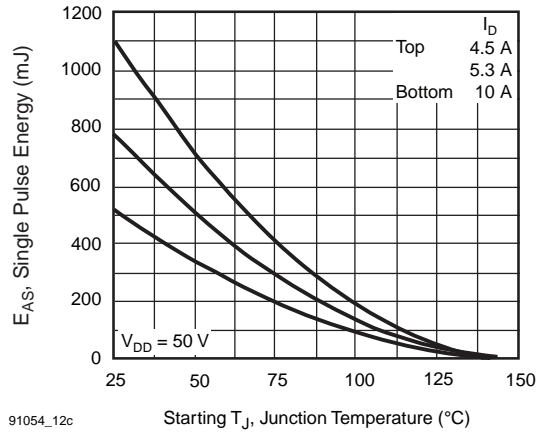


Fig. 12b - Unclamped Inductive Waveforms



91054_12c

Fig. 12c - Maximum Avalanche Energy vs. Drain Current

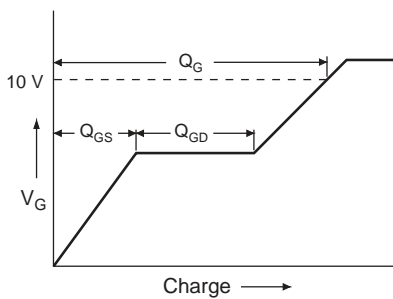


Fig. 13a - Basic Gate Charge Waveform

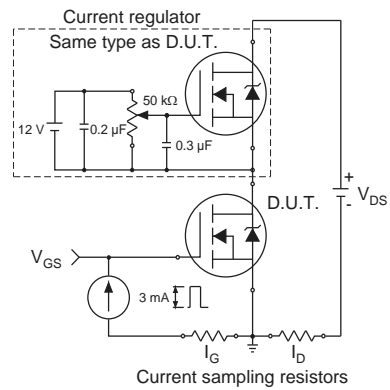
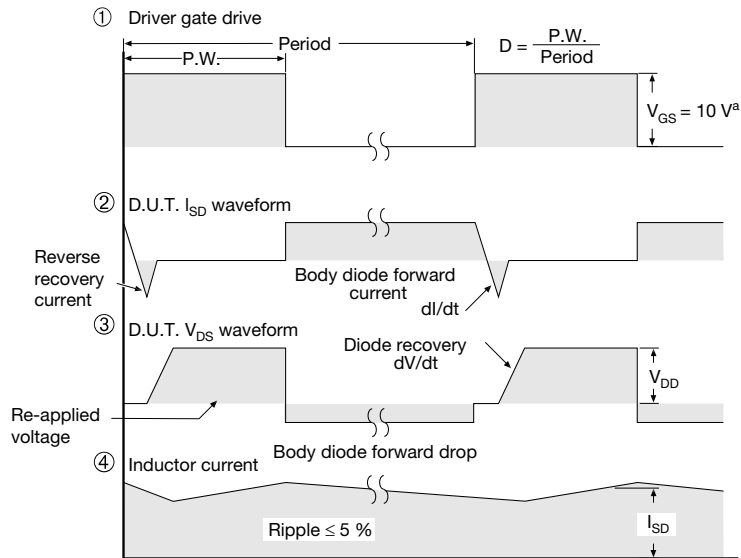
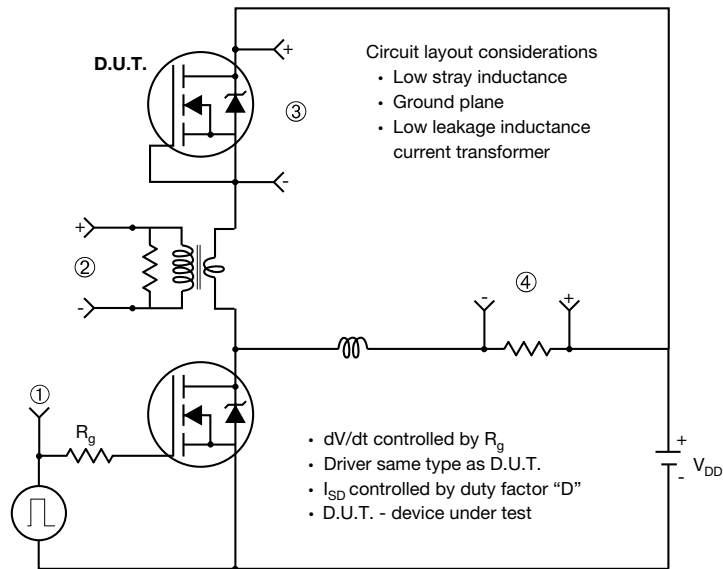


Fig. 13b - Gate Charge Test Circuit

Peak Diode Recovery dV/dt Test Circuit

Note

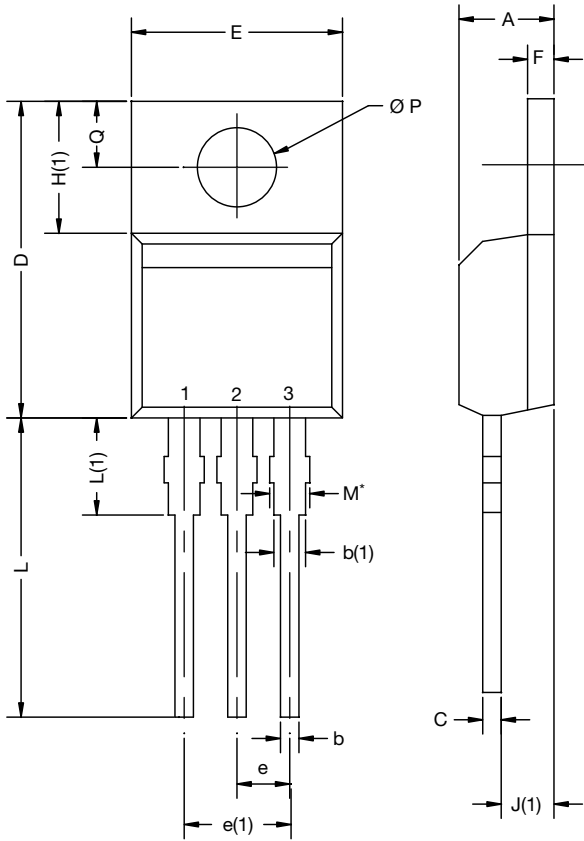
 a. $V_{GS} = 5 V$ for logic level devices

Fig. 14 - For N-Channel

Vishay Siliconix maintains worldwide manufacturing capability. Products may be manufactured at one of several qualified locations. Reliability data for Silicon Technology and Package Reliability represent a composite of all qualified locations. For related documents such as package/tape drawings, part marking, and reliability data, see www.vishay.com/ppg?91054.



TO-220-1

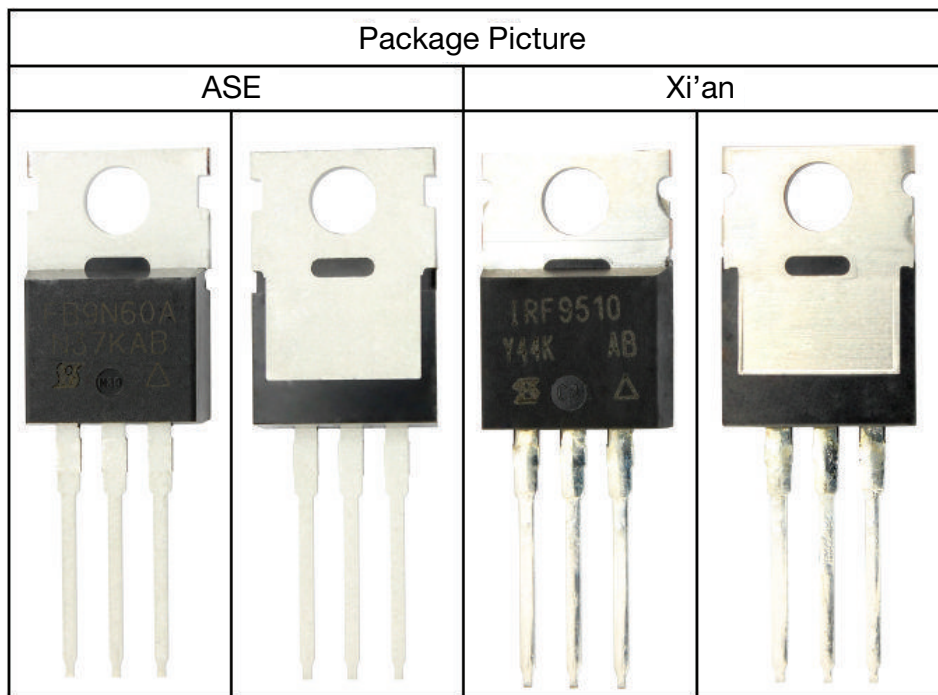


DIM.	MILLIMETERS		INCHES	
	MIN.	MAX.	MIN.	MAX.
A	4.24	4.65	0.167	0.183
b	0.69	1.02	0.027	0.040
b(1)	1.14	1.78	0.045	0.070
c	0.36	0.61	0.014	0.024
D	14.33	15.85	0.564	0.624
E	9.96	10.52	0.392	0.414
e	2.41	2.67	0.095	0.105
e(1)	4.88	5.28	0.192	0.208
F	1.14	1.40	0.045	0.055
H(1)	6.10	6.71	0.240	0.264
J(1)	2.41	2.92	0.095	0.115
L	13.36	14.40	0.526	0.567
L(1)	3.33	4.04	0.131	0.159
Ø P	3.53	3.94	0.139	0.155
Q	2.54	3.00	0.100	0.118

ECN: X15-0364-Rev. C, 14-Dec-15
DWG: 6031

Note

- M* = 0.052 inches to 0.064 inches (dimension including protrusion), heatsink hole for HVM





Disclaimer

ALL PRODUCT, PRODUCT SPECIFICATIONS AND DATA ARE SUBJECT TO CHANGE WITHOUT NOTICE TO IMPROVE RELIABILITY, FUNCTION OR DESIGN OR OTHERWISE.

Vishay Intertechnology, Inc., its affiliates, agents, and employees, and all persons acting on its or their behalf (collectively, "Vishay"), disclaim any and all liability for any errors, inaccuracies or incompleteness contained in any datasheet or in any other disclosure relating to any product.

Vishay makes no warranty, representation or guarantee regarding the suitability of the products for any particular purpose or the continuing production of any product. To the maximum extent permitted by applicable law, Vishay disclaims (i) any and all liability arising out of the application or use of any product, (ii) any and all liability, including without limitation special, consequential or incidental damages, and (iii) any and all implied warranties, including warranties of fitness for particular purpose, non-infringement and merchantability.

Statements regarding the suitability of products for certain types of applications are based on Vishay's knowledge of typical requirements that are often placed on Vishay products in generic applications. Such statements are not binding statements about the suitability of products for a particular application. It is the customer's responsibility to validate that a particular product with the properties described in the product specification is suitable for use in a particular application. Parameters provided in datasheets and / or specifications may vary in different applications and performance may vary over time. All operating parameters, including typical parameters, must be validated for each customer application by the customer's technical experts. Product specifications do not expand or otherwise modify Vishay's terms and conditions of purchase, including but not limited to the warranty expressed therein.

Except as expressly indicated in writing, Vishay products are not designed for use in medical, life-saving, or life-sustaining applications or for any other application in which the failure of the Vishay product could result in personal injury or death. Customers using or selling Vishay products not expressly indicated for use in such applications do so at their own risk. Please contact authorized Vishay personnel to obtain written terms and conditions regarding products designed for such applications.

No license, express or implied, by estoppel or otherwise, to any intellectual property rights is granted by this document or by any conduct of Vishay. Product names and markings noted herein may be trademarks of their respective owners.

B

Electrolytic Capacitor

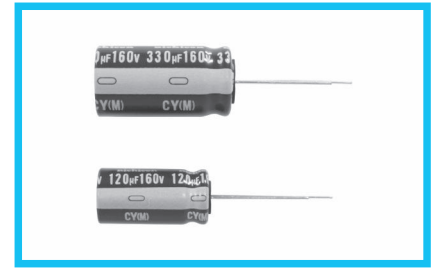
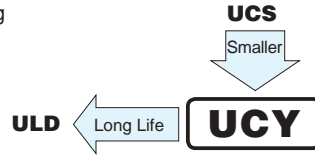
In this annex we can find the datasheet of one of the capacitors used in this project. It consists on an aluminum electrolytic capacitor made by nichicon and named as UCY2V680MHD.

ALUMINUM ELECTROLYTIC CAPACITORS

UCY Miniature Sized, High Ripple Current,
High Reliability



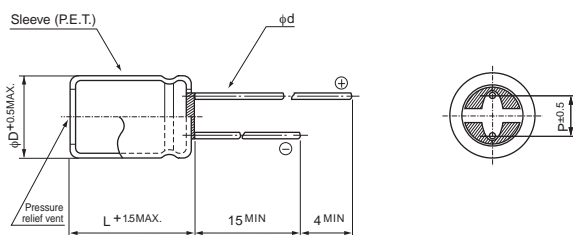
- High ripple current and Long Life product withstanding load life of 10000 to 12000 hours at +105°C.
- Suited for ballast application.
- Compliant to the RoHS directive (2011/65/EU).



Specifications

Item	Performance Characteristics														
Category Temperature Range	-40 to +105°C (160 to 400V), -25 to +105°C (420 to 500V)														
Rated Voltage Range	160 to 500V														
Rated Capacitance Range	6.8 to 680µF														
Capacitance Tolerance	±20% at 120Hz, 20°C														
Leakage Current	After 1 minute's application of rated voltage at 20°C, leakage current is not more than 0.04CV+100 (µA)														
Tangent of loss angle (tan δ)	Measurement frequency : 120Hz at 20°C														
	Rated voltage (V)	160	200	250	350	400	420	450	500						
	tan δ (MAX.)	0.20	0.20	0.20	0.24	0.24	0.24	0.24	0.24						
Stability at Low Temperature	Measurement frequency : 120Hz														
	Rated voltage (V)	160	200	250	350	400	420	450	500						
	Impedance ratio ZT / Z20 (MAX.)	Z=-25°C / Z+20°C	3	3	3	5	5	6	6						
		Z=-40°C / Z+20°C	6	6	6	6	6	-	-						
Endurance	The specifications listed at right shall be met when the capacitors are restored to 20°C after D.C. bias plus rated ripple current is applied for 12000 hours (10000 hours for 20L or less, 500V) at 105°C, the peak voltage shall not exceed the rated voltage.						<table border="1"> <tr> <td>Capacitance change</td> <td>Within ±20% of the initial capacitance value</td> </tr> <tr> <td>tan δ</td> <td>200% or less than the initial specified value</td> </tr> <tr> <td>Leakage current</td> <td>Less than or equal to the initial specified value</td> </tr> </table>			Capacitance change	Within ±20% of the initial capacitance value	tan δ	200% or less than the initial specified value	Leakage current	Less than or equal to the initial specified value
Capacitance change	Within ±20% of the initial capacitance value														
tan δ	200% or less than the initial specified value														
Leakage current	Less than or equal to the initial specified value														
Shelf Life	After storing the capacitors under no load at 105°C for 1000 hours and then performing voltage treatment based on JIS C 5101-4 clause 4.1 at 20°C, they shall meet the specified values for the endurance characteristics listed above.														
Marking	Printed with white color letter on dark brown sleeve.														

Radial Lead Type

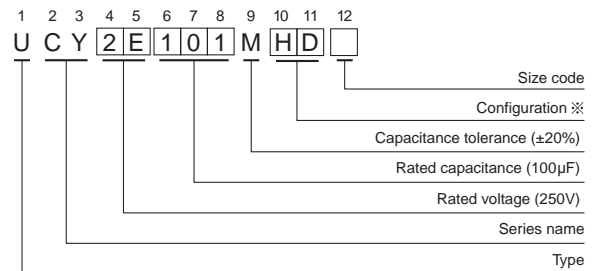


	(mm)			
φD	10	12.5	16	18
P	5.0	5.0	7.5	7.5
φd	0.6	0.6 [※]	0.8	0.8

※ In case L > 25 for the φ12.5 dia. unit, lead dia. φd = 0.8mm.

- Please refer to page 20 about the end seal configuration.

Type numbering system (Example : 250V 100µF)



※ Configuration

φ D	Pb-free leadwire Pb-free PET sleeve
10	PD
12.5 to 18	HD

Please refer to page 20, 21, 22 about the formed or taped product spec.
Please refer to page 4 for the minimum order quantity.

- Dimension table in next page.

UCY

■ Dimensions

Cap	Code	V		160		200		250		350		400		420		450		500			
		2C	2D	2E	2V	2G	W6	2W	2H												
6.8	6R8											10 × 16	140	10 × 16	105	10 × 16	105				
10	100											10 × 16	150	10 × 20	135	10 × 20	135	12.5 × 20	160		
12	120								10 × 16	160		10 × 20	175	10 × 20	150	10 × 20	150				
15	150								10 × 20	180		10 × 20	180	10 × 25	185	10 × 25	185	12.5 × 25	220		
18	180								10 × 20	215		10 × 25	235	10 × 31.5	215	10 × 31.5	215	12.5 × 31.5	240		
																		▲ 12.5 × 20	255	● 16 × 20	240
22	220				10 × 16	225	10 × 16	225	10 × 25	255		10 × 31.5	275	12.5 × 20	285	12.5 × 25	300	12.5 × 35.5	280		
									○ 10 × 20	215										▲ 16 × 25	280
										● 12.5 × 20	325										● 18 × 20
27	270				10 × 16	235	10 × 20	255	10 × 31.5	305		12.5 × 20	360	12.5 × 25	340	12.5 × 25	340	12.5 × 40	310		
									○ 10 × 25	255										▲ 16 × 25	310
33	330	10 × 16	260	10 × 20	305	10 × 20	305	10 × 25	380	12.5 × 25	385	12.5 × 31.5	400	12.5 × 31.5	400	12.5 × 31.5	400	16 × 31.5	350		
									● 12.5 × 20	400	● 16 × 20	450	● 16 × 20	450	● 16 × 20	385	● 16 × 20	385	● 18 × 25	350	
39	390	10 × 16	295	10 × 20	325	10 × 25	345	12.5 × 25	455	12.5 × 25	455	12.5 × 31.5	465	12.5 × 31.5	430	12.5 × 35.5	460	16 × 35.5	380		
													○ 12.5 × 25	385			● 18 × 20	440			
47	470	10 × 20	375	10 × 20	360	10 × 31.5	405	12.5 × 25	510	12.5 × 25	510	16 × 20	520	12.5 × 35.5	505	12.5 × 40	525	16 × 40	440		
				● 12.5 × 20	490	○ 10 × 25	345	● 16 × 20	540	▲ 12.5 × 31.5	510	▲ 16 × 25	500	▲ 16 × 25	500	▲ 16 × 25	500	▲ 18 × 31.5	440		
56	560	10 × 20	380	10 × 25	415	12.5 × 20	515	12.5 × 31.5	590	12.5 × 31.5	590	12.5 × 35.5	630	12.5 × 35.5	630	16 × 31.5	585	18 × 35.5	480		
									▲ 16 × 20	565	▲ 16 × 25	585	▲ 16 × 25	585	12.5 × 40	570	● 18 × 25	560			
													● 18 × 20	600							
68	680	10 × 25	455	10 × 31.5	485	12.5 × 25	615	12.5 × 35.5	695	12.5 × 35.5	695	12.5 × 40	720	16 × 31.5	645	16 × 35.5	660	18 × 40	525		
		● 12.5 × 20	590	● 12.5 × 20	650	● 16 × 20	650	● 16 × 25	700	○ 16 × 25	640	● 18 × 25	615	16 × 35.5	660						
									▲ 18 × 20	690	● 18 × 25	735									
82	820	10 × 31.5	534	12.5 × 25	645	12.5 × 31.5	715	16 × 31.5	740	16 × 31.5	740	16 × 31.5	805	16 × 35.5	725	16 × 40	750				
		○ 10 × 25	455	○ 12.5 × 20	645	○ 12.5 × 25	615	▲ 12.5 × 40	785	○ 16 × 25	700	● 18 × 25	765	▲ 18 × 31.5	730	▲ 18 × 31.5	730				
		● 12.5 × 20	640	● 16 × 20	690	● 16 × 20	690	○ 16 × 25	700	● 18 × 25	765										
100	101	12.5 × 20	645	12.5 × 25	695	16 × 20	715	16 × 31.5	825	16 × 31.5	825	16 × 35.5	850	16 × 40	825	18 × 35.5	835				
				● 16 × 20	710	▲ 12.5 × 35.5	785	● 18 × 25	790	▲ 18 × 31.5	875	▲ 18 × 31.5	875	▲ 18 × 35.5	835						
120	121			16 × 20	775	16 × 25	845	16 × 35.5	925	18 × 31.5	940	18 × 40	930	18 × 40	930						
		12.5 × 25	760	▲ 12.5 × 31.5	810	○ 12.5 × 35.5	785	▲ 18 × 31.5	940	▲ 16 × 40	950	▲ 18 × 46	945	▲ 18 × 46	945						
						● 12.5 × 40	890	▲ 18 × 20	815	● 18 × 35.5	960										
150	151	12.5 × 31.5	905	12.5 × 35.5	965	18 × 25	970	18 × 35.5	1080	18 × 40	1030										
		○ 12.5 × 25	760	● 16 × 25	945	▲ 12.5 × 40	990	▲ 16 × 40	1000												
		● 16 × 20	945	▲ 18 × 20	910																
180	181	16 × 20	1000	12.5 × 40	1090	16 × 31.5	1110	18 × 40	1205	18 × 46	1110										
		○ 12.5 × 31.5	905	▲ 16 × 25	1035	▲ 18 × 25	1050														
		▲ 12.5 × 35.5	1050	● 18 × 20	910																
220	221	12.5 × 40	1200	16 × 31.5	1230	16 × 40	1295	18 × 46	1300												
		○ 12.5 × 35.5	1050	▲ 12.5 × 40	1090	○ 16 × 35.5	1220														
		● 16 × 25	1185	● 18 × 25	1185	● 18 × 31.5	1160														
270	271	18 × 25	1235	16 × 35.5	1400	18 × 35.5	1450														
		▲ 12.5 × 40	1300	▲ 18 × 31.5	1410	▲ 16 × 40	1350														
330	331	16 × 31.5	1510	16 × 40	1595	18 × 46	1600														
		▲ 18 × 25	1445	▲ 18 × 31.5	1560	○ 18 × 40	1530														
390	391	16 × 40	1730	18 × 40	1780																
		○ 16 × 35.5	1510	○ 18 × 35.5	1690																
470	471	18 × 35.5	1920	18 × 40	1850																
		▲ 16 × 40	1730	▲ 18 × 46	1900																
560	561	18 × 40	2130																		
680	681	18 × 46	2300																Case size φD × L (mm) ※		

● Frequency coefficient of rated ripple current

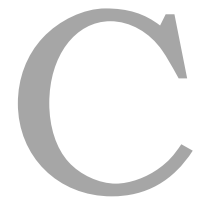
Frequency	50Hz	120Hz	1kHz	10kHz	100kHz or more
Coefficient	0.80	1.00	1.60	1.80	2.00

※ : Rated ripple current (mArms) at 105°C 120Hz

▲ : In this case, ⑩ will be put at 12th digit of type numbering system.

● : In this case, ③ will be put at 12th digit of type numbering system.

○ : In this case, ⑨ will be put at 12th digit of type numbering system.



Ceramic Capacitor

In this annex we can find the datasheet of one of the capacitors used in this project. It consists on a ceramic capacitor made by TDK and named as C3216X7T2W104M160AA.

C3216X7T2W104M160AA

TDK Item Description : C3216X7T2W104MT****

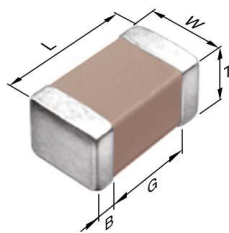


Application & Main Feature

Commercial Grade (Mid Voltage (100 to 630V))

Series

C3216 [EIA CC1206]



Dimensions

L	3.20mm +/-0.2mm
W	1.60mm +/-0.2mm
T	1.60mm +/-0.2mm
B	0.20mm Min.
G	1.00mm Min.

Temperature Characteristic

X7T (-55 to 125 degC +22,-33%)

Rated Voltage

2W (450Vdc)

Capacitance

100nF

Capacitance Tolerance

M (+/-20%)

Dissipation Factor

2.5% Max.

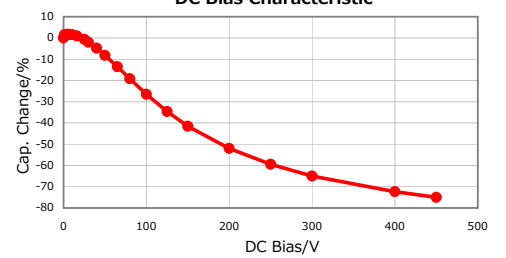
Insulation Resistance

5Gohm Min.

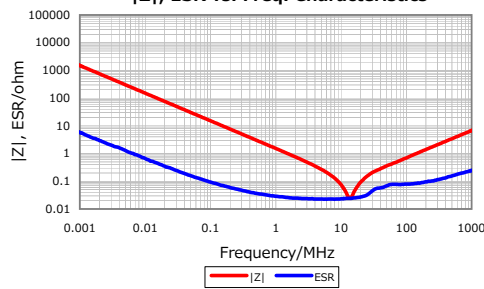
AEC-Q200

Not Applicable

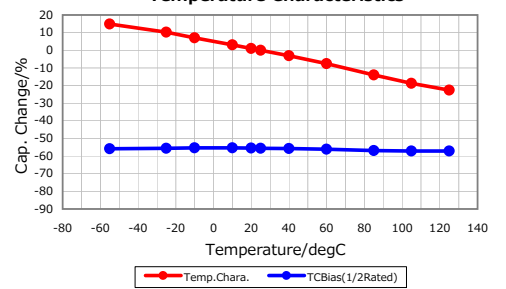
DC Bias Characteristic



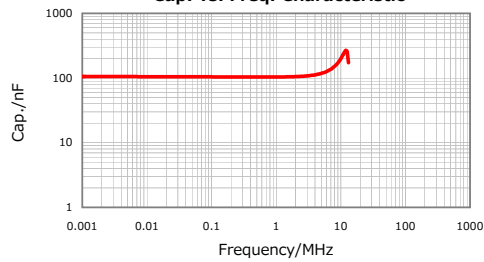
|Z|, ESR vs. Freq. Characteristics



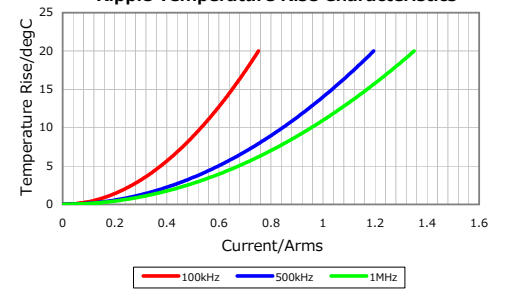
Temperature Characteristics



Cap. vs. Freq. Characteristic



Ripple Temperature Rise Characteristics



Characterization Sheet (Multilayer Ceramic Chip Capacitors)



All specifications are subject to change without notice.

January 4, 2016

References

- [1] I. Boldea, “Electric generators and motors: An overview,” *CES Transactions on Electrical Machines and Systems*, vol. 1, pp. 3–14, March 2017.
- [2] J. J. Loferski, “Theoretical considerations governing the choice of the optimum semiconductor for photovoltaic solar energy conversion,” *Journal of Applied Physics*, vol. 27, no. 7, pp. 777–784, 1956.
- [3] D. G. Holmes and T. A. Lipo, *Modulation of SinglePhase Voltage Source Inverters*, pp. 744–. Wiley–IEEE Press, 2003.
- [4] “IEEE recommended practice and requirements for harmonic control in electric power systems,” *IEEE Std 519-2014 (Revision of IEEE Std 519-1992)*, pp. 1–29, June 2014.
- [5] M. Peterson, B. N. Singh, and P. Rastgoufard, “Active and passive filtering for harmonic compensation,” in *2008 40th Southeastern Symposium on System Theory (SSST)*, pp. 188–192, March 2008.
- [6] P. T. Krein, R. S. Balog, and M. Mirjafari, “Minimum energy and capacitance requirements for single-phase inverters and rectifiers using a ripple port,” *IEEE Transactions on Power Electronics*, vol. 27, pp. 4690–4698, Nov 2012.
- [7] S. R. “Tabulated values of the Shockley–Queisser limit for single junction solar cells,” *Solar Energy*, vol. 130, pp. 139 – 147, 2016.
- [8] M. Seyedmahmoudian, B. Horan, T. K. Soon, R. Rahmani, A. M. T. Oo, S. Mekhilef, and A. Stojcevski, “State of the art artificial intelligence-based MPPT techniques for mitigating partial shading effects on PV systems – A review,” *Renewable and Sustainable Energy Reviews*, vol. 64, pp. 435 – 455, 2016.
- [9] A. Safari and S. Mekhilef, “Simulation and hardware implementation of incremental conductance MPPT with direct control method using Cuk converter,” *IEEE Transactions on Industrial Electronics*, vol. 58, pp. 1154–1161, April 2011.
- [10] N. Femia, D. Granozio, G. Petrone, G. Spagnuolo, and M. Vitelli, “Predictive adaptive MPPT perturb and observe method,” *IEEE Transactions on Aerospace and Electronic Systems*, vol. 43, pp. 934–950, July 2007.
- [11] A. Pandey, N. Dasgupta, and A. K. Mukerjee, “Design issues in implementing MPPT for improved tracking and dynamic performance,” in *IECON 2006 - 32nd Annual Conference on IEEE Industrial Electronics*, pp. 4387–4391, Nov 2006.
- [12] N. Femia, G. Petrone, G. Spagnuolo, and M. Vitelli, “Optimization of perturb and observe maximum power point tracking method,” *IEEE Transactions on Power Electronics*, vol. 20, pp. 963–973, July 2005.

References

- [13] S. Jain and V. Agarwal, "A new algorithm for rapid tracking of approximate maximum power point in photovoltaic systems," *IEEE Power Electronics Letters*, vol. 2, pp. 16–19, March 2004.
- [14] K. S. Tey and S. Mekhilef, "Modified incremental conductance MPPT algorithm to mitigate inaccurate responses under fast-changing solar irradiation level," *Solar Energy*, vol. 101, pp. 333–342, 2014.
- [15] D. W. Hart, *Introduction to Power Electronics*. 1997.
- [16] V. Gaikwad, S. Mutha, R. Mundhe, O. Sagar, and T. Chinchole, "Survey of PWM techniques for solar inverter," in *2016 International Conference on Global Trends in Signal Processing, Information Computing and Communication (ICGTSPICC)*, pp. 501–504, Dec 2016.
- [17] J.-Y. LEE and Y.-Y. SUN, "A new SPWM inverter with minimum filter requirement," *International Journal of Electronics*, vol. 64, no. 5, pp. 815–826, 1988.
- [18] B. Hua, Z. Zhengming, M. Shuo, L. Jianzheng, and S. Xiaoying, "Comparison of three PWM strategies-SPWM, SVPWM one-cycle control," in *The Fifth International Conference on Power Electronics and Drive Systems, 2003. PEDS 2003.*, vol. 2, pp. 1313–1316 Vol.2, Nov 2003.
- [19] W. C. Duesterhoeft, M. W. Schulz, and E. Clarke, "Determination of instantaneous currents and voltages by means of alpha, beta, and zero components," *Transactions of the American Institute of Electrical Engineers*, vol. 70, pp. 1248–1255, July 1951.
- [20] R. H. Park, "Two-reaction theory of synchronous machines generalized method of analysis–part I," *Transactions of the American Institute of Electrical Engineers*, vol. 48, pp. 716–727, July 1929.
- [21] G. Kron, "The application of tensors to the analysis of rotating electrical machinery," *GE Review*, 1938.
- [22] Y. Lei, C. Barth, S. Qin, W. C. Liu, I. Moon, A. Stillwell, D. Chou, T. Foulkes, Z. Ye, Z. Liao, and R. C. N. Pilawa-Podgurski, "A 2-kW single-phase seven-level flying capacitor multilevel inverter with an active energy buffer," *IEEE Transactions on Power Electronics*, vol. 32, pp. 8570–8581, Nov 2017.
- [23] R. W. Erickson and D. Maksimovic, *Fundamentals of Power Electronics*. Springer Science & Business Media, 2007.
- [24] M. Liserre, F. Blaabjerg, and S. Hansen, "Design and control of an LCL–filter–based three–phase active rectifier," *IEEE Transactions on Industry Applications*, vol. 41, pp. 1281–1291, Sept 2005.
- [25] W. Wu, Y. He, T. Tang, and F. Blaabjerg, "A new design method for the passive damped LCL and LLCL filter–based single–phase grid–tied inverter," *IEEE Transactions on Industrial Electronics*, vol. 60, pp. 4339–4350, Oct 2013.
- [26] W. Wu, Y. He, and F. Blaabjerg, "An LLCL power filter for single–phase grid–tied inverter," *IEEE Transactions on Power Electronics*, vol. 27, pp. 782–789, Feb 2012.
- [27] R. N. Beres, X. Wang, F. Blaabjerg, M. Liserre, and C. L. Bak, "Optimal design of high–order passive–damped filters for grid–connected applications," *IEEE Transactions on Power Electronics*, vol. 31, pp. 2083–2098, March 2016.
- [28] "IEEE application guide for IEEE Std 1547(tm), IEEE standard for interconnecting distributed resources with electric power systems," *IEEE Std 1547.2-2008*, pp. 1–217, April 2009.

- [29] S. Sen, K. Yenduri, and P. Sensarma, “Step-by-step design and control of LCL filter based three phase grid-connected inverter,” in *2014 E International Conference on Industrial Technology (ICIT)*, pp. 503–508, Feb 2014.
- [30] Y. Lang, D. Xu, S. R. Hadianamrei, and H. Ma, “A novel design method of LCL type utility interface for three-phase voltage source rectifier,” in *2005 IEEE 36th Power Electronics Specialists Conference*, pp. 313–317, June 2005.
- [31] B. Bolsens, K. D. Brabandere, J. V. den Keybus, J. Driesen, and R. Belmans, “Model-based generation of low distortion currents in grid-coupled pwm-inverters using an lcl output filter,” in *2004 IEEE 35th Annual Power Electronics Specialists Conference (IEEE Cat. No.04CH37551)*, vol. 6, pp. 4616–4622 Vol.6, June 2004.
- [32] P. Channegowda and V. John, “Filter optimization for grid interactive voltage source inverters,” *IEEE Transactions on Industrial Electronics*, vol. 57, pp. 4106–4114, Dec 2010.
- [33] M. Vujacic, M. Srndovic, M. Hammami, and G. Grandi, “Evaluation of DC voltage ripple in single-phase H-bridge PWM inverters,” in *IECON 2016 - 42nd Annual Conference of the IEEE Industrial Electronics Society*, pp. 3235–3240, Oct 2016.
- [34] R. Balog and P. T. Krein, “Automatic tuning of coupled inductor filters,” in *2002 IEEE 33rd Annual IEEE Power Electronics Specialists Conference. Proceedings (Cat. No.02CH37289)*, vol. 2, pp. 591–596 vol.2, 2002.
- [35] H. Wang and F. Blaabjerg, “Reliability of capacitors for DC-link applications in power electronic converters—an overview,” *IEEE Transactions on Industry Applications*, vol. 50, pp. 3569–3578, Sept 2014.

